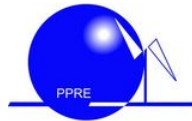# Carl von Ossietzky Universität Oldenburg

Institute of Physics

Sustainable Renewable Energy Technologies (SuRE)

Master's Thesis

Title:

"Supporting Capacity Expansion Planning in REMix by Detailed AC-Optimal Power Flow Experiments for Voltage Stability Modelling"

Presented by:	Kehinde Oseni Salami
First examiner:	Dr. Robert Beckmann
Second examiner:	Prof. Dr. Carsten Agert
Supervisors:	Dr. Karl-Kien Cao
Host Institution:	DLR Institute of Networked Energy Systems
Place, Date:	Oldenburg, March 15, 2024

Acknowledgements

First and foremost, I extend my deepest gratitude to Almighty Allah (God) for the strength, wisdom, and unwavering faith, and for His blessings that have guided me through this endeavor.

I would like to express my heartfelt appreciation to my loving wife, who has been a pillar of support, encouragement, and understanding throughout this academic journey. Her patience and love have been the bedrock upon which I have leaned in times of both challenge and celebration. To my Son, Abdullah, your innocent smiles and joyous laughter have been a constant source of motivation, reminding me of life's brighter aspects amidst the rigorous demands of research.

My gratitude extends to my dear parents, who have been my first teachers and mentors. Their unconditional love, sacrifices, and belief in me have shaped the person I am today. Their support and encouragement over the years have been indispensable to my personal and academic growth.

To Karl-Kien Cao, my direct supervisor, I extend my sincerest appreciation. His expertise, mentorship, and guidance have been indispensable from the beginning to the end of this thesis. I remember days when I required much more of his time than scheduled, among other sacrifices he rendered. I remain greatly thankful for everything, Kien.

Special appreciation goes to Robert Beckmann, whose invaluable feedback and guidance contributed greatly to the completion of this thesis. He also made my integration into the DLR site at Wechloy campus smooth from the very first day of my research.

I would also like to extend my gratitude to the staff of the Energy System Analysis at the DLR institute, particularly Jan Buschmann, Francesco Witte, and Gereon Recht. Their valuable support, feedback, and advice have significantly enriched this project.

I am immensely grateful to my examiners, Robert Beckmann and Prof. Dr. Carsten Agert,

whose expert guidance, insightful feedback, and constructive criticism have been invaluable throughout this process. Their dedication, expertise, and willingness to share knowledge have significantly contributed to the quality of this work.

My appreciation also extends to the German Government, through the DAAD, whose generous funding made my Master's studies in Renewable Energy possible.

Furthermore, my deepest appreciation goes to the lecturers and staff of PPRE and SuRE. Their vast knowledge and guidance have been pivotal in my academic and career growth, especially here in Europe, enabling me to reach this milestone.

To all who have contributed to this journey in various ways, I offer my sincere thanks. This accomplishment is not mine alone but a reflection of the collective effort, support, and faith of everyone mentioned above.

Abstract

This thesis addresses the critical challenge of maintaining voltage stability in power systems with high renewable energy penetration during capacity expansion planning (CEP) in the Renewable Energy Mix (REMix) optimization framework. Given the intermittent nature of renewable energy sources and their impact on grid stability, this study proposes a comprehensive methodology that integrates voltage stability considerations, specifically the Voltage Collapse Proximity Indicator (VCPI), into the CEP process using the REMix energy system model. This work uses MATLAB as a supporting modelling software for running detailed AC optimal power flow. The research conducted in this thesis demonstrates the feasibility and effectiveness of incorporating VCPI to ensure voltage stability across the power network.

The research employs a systematic model generation expansion planning approach using the IEEE RTS 24-bus system. Comparative analysis of observed scenarios with and without VCPI integration reveals that including additional voltage stability constraints leads to more reliable and cost-effective expansion planning, emphasizing the critical role of the voltage stability index in enhancing grid resilience and reducing power losses.

Furthermore, this work extends the scope of typical REMix applications by introducing the concept of a voltage security-constrained optimal power flow algorithm, offering insights into optimizing power systems design and operation in the context of growing renewable energy integration. The particle swarm optimization (PSO) algorithm used to solve the optimal power flow (OPF) is part of the supporting tool. The findings highlight the potential for significant operational cost savings and improved system reliability through informed CEP decisions considering voltage stability. This thesis contributes to the body of knowledge by bridging the gap in existing REMix applications, offering a novel approach to ensuring voltage stability in renewable-rich power networks, thereby supporting the transition towards sustainable and stable electricity systems.

The thesis concludes by suggesting future research directions, including integrating VCPI into linearized optimal power flow models in REMix for larger-scale applications and exploring alternative optimization solvers to enhance model compatibility and efficiency. This

work underscores the importance of incorporating voltage stability considerations in CEP, paving the way for more sustainable and resilient power systems in the high renewable energy integration era.

Contents

List of Figures

List of Tables

List of Abbreviations

CEP Capacity Expansion Planning

GEP Generation Expansion Planning

TEP Transmission Expansion Planning

DLR Deutsches Zentrum für Luft- und Raumfahrt

FVSI Fast Voltage Stability Index

GAMS General Algebraic Modeling System

IVSI Improved Voltage Stability Index

LVSI Line Voltage Stability Index

LQP Line Stability Factor

Lmn Line Stability Index

NCPI Novel Collapse Prediction Index

REMix Renewable Energy Mix

VCPI Voltage Collapse Proximity Indicator

VSC-OPF Voltage Stability-Constrained Optimal Power Flow

VSI Voltage Stability Index

VSIs Voltage Stability Indices

OPF Optimal power flow

AC-OPF Alternating current optimal power flow

DC-OPF Direct current optimal power flow

OC Operation cost

GEP OF Generation Expansion Planning Objective Function

Invest investment cost for a technology unit (in MEUR/MW)

OMFix fix operation and maintenance costs (in MEUR/MW/year)

OMVar variable operation and maintenance cost (in MEUR/MWh)

PSO Particle Swarm Optimization

WPP Wind Power Plant

p.u Per Unit

Mio Million

Tsd Thousand

List of Symbols

Symbol	Description
i, j	Indices of the buses
Ω_b	set of all buses
a_i, b_i, and c_i	Cost coefficients of active power generation at bus i
P_{Gi}	Active power generations at the bus i
Q_{Gi}	Reactive power generations at the bus i
P_{Di}	Active power demand at the bus i
Q_{Di}	Reactive power demand at the bus i
G_{ij}	Transfer conductance between the buses i and j
B_{ij}	Transfer susceptance between the buses i and j
θ_{ij}	Phase angle difference between the voltages at buses i and j
$C_{I,t}$	Capital cost
$C_{OM,t}$	Operation and maintenance cost
$C_{F,t}$	Fuel cost
$C_{E,t}$	Environmental cost
T	Planning year
V_i	Sending voltage magnitude
P_i	Sending active power
Q_i	Sending reactive power
δ_i	Sending voltage angle
I	Transmission line current
R	Resistance of the transmission line
X	Reactance of the transmission line
Z	Impedance of the transmission line
θ	Impedance angle
V_j	Receiving voltage magnitude
P_j	Receiving active power

Q_j	Receiving reactive power
δ_j	Receiving voltage angle
δ	Difference between the sending and receiving voltage angles
$P_{j(max)}$	Maximum transferable active power
$Q_{j(max)}$	Maximum transferable reactive power
P_{loss}	Active power loss
Q_{loss}	Reactive power loss
$VCPI(power)$	VCPI using active power
$VCPI(powerloss)$	VCPI using active power loss
$X(t)$	Particle position
$V(t)$	Particle velocity
G_{best}	Global best
P_{best}	Personal best
r_1, r_2	Random numbers in the interval of (0,1) with uniform distribution
C_1, C_2	Coefficients of accelerated particles
$V(t-1)$	Inertial weight of the particle

Chapter 1

Introduction

1.1 Background and Motivation for the Thesis

The modern electric power system is a complex and dynamic network experiencing significant transformation, especially due to the continuous integration of renewable energy sources. The intermittent and unpredictable nature of renewable energy sources, such as solar and wind, causes fluctuations in power generation and makes it difficult to maintain a balanced and stable power grid. Moreover, the distributed nature of these sources requires a re-examination of traditional voltage stability assessment and enhancement techniques. While this integration brings sustainability benefits, it also introduces new challenges in maintaining system stability, particularly voltage stability during Capacity Expansion Planning (CEP). This challenge has become increasingly significant due to the connection of various blackouts worldwide with voltage-related occurrences [1, 2, 3]. As a result, planning engineers have directed significantly greater attention towards addressing the issue of optimal power flow under voltage stability constraint when considering capacity expansion planning [1].

Power system stability has been recognized since the 1920s as a critical aspect of safe system operation [4]. It is the ability of an electrical network to return to its normal operating condition whenever the system suffers a disturbance. The stability of a power system depends not only on its operating conditions but also on the nature of the physical disturbances. Power system stability is classified into three main classes: rotor angle stability, frequency stability, and voltage stability [4]. This classification, while useful in addressing the inherent complexity of a power network, also highlights the inter-dependencies between these stability domains. For example, in a network, voltage collapse may lead to large disturbances in rotor angle and frequency. Likewise, large frequency deviations can cause pronounced changes in voltage magnitude, demonstrating the interconnected nature of these stability aspects. Thus, the voltage is a critical component for the stability of the power network.

Various approaches and methodologies have been put forward in research to assess power system voltage stability [5, 6]. In this regard, several static voltage stability indicators

have gained extensive usage in evaluating and predicting the system closeness to voltage instability [1]. These indicators have been classified into two categories: bus voltage and line flow stability indices. In the category of bus voltage stability indices, the weakest bus is identified by utilizing data concerning the stability status of the buses such as L-index [7], voltage collapse prediction index [8], Voltage Stability Index (VSI) [9] and Improved Voltage Stability Index (IVSI) [10].

On the other hand, line-based indices are utilized to pinpoint critical lines within an interconnected system. Notable examples include the Fast Voltage Stability Index (FVSI) [11], the Line Stability Index (Lmn) [12], the Voltage Collapse Proximity Indicator (VCPI) [13], the Line Stability Factor (LQP) [14] and Novel Collapse Prediction Index (NCPI) [15]. These line indices are instrumental in assessing the pivotal lines significantly impacting the overall system stability. According to [1], the attributes of the line voltage stability indices served as a driving force behind the intention to develop a Voltage Stability-Constrained Optimal Power Flow (VSC-OPF) grounded in these line voltage indices. These indicators include power and voltage variations, thus providing reliable information on how close the voltage is to instability. Among the various indicators, the Voltage Collapse Proximity Indicator (VCPI) stands out for its superior accuracy and resilience in forecasting voltage collapse [1, 16].

The process of planning grid capacity expansion to meet future load demands is becoming increasingly complex with the integration of renewable energy. Traditional CEP models designed for predictable centralized power generation systems need to be reevaluated and adjusted to account for the variability and uncertainty that come with renewable energy. This requires developing advanced modelling techniques that effectively integrate voltage stability constraints into CEP, especially for grids with high renewable energy penetration. Such models must be able to simulate various factors that affect voltage stability, such as load fluctuations, changes in network topology, and the stochastic nature of renewable energy. It should also provide actionable insights to network planners and operators to ensure voltage stability during the CEP processes.

In the research field of energy systems analysis, models are used to optimize energy systems, including grid expansion planning. One of these models is the REMix [17] developed at Deutsches Zentrum für Luft- und Raumfahrt (DLR). This modelling framework allows users to set up optimization problems written in General Algebraic Modeling System (GAMS) for addressing real power systems [18, 19]. This thesis aims to significantly contribute to power system engineering by enhancing the integration of voltage stability considerations within CEP, especially in power networks with substantial renewable energy sources. By integrating grid expansion planning concepts with the REMix model, this research bridges the gap where REMix has not yet considered voltage stability constraints. This study develops and validates an advanced model that combines REMix optimization capabilities with robust

voltage stability measures to ensure a secure power supply for future power systems, thus fostering the sustainable evolution of electricity networks.

1.2   Research Objectives

This thesis aims to introduce the concept of voltage stability during capacity expansion planning in electrical networks. To achieve this purpose, the following specific objectives have been formulated:

1. **Develop a Comprehensive Understanding:** To gain an in-depth understanding of the current state of voltage stability analysis methods and how these methods are integrated into CEP models, particularly in networks with high renewable energy penetration.

2. **Analysis and Comparison:** To conduct a comparative analysis of various voltage stability indices and their effectiveness in ensuring network stability during capacity expansion.

3. **Integrating Voltage Stability Constraint in Optimal Power Flow:** To incorporate a voltage stability constraint into an established optimal power flow algorithm in MATLAB [20] and REMix.

4. **Model Adaptation into CEP:** To develop and validate a model that effectively incorporates voltage stability constraints in CEP. This model will consider the unique characteristics of renewable energy sources and their impact on voltage stability.

5. **Implementation and Testing:** To implement the developed model in a test network, such as the IEEE 24 bus system, and validate CEP with and without voltage security constraints.

6. **Innovative Solutions and Recommendations:** To explore and propose innovative solutions that enhance voltage stability during the CEP process and to provide recommendations for future research and practical applications in the field.

1.3   Thesis Structure

The thesis is structured into five chapters, each focusing on a distinct aspect of the research work. Chapter 1, *Introduction*, outlines the background, motivation, objectives, and contribution of the study. Chapter 2, *Theoretical Background*, discusses mainly the fundamentals of power system stability, voltage stability indices, and Capacity Expansion Planning (CEP) methodologies. Chapter 3, *Methodology* describes the approach used for modelling voltage

stability in CEP, including the tools and software employed. Chapter 4, *Results and discussion*, presents the application of the developed model to test cases and discusses the findings. The discussion part further analyzes the results, compares them with existing approaches, and discusses their implications. Finally, Chapter 5, *Conclusion and future research outlook*, summarizes the study's findings, highlights its contributions, and suggests areas for future research for continuous advancement and application of REMix for power system research.

1.4   Contribution of the Thesis

This research aims to contribute to the field of electrical engineering by developing a comprehensive model that integrates voltage stability considerations into the CEP process, particularly for networks with high renewable energy integration. The research is expected to provide valuable insights into the challenges and solutions for maintaining voltage stability in modern power systems while trying to expand the grid network, thus supporting the ongoing transition to more sustainable and reliable electricity networks.

Chapter 2

Theoretical Background

This chapter delves into the theoretical background of the thesis, discussing the fundamental concepts related to power system stability and capacity expansion planning, as well as the different analysis and simulation methods. These include power flow calculation and optimal power flow, which are critical for understanding the dynamics of power systems. Additionally, the chapter explores the expansion planning methods, providing insights into how power systems can be scaled and developed. Moreover, it addresses voltage stability indices, a key aspect in ensuring the reliable operation of power systems.

2.1 Power Flow

The complexity of modern power systems networks has continued to grow, making it difficult to represent without models. As a result, mathematically simplified models form the basis of modern power system analysis. Over the years, electrical engineers have agreed on systematic ways of representing all components in the power network. The network equations can be developed systematically in different ways. In power systems, the formulation of network equations is in power. As such, they are known as *power flow equation*. Usually, these equations are non-linear and must be solved using an iterative technique [21]. Gauss-Siedel, Newton-Raphson, and Fast decoupled power flow methods are three commonly used techniques. They form the backbone of power flow analysis and design. In solving a power flow problem, the first is modelling the buses and network admittance matrix across the lines [22].

Buses mark all power entry and exit points, and lines are the connecting elements that allow the flow of electricity between these points within a network. Also, the system is first assumed to be operating under balanced conditions. Quantities of concern at each of the buses and on the lines include voltage magnitude $|V|$, phase angle δ, real power P and reactive power Q [21]. In every network, the buses are classified into three types. The first type of bus is the slack bus, reference bus, or swing bus; this is taken as the reference bus

where the magnitude and phase angle of the voltage are specified. Only one bus can be taken as a slack bus, usually with the largest generator capacity.

The second type is the load bus or P-Q bus; the active and reactive powers are known in this bus. However, the magnitude and phase angle of the bus voltages are not specified and need to be determined. Only the load may be connected at this bus, or both load and generator are connected, or nothing is connected. Generator bus or P-V bus is the third type. At this bus, the real power and voltage magnitude are known. The voltage angle and the reactive power are to be evaluated. Only generators are connected to this bus. The next step is to apply any convenient technique to solve the power flow problem.

Figure 2.1 shows a typical bus in a power system network. For analysis, a π model is used to represent the transmission lines, and the lines' impedance is converted to per-unit admittance using the same MVA base value [21].
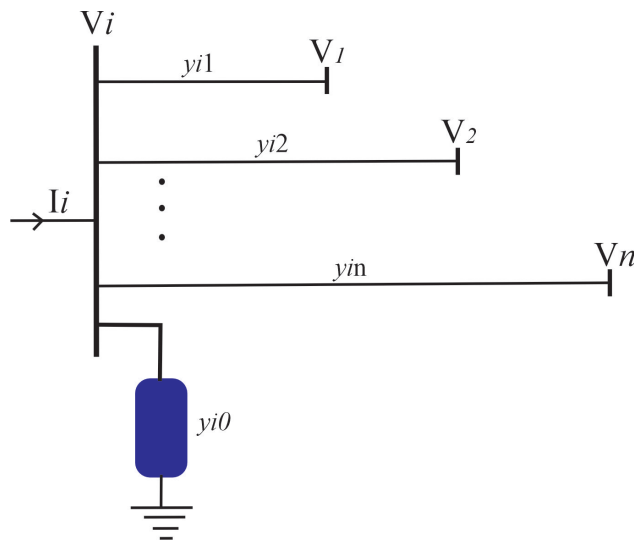
Figure 2.1: A typical power system bus

Using the Kirchhoff current law at the bus, the following expressions are derived.

$$I_i = V_i \left(\sum_{j=0}^{n} y_{ij} \right) - \sum_{j=1}^{n} y_{ij} V_j \quad j \neq i \tag{2.0}$$

The real and reactive power at bus i are related by [21]

$$P_i + jQ_i = V_i I_i^* \tag{2.1}$$

or

$$I_i = \frac{P_i - jQ_i}{V_i^*} \tag{2.2}$$

In equation (2.0), substitute I_i to give

$$\frac{P_i - jQ_i}{V_i^*} = V_i \sum_{j=0}^{n} y_{ij} - \sum_{j=1}^{n} y_{ij} V_j \quad j \neq i \tag{2.3}$$

6

Equation (2.3) gives the mathematical expression for the load flow problem, which results in a set of nonlinear algebraic equations [21]. The solution to the power flow equation can be found through an iterative procedure in which Gauss-Seidel, Newton-Raphson, or fast separation algorithms can be used [22].

2.2   Introduction to Power Systems Stability

For power systems, stability is a measure of a system ability to remain in or return to a stable state after a disturbance, such as a fault or sudden change in load. This stability depends on the operating condition and the nature of the physical disturbance [4]. Stability analysis aims to understand energy systems' dynamic behavior and ability to withstand and quickly recover from events that deviate from normal operating conditions.

As electricity demand increases and the power grid modernizes to incorporate renewable energy and new consumer demands, the concept of capacity expansion planning becomes more important. This approach aims to intelligently and sustainably improve energy system infrastructure. This includes optimizing the addition of new generation resources, transmission lines, and other infrastructure in line with future demand forecasts. Effective capacity expansion planning maintains power system stability and ensures robustness to accommodate growth and technological change, ensuring reliable power supply for an evolving energy landscape.

According to [23], power system stability is now classified as shown in figure 2.2. Compared to the original classification in [4], two new stability classes have been introduced, which are "converter-driven stability" and "resonant stability." These two new classes were added by the increasing use of converter interfaced generation in power networks [23]. With the addition of power electronics dynamics, the time scale critical for power system stability has been extended downward to electromagnetic transients [23].
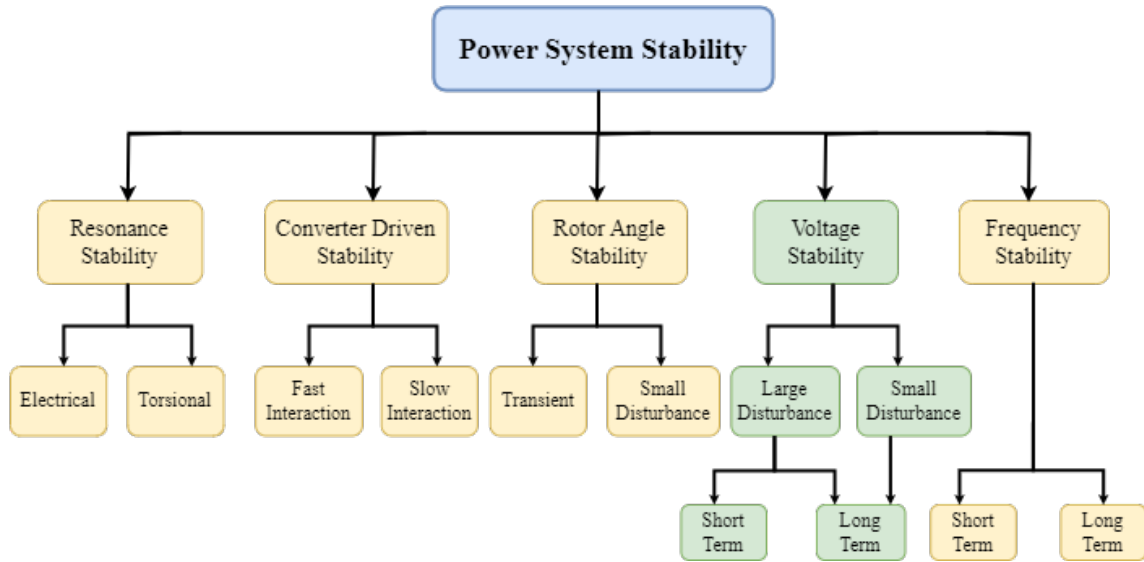
Figure 2.2: Classification of Power System Stability

Classifying power system stability is an effective and practical means of dealing with the complexity of the problem, but the stability of the entire system must always be kept in mind [4].

2.2.1 Voltage Stability in Power Systems

Voltage stability in power systems refers to the ability of a system to maintain steady voltages at all buses in the system after being subjected to a disturbance from a pre-disturbance equilibrium state [4]. This is important for system reliability, especially as demand increases and more power electronic devices are integrated into the grid. Voltage stability depends on the ability of the combined generation and transmission system to supply the electricity demanded by the load in a power network [23, 24]. This capability is limited by the maximum power transfer on a given set of buses and is associated with the voltage drop that occurs when active and/or reactive power flows through the inductive reactance of the power transmission network [23].

Voltage collapse is more complex than voltage stability and refers to voltage instability, leading to power outages or very low voltages in the power grid [25]. Depending on the magnitude of the disturbance, it is classified as a large disturbance or a small disturbance. Large-disturbance voltage stability refers to the ability of a system to maintain steady voltages after a major disturbance such as system faults, circuit contingencies, or power outages [25]. This has a time-frame between zero to about ten seconds. On the other hand, Small disturbance voltage stability is the ability of a system to maintain steady voltages after a small disturbance. These disturbances can also be categorized into short-term and long-term voltage stability.

While short-term voltage stability includes the dynamics of rapidly responding load components such as induction motors, electronically controlled loads, HVDC links, and inverter-based generators, Long-term voltage stability involves low-speed devices such as tap transformers, thermostatically controlled loads, and generator current limiters [23]. Issues with voltage stability can lead to progressive voltage drops, which, if not resolved, may result in a voltage collapse or blackout. Power systems are now equipped with various control mechanisms, such as tap-changing transformers, voltage regulators, and reactive power support from capacitors or generators to avoid such scenarios. The planning and analysis of voltage stability involve detailed modelling of the power system to simulate and understand the behavior of voltages under different loading conditions and to determine the appropriate control actions needed to mitigate any potential instability that can occur.

2.3   Optimal Power Flow

OPF is an optimization concept primarily used in power system operations and planning to determine a power system most efficient, economic, and safe operation under a given set of constraints. In OPF problem, power flow calculation alongside economic dispatch problem are solved simultaneously [26, 27]. The economic dispatch involves allocating generation units to minimize the total operational cost. With the increasing demand for electricity and integration of renewable energy sources, OPF will continue to play a crucial role in maintaining the stability and efficiency of power systems [19, 28]. OPF was initially focused on minimizing fuel costs but has evolved to address other objectives, such as minimizing losses, reducing emissions, and maintaining voltage profiles. As in other optimization problems, the mathematical formulation of the OPF involves three major stages: defining an objective function, setting constraints, and defining a solution technique.

The objective function is a mathematical illustration of the target purpose: cost minimization or even power loss minimization. The constraints include the network's power balance, voltage limits, line flow limits, equipment operating limits, etc. The solution technique then determines the kind of programming or solver to be used. This could be linear programming or a method, nonlinear programming, or heuristic methods. Due to the non-linearity of the power flow equation in AC networks, OPF was initially formulated as a nonlinear, nonconvex optimization problem. Therefore, finding the global optimum for non-linear problems is difficult and computationally intensive [19, 29]. The voltage stability index is integrated into OPF and is used in this thesis to avoid voltage collapse.

2.3.1   AC Optimal Power Flow

AC-OPF simultaneously co-optimizes the active and reactive power dispatch according to the defined operational and physical network constraints to minimize the system operating cost or other objective functions [30]. The AC-OPF formulation is a non-convex, non-linear optimization problem that is known to be non-deterministic and polynomial-time hard [30, 31, 32]. The solution to alternating current power flow involves a system of equations that includes the distribution of both active and reactive power in terms of voltage magnitude and angle and corresponds to Kirchhoff's laws solution [30, 33]. The formulation of the AC-OPF in polar coordinate is as follows [34];

Let i, j be the indices of the buses and Ω_b be the set of all buses. Considering an objective function to minimize the operation cost of the system. The generator cost curves are modelled by quadratic functions, which is expressed as Operation cost (OC);

$$\min \text{OC} = \sum_{i \in \Omega_b} (a_i P_{Gi}^2 + b_i P_{Gi} + c_i)\, USD/h \tag{2.4}$$

Where OC is the total operational cost. The cost coefficients of active power generation at bus i are denoted by a_i, b_i, and c_i, with units USD/MW^2h, USD/MWh, and USD/h respectively. The constraints are described by;

$$P_{G_i} - P_{D_i} = \sum_{j \in \Omega_b} P_{ij} \tag{2.5}$$

$$Q_{G_i} - Q_{D_i} = \sum_{j \in \Omega_b} Q_{ij} \tag{2.6}$$

$$P_{ij} = |V_i|^2 G_{ij} - |V_i||V_j|(G_{ij} \cos \theta_{ij} + B_{ij} \sin \theta_{ij}) \tag{2.7}$$

$$Q_{ij} = -|V_i|^2(B_{ij} + b_{sh_{ij}}) - |V_i||V_j|(G_{ij} \sin \theta_{ij} - B_{ij} \cos \theta_{ij}) \tag{2.8}$$

$$P_{G_i}^{\min} \leq P_{G_i} \leq P_{G_i}^{\max} \tag{2.9}$$

$$Q_{G_i}^{\min} \leq Q_{G_i} \leq Q_{G_i}^{\max} \tag{2.10}$$

$$(P_{ij})^2 + (Q_{ij})^2 \leq (S_{ij}^{\max})^2 \tag{2.11}$$

$$|V_i|^{\min} \leq |V_i| \leq |V_i|^{\max} \tag{2.12}$$

$$\theta_{ij}^{\min} \leq \theta_{ij} \leq \theta_{ij}^{\max} \tag{2.13}$$

Where P_{Gi} and Q_{Gi} are the active and reactive power generations at the bus i respectively. P_{Di} and Q_{Di} are the active and reactive power demand at bus i respectively. Equation (2.5) and Equation (2.6) represent active and reactive power flows across line ij respectively. G_{ij} and B_{ij} are the transfer conductance and susceptance between the buses i and j respectively. The phase angle difference between the voltages at buses i and j is θ_{ij}. Equation (2.9) and Equation (2.10) are the generation limits of each generator in any network. Equation (2.11) applies the transmission lines' thermal limit to the optimal power flow. Equation (2.12)

ensures that the bus voltages are within a certain limit. Equation (2.13) imposes the voltage angle limitation at the nodes.

2.3.2 DC Optimal Power Flow

The DC-OPF is a linear simplification of AC-OPF that only considers real power and ignores reactive power dispatch. This linear problem is convex and ensures that the local optimum is a global optimum. DC-OPF is fast and, as a result, employed in solving large problems. The linearity of DC-OPF is achieved through several assumptions [35];

- The ratio of the reactance to the resistance of a line should be large enough that the resistance can be neglected.

- The magnitudes of the voltage are assumed to be 1pu.

- Voltage angle differences are small

The optimization problem of the DC-OPF is the same for AC-OPF as given in Equation (2.4). However, some of the constraints are modified as follows [35];

$$P_{ij} = \frac{\delta_i - \delta_j}{x_{ij}} \quad \forall ij \in \Omega_l \tag{2.14}$$

$$P_{G_i} - P_{D_i} = \sum_{j \in \Omega_b} P_{ij} \tag{2.15}$$

$$-P_{ij}^{\max} \le P_{ij} \le P_{ij}^{\max} \quad \forall ij \in \Omega_l \tag{2.16}$$

$$P_{G_i}^{\min} \le P_{G_i} \le P_{G_i}^{\max} \tag{2.17}$$

From the above relations, Equation (2.14) corresponds to the DC power flow linearization, in which the active power flow across every line is equivalent to the ratio of the difference in the voltage angle to the reactance across the line connecting bus i and j. Equation (2.15) is equivalent to the Equation (2.5) from the AC-OPF. Here, the bus power balance at each bus i is related to Kirchhoff's Current Law, indicating that the difference between power generation and the power demand at a node must be equal to the power drawn by each of the branches [29].Equation (2.16) gives the active power flow limits for each branch. Constraint (2.17) is the same with the (2.9) in the AC-OPF, which shows the maximum and minimum limits for the generation of power at each generator. The technical terms in DC-OPF modelling are all linear, which makes it an important concept in power system analysis. The cost function is the only nonlinear part. However, this tool does not give the actual voltage and reactive power at the different sections of the system.

2.4 Capacity Expansion Planning (CEP)

Capacity Expansion Planning CEP involves making decisions about new generation plants and transmission systems based on prescribed future demands. OPF plays a key role here, providing detailed insights into current operational constraints and grid efficiency. Understanding the optimal flow of power under current conditions allows planners and researchers to understand where additional capacity is needed and what investments (new power plants, transmission lines, technology upgrades, etc.) will yield the most cost-effective and reliable improvements without compromising the system stability [36]. This process ensures that the expansion is not only economically sound but also aligns with the technical capabilities and constraints of the existing network, thereby facilitating a more robust and efficient power system in the long run. The common types of capacity expansion planning in power systems are Generation Expansion Planning (GEP), Transmission Expansion Planning (TEP), and Storage Expansion Planning (SEP). However, this work focuses on GEP.

2.4.1 Generation Expansion Planning

Generation Expansion Planning makes decisions about future investments in generation mix to maintain an appropriate margin between demand and supply, considering future power demand and potential changes in the transmission system network [37]. GEP aims to effectively determine the type, size and timing of construction of new power plants over some time. Usually, GEP is considered as a dynamic or multi-stage planning due to the study period. To carry out a GEP, it is formulated as an optimization problem where objective functions and constraints have been well defined [38].

In the past, the objective functions have been centered around investment cost, operation and maintenance, and fuel cost due to the conventional nature of most power plants. However, the impact of global warming and the various government carbon policies have resulted in adding emission tax into the objective function [38]. Also, more conversion systems for renewable sources are now integrated into the grid to offer an alternative to carbon emissions by conventional plants. In generation expansion planning modelling, the objective function is to minimize the total planned cost, including capital costs for new generation units, variable and fixed operating and maintenance costs for new generation units, annual fuel costs for existing and new generation units and environmental cost for the different planning year [39, 38, 40]. The Generation Expansion Planning Objective Function (GEP OF) model is given as shown in equation (2.18);

$$\text{GEP OF} = \min \sum_{t \in T}(C_{I,t} + C_{OM,t} + C_{F,t} + C_{E,t}) \qquad (2.18)$$

Where T is the planning year, $C_{I,t}$, $C_{OM,t}$, $C_{F,t}$ and $C_{E,t}$ are the capital cost, operation and maintenance cost $(O\&M)$, fuel cost, and environmental cost, respectively, in year t

[40]. To achieve an optimal expansion solution, sets of technical and economic constraints are considered in the model, including capacity limit, power balances, and environmental constraints.

2.4.2 Method for Modelling GEP

Equation (2.18) gives the objective function relation for modelling generation expansion planning. The relations of the individual components of capital cost (or investment cost) $(C_{I,t})$, operation and maintenance cost $(C_{OM,t})$, fuel cost $(C_{f,t})$ and environmental cost $(C_{E,t})$ are given by [40] for modelling;

$$C_{I,t} = \sum_{g \in G} \sum_{i \in g} c_{t,g,i}^{new} X_{t,g,i}^{new} \tag{2.19}$$

$$C_{OM,t} = \sum_{g \in G} \sum_{i \in g} \left(PG_{t,g,i}^{fixed} X_{t,g,i} + PG_{t,g,i}^{var} X_{t,g,i} \right) \tag{2.20}$$

$$C_{F,t} = \sum_{g \in G} \sum_{i \in g} FL_{t,g,i} E_{t,g,i} \tag{2.21}$$

$$C_{E,t} = \sum_{g \in G} \sum_{i \in g} (c_{t,g,i}^{carbon} E_{t,g,i}) \tag{2.22}$$

Here, G represents the set of generation sources. The terms $X_{t,g,i}^{new}$ and $X_{t,g,i}$ refer to the newly installed capacity and the total installed capacity, respectively, for a specific unit i within the generation source type g in a specified year t [40]. The capital cost for each capacity of unit i in generation type g during year t is denoted by $c_{t,g,i}^{new}$. Additionally, $PG_{t,g,i}^{fixed}$ and $PG_{t,g,i}^{var}$ represent the fixed and variable operation and maintenance costs per unit capacity and per kilowatt hour, respectively, for the same unit and generation type. The cost of fuel per kilowatt hour for each unit in power supply type g during year t is indicated by $FL_{t,g,i}$. The costs associated with carbon emissions for the same unit, power supply type, and year is given by $c_{t,g,i}^{carbon}$ [40]. The annual power generation for unit i in generation type g during year t is expressed as $E_{t,g,i} = H_{t,g,i} \cdot X_{t,g,i}$, where $H_{t,g,i}$ stands for the annual utilization hours for that unit [40]. Key constraints considered in the model include;

$$X_{t-1,g,i}^{new} \leq X_{t,g,i}^{new} \tag{2.23}$$

Constraint (2.23) maintains the installation status of the generation unit, which can be either a conventional generator or a wind turbine.

$$0 \leq PG_{t,g,i} \leq PG_{g,i}^{max} \times X_{t,g,i} \tag{2.24}$$

Constraint (2.24) gives the technical characteristics of the generators. The optimal power flow constraints are the same as in (2.5) - (2.13).

2.4.3 Transmission Expansion Planning

Transmission Expansion Planning aims to identify various assets such as overhead lines, submarine cables, transformers, and other line components to be installed in the network, taking into account a long-term expansion planning horizon for the power network [41]. TEP can be classified as static or dynamic planning depending on the treatment of the study period. A static TEP assumes that system enhancements are implemented immediately and at a single point in the future, whereas the dynamic TEP considers dividing the planning period into several years or the planning horizon into several hours. Although, in dynamic TEP, the enormous computational effort is required to achieve an optimal solution, the method provides economically efficient solutions [42]. Most of the TEP issues involve minimizing the capital cost of installing additional transmission lines under power system conditions, such as voltage limits, line currents, and generator production limits [43].

2.5 Grid Stability Analysis Techniques

During grid studies, various techniques that are crucial for ensuring the reliability and robustness of power systems are carried out. These techniques are used to analyze network behavior under different conditions and plan scenarios that could potentially lead to instability. As capacity expansion planning proceeds, it is crucial to maintain the continuous stability of the network, which is why analysis techniques such as load flow analysis, dynamic stability analysis, voltage stability analysis, frequency response analysis, contingency analysis, statistical and probabilistic analysis, and harmonic analysis are employed. This thesis focuses on optimal power flow, voltage stability analysis, dynamic stability, and contingency analysis to ensure system stability during capacity expansion planning.

2.5.1 Voltage Stability Indices

Voltage Stability Indices (VSIs) are used to determine whether a system is stable and how close the system is to instability or collapse. As earlier stated, many methods have been proposed in the literature to study voltage stability in power systems. According to [15, 44], VSIs can be grouped into four types which are bus variables based-indices, line variables based-indices, jacobian matrix-based indices and Phasor Measurement Units (PMU) based indices. Line Voltage Stability Index (LVSI) are line variable-based indices used to determine power systems' weak buses and critical lines and are particularly useful in evaluating the voltage stability of lines and buses [15]. This line-based index can be employed in optimization problems to determine regions with weak buses and lines, which makes it useful for consideration during capacity expansion planning. The different types of line variables-based indices are classified as follows. Considering the two-node network,
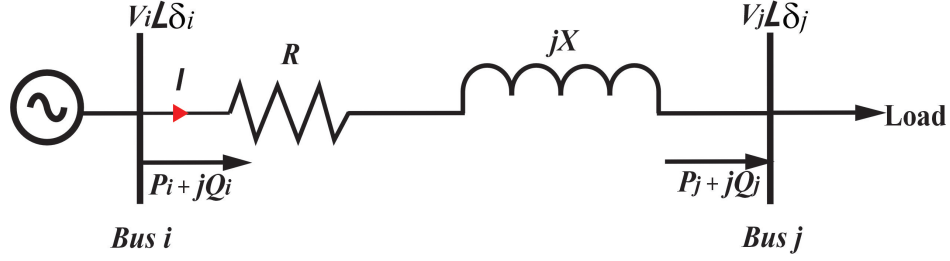
Figure 2.3: Single line diagram of generator-power transmission line- load

Where; V_i = Sending voltage magnitude, P_i = Sending active power, Q_i = Sending reactive power, δ_i = Sending voltage angle, I = Transmission line current, R = Resistance of the transmission line, X = Reactance of the transmission line, Z = Impedance of the transmission line, θ = Impedance angle, V_j = Receiving voltage magnitude, P_j = Receiving active power, Q_j = Receiving reactive power, δ_j = Receiving voltage angle, δ = The difference between the sending and receiving voltage angles.

1. Line Stability Index (Lmn) [45] derived the line stability index Lmn concept based on a power transmission concept in a single line. The stability index is defined as in (2.25);

$$\text{Lmn} = \frac{4XQ_j}{(V_i \sin(\theta - \delta))^2} \leq 1 \tag{2.25}$$

The limitation of this index is that it neglects shunt admittance and real power effect. Hence cannot predict voltage collapse at very high real or apparent power loads [15]. Considering power flow calculation, the system is said to be stable when the index is less than or equal to 1.

2. Line Stability Factor (LQP) The line stability factor is given by [14] using a single power transmission line analysis;

$$\text{LQP} = 4 \left(\frac{X}{V_i^2} \left(\frac{P_i^2 X}{V_i^2} + Q_i \right) \right) \leq 1 \tag{2.26}$$

In this index, the line is considered lossless and there is no relative direction of power flow. Also, The system is said to be stable when the line stability factor is less than or equal to 1.

3. Fast Voltage Stability Index (FVSI) Fast Voltage Stability Index, proposed by [11], can be used to determine voltage collapse on a line. FVSI is given as in (2.27)

$$\text{FVSI} = \frac{4Z^2 Q_i}{V_i^2 X} \leq 1 \tag{2.27}$$

This voltage stability index is less accurate because it ignores key line parameters such as the active power variations and angle differences.

4. Novel Collapse Prediction Index (NCPI) The Novel Collapse Prediction Index is an improved version of FVSI. This index partially ignores the resistance of the power transmission line while considering the influence of active and reactive power flows on the

15

voltage stability of the system. As modelled by [15], NCPI considers the receiving end reactive power magnitude and the relative direction of active and reactive power flow. NCPI is given by (2.27)

$$\text{NCPI} = \frac{4Z^2}{XV_i^2} \left(\frac{Z^2 P_j^2}{XV_i^2} + |Q_i| \right) \leq 1 \tag{2.28}$$

5. Voltage Collapse Proximity Indicator (VCPI) The Voltage Collapse Proximity Indicator is based on the concept of maximum power transmitted over the lines in a network. VCPI can be used to determine weak buses in a network or predict voltage collapse in a line. The VCPI index is simple and flexible for real-time simulation and simulation of all kinds of topology and load changes in the network [46]. VCPI is defined by;

$$\text{VCPI(power)} = \frac{P_j}{P_{j(\text{max})}} = \frac{Q_j}{Q_{j(\text{max})}} \tag{2.29}$$

where $P_{j(max)}$ and $Q_{j(max)}$ are given by

$$P_{j(\text{max})} = \frac{V_i^2}{Z_i} \frac{\cos \phi}{4 \cos^2 \left(\frac{\theta - \phi}{2} \right)} \tag{2.30}$$

$$Q_{j(\text{max})} = \frac{V_i^2}{Z_i} \frac{\sin \phi}{4 \cos^2 \left(\frac{\theta - \phi}{2} \right)} \tag{2.31}$$

The VCPI(power) is said to be the ratio of the real power transferred to the receiving end to the maximum real power that can be transferred. The system is said to be stable when the indices value is less than or equal to unity when solving a load flow problem.

It is important to emphasize that all the indices for line voltage stability are grounded in identical theoretical principles, with the only variation stemming from the specific assumptions applied in each of the index [15, 44, 47, 48].In the case of Lmn formulation, it ignores the effect of active power and shunt admittance, making it fail to predict collapse in high active or apparent power loading situations. For LQP, lines are considered losses, which is unrealistic and pays no attention to relative direction power flow [15]. FVSI does not account for active power variation, angle difference, and shunt admittance. In the case of NCPI, it partially ignores the resistance of the transmission lines. VCPI, on the other hand, includes all the parameters directly affecting voltage stability, including line impedance magnitude and angle, active and reactive power, voltage at the sending bus, active power flow across the transmission line, and the load impedance phase angle. All these parameters embedded into the VCPI makes it a robust tool for determining how close a system is to instability.

2.5.2   Derivation of Voltage Collapse Proximity Indicator

Using the concept described in [49] to model the line diagram in figure 2.3 above, the single transmission line model in Figure 2.4 is obtained;
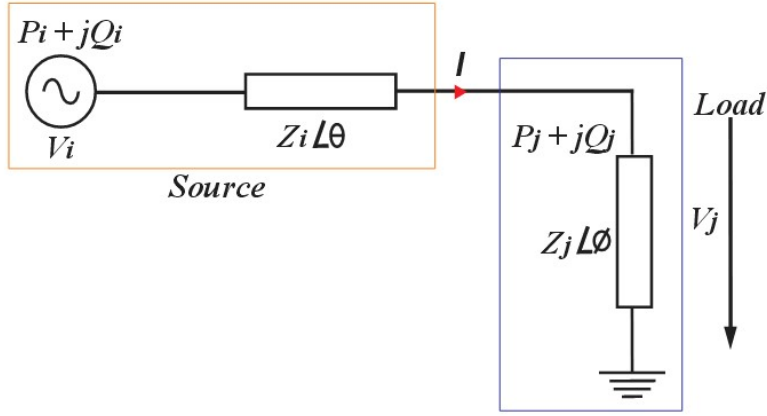
Figure 2.4: Single Transmission Line Model

Where V_i is the sending end voltage, V_j is the receiving end voltage, θ is the line impedance angle, $Z_i \angle \theta$ is the line impedance, $Z_L \angle \phi$ is the corresponding load impedance, and $\phi = \tan^{-1}(Q/P)$ is the phase angle of the load impedance.

The VCPI index is based on the concept of the maximum power transferred on the transmission lines of the network, as illustrated in figure 2.4. Here, it is assumed that the load carried by the line is considered the power delivered exclusively through that line at its receiving end instead of being viewed as the total load at the node [13].

Considering a typical scenario where the phase angle ϕ of the load impedance remains unchanged, but its magnitude fluctuates[13, 49]. It is common to maintain a constant power factor in the electrical system. As the load increases, the magnitude of the load impedance Z_L decreases, and the current in the system increases, resulting in a voltage drop at the receiving point of the load [13, 49]. Thus, the voltage present at the load terminal decreases;

$$I = \frac{V_i}{\sqrt{(Z_i \cos \theta + Z_j \cos \phi)^2 + (Z_i \sin \theta + Z_j \sin \phi)^2}} \tag{2.32}$$

$$V_j = Z_j * I = \frac{Z_j}{Z_i} \frac{V_i}{\sqrt{1 + (Z_j/Z_i)^2 + 2(Z_j/Z_i)\cos(\theta - \phi)}} \tag{2.33}$$

Thus, the active and the reactive power at the receiving end of the transmission line is given as;

Receiving Active Power P_j;

$$P_j = V_j I \cos \phi \tag{2.34}$$

Receiving Reactive Power Q_j;

$$Q_j = V_j I \sin \phi \tag{2.35}$$

Substituting Equations (2.32) and (2.33) into (2.34), the receiving end active power can be written as;

$$P_j = \frac{(V_i)^2/Z_i}{1 + (Z_j/Z_i)^2 + 2(Z_j/Z_i)\cos(\theta - \phi)} \frac{Z_j}{Z_i} \cos \phi \tag{2.36}$$

17

Also, substituting Equations (2.32) and (2.33) into (2.35), the receiving end reactive power can be written as;

$$Q_j = \frac{(V_i)^2/Z_i}{1 + (Z_j/Z_i)^2 + 2(Z_j/Z_i)\cos(\theta - \phi)} \frac{Z_j}{Z_i} \sin\phi \tag{2.37}$$

In a similar manner, the losses of the power lines can be computed [13]; Active power loss P_{loss};

$$P_{loss} = I^2 Z_i \cos\theta \tag{2.38}$$

Reactive power loss Q_{loss};

$$Q_{loss} = I^2 Z_i \sin\theta \tag{2.39}$$

Substituting Equation (2.32) into (2.38) and (2.38), the losses can be written as;

$$P_{loss} = \left(\frac{V_i}{Z_i}\right)^2 \frac{1 + (Z_j/Z_i)^2 + 2(Z_j/Z_i)\cos(\theta - \phi)}{Z_i \cos\theta} \cos\phi \tag{2.40}$$

$$Q_{loss} = \left(\frac{V_i}{Z_i}\right)^2 \frac{1 + (Z_j/Z_i)^2 + 2(Z_j/Z_i)\cos(\theta - \phi)}{Z_i \cos\theta} \sin\phi \tag{2.41}$$

According to [49], maximum power transferred to the load is obtained when $\frac{\partial P}{\partial Z_L} = 0$, which corresponds to $Z_L/Z_i = 1$. Thus, $Z_L = Z_i$. Substituting $Z_L = Z_i$ in (2.34), the maximum transferable power P_{max} can be deduced as follows:

$$P_{j(max)} = \frac{V_i^2}{Z_i 4\cos^2\left(\frac{\theta - \phi}{2}\right)} \cos\phi \tag{2.42}$$

In a similar way, the maximum transferable reactive power Q_{max}, maximum power losses $P_{(loss)max}$ and $Q_{(loss)max}$ are obtained in the following expressions:

$$Q_{j(max)} = \frac{V_i^2}{Z_i 4\cos^2\left(\frac{\theta - \phi}{2}\right)} \sin\phi \tag{2.43}$$

$$P_{loss(max)} = \frac{V_i^2}{Z_i 4\cos^2\left(\frac{\theta - \phi}{2}\right)} \sin\theta \tag{2.44}$$

$$Q_{loss(max)} = \frac{V_i^2}{Z_i 4\cos^2\left(\frac{\theta - \phi}{2}\right)} \sin\theta \tag{2.45}$$

Taking into account the established upper limits for these parameters, the Voltage Collapse Proximity Indicators are derived as given in the following equations:

$$VCPI(activepower) = \frac{P_j}{P_{j(max)}} \tag{2.46}$$

$$VCPI(reactivepower) = \frac{Q_j}{Q_{j(max)}} \tag{2.47}$$

$$VCPI(activepowerloss) = \frac{P_{loss}}{P_{(loss)max}} \tag{2.48}$$

$$VCPI(reactivepowerloss) = \frac{Q_{loss}}{Q_{(loss)max}} \tag{2.49}$$

[13] showed that through experimental results the active power VCPI and reactive power VCPI are equivalent. Similarly, the two losses are equivalent. As a result, the VCPI equations are reduced to two as follows:

$$VCPI(power) = \frac{P_j}{\frac{V_i^2}{Z_i 4\cos^2\left(\frac{\theta-\phi}{2}\right)}\cos\phi} \tag{2.50}$$

$$VCPI(powerloss) = \frac{P_{loss}}{\frac{V_i^2}{Z_i 4\cos^2\left(\frac{\theta-\phi}{2}\right)}\sin\theta} \tag{2.51}$$

Conventional power flow calculations are used to get the values of P_j, Q_j, $P_{j(max)}$, and $Q_{j(max)}$ [13]. For this thesis, VCPI (power) is implemented alongside the capacity expansion model.

2.6 Particle Swarm Optimization

Particle Swarm Optimization (PSO) is a collective stochastic optimization technique based on a population search algorithm. In 1995, Kennedy and Eberhart introduced particle swarm optimization, an intelligent heuristic optimization algorithm that has since surpassed the genetic algorithm in certain applications [50, 51]. In PSO, the potential solutions known as particles navigate the solution space by tracking the particles flight that presently represent the optimal solutions. Moreso, during the flight duration, particles can utilize their knowledge of flight and the collective flight patterns of the group to adjust themselves accordingly [52]. As a result, the optimal solution can now be reached after multiple iterations. PSO algorithms are of two types, namely, global PSO (GPSO) and local PSO (LPSO) [50, 53, 54]. While GPSO focuses solely on finding the optimal global solution, LPSO methods are tailored for practical optimization tasks requiring multiple global solutions [50, 55]. The equations for the position and velocity of a particle are provided as follows [50].

$$X(t) = X(t-1) + V(t) \tag{2.52}$$

$$V(t) = V(t-1) + C_1 \cdot r_1 \cdot (p_{\text{best}} - X(t-1)) + C_2 \cdot r_2 \cdot (g_{\text{best}} - X(t-1)) \tag{2.53}$$

Where, $X(t)$ is the particle position. $V(t)$ is the particle velocity. G_{best} is the global best. P_{best} is the personal best. r_1 and r_2 are two random numbers in the interval of $(0, 1)$ with uniform distribution. C_1 and C_2 are the coefficients of accelerated particles. $V(t-1)$ is the inertial weight of the particle. Figure 2.5 illustrates the flowchart of PSO algorithm [50].
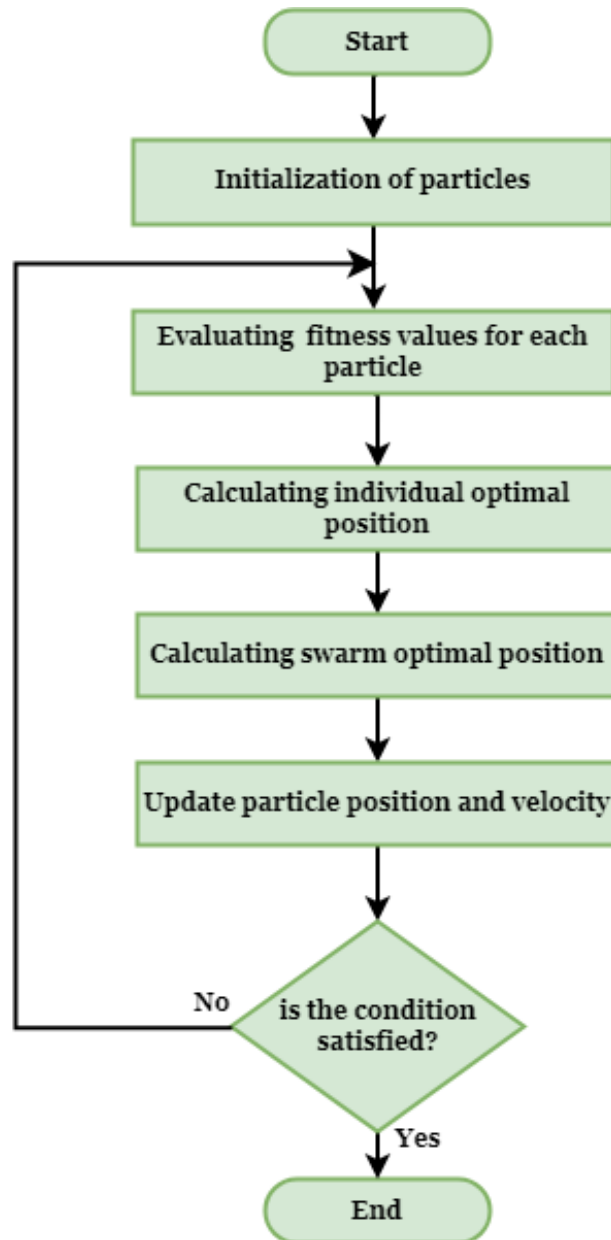
Figure 2.5: Flowchart of PSO algorithm

Chapter 3

Methodology

This chapter describes the methodology employed to achieve the research objectives outlined in this thesis, which entails the implementation of voltage stability modelling during capacity expansion planning in REMix. The process encompasses five significant steps. The first step involves developing and implementing a DC-OPF capacity expansion planning model in REMix environment and an AC-OPF model in the supporting software. This thesis uses Matlab as supporting software to compute more detailed network parameters to study voltage stability and carry out capacity expansion planning. The resulting MATLAB model is the "supporting model" or "validation model". The second step involves defining voltage stability within the context of this thesis. Different voltage stability indices exist, and the one that gives the earliest prediction when a line is close to collapse is applied for this work. The next step entails algorithm development for voltage security constrained optimal power flow VSC-OPF, in which the VSC-OPF is developed in the supporting model to determine specific parameters for the REMix model. The fourth step involves adapting the GEP model to include the proposed VSC-OPF algorithm to enhance the voltage stability while optimizing the system cost. The last step involves defining two different generation expansion planning GEP case studies consisting of four scenarios for a standard IEEE RTS 24-bus network. The proposed models are validated to ensure voltage stability during GEP modelling in REMix. Figure 3.1 shows the schematic representation of this thesis.

01	02	03	04	05
Model topology and OPF for generic power system network	Defining voltage stability for the thesis	Voltage security constrained optimal power flow algorithm development (VSC-OPF)	Integration of GEP model with VSC-OPF	2 GEP Case Studies and Validation
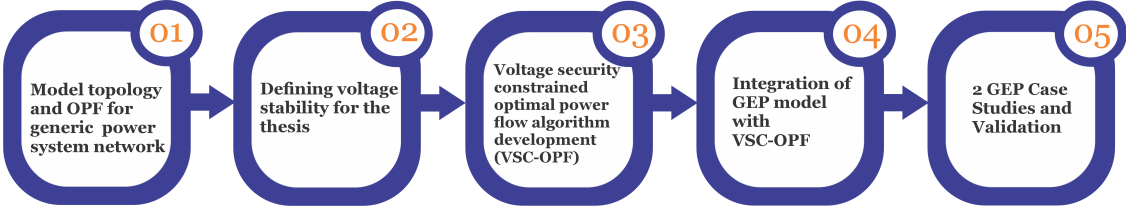
Figure 3.1: Project Methodology

3.1 REMix Tool

REMix is an acronym for "Renewable Energy Mix for a Sustainable Energy Supply". It is a modelling framework developed at the DLR and involves a set of linear optimization models written in GAMS. It is a collection of compatible source codes needed for a particular model. These source codes can be combined modularly, allowing users to reuse the same modelling concepts and associated source codes to address different content focuses. This approach is based on a common set of available model features. Most interesting to know that REMix is developed for studies in the field of energy system modelling. Figure 3.2 from [56] gives the way the model developed by REMix can be categorized.
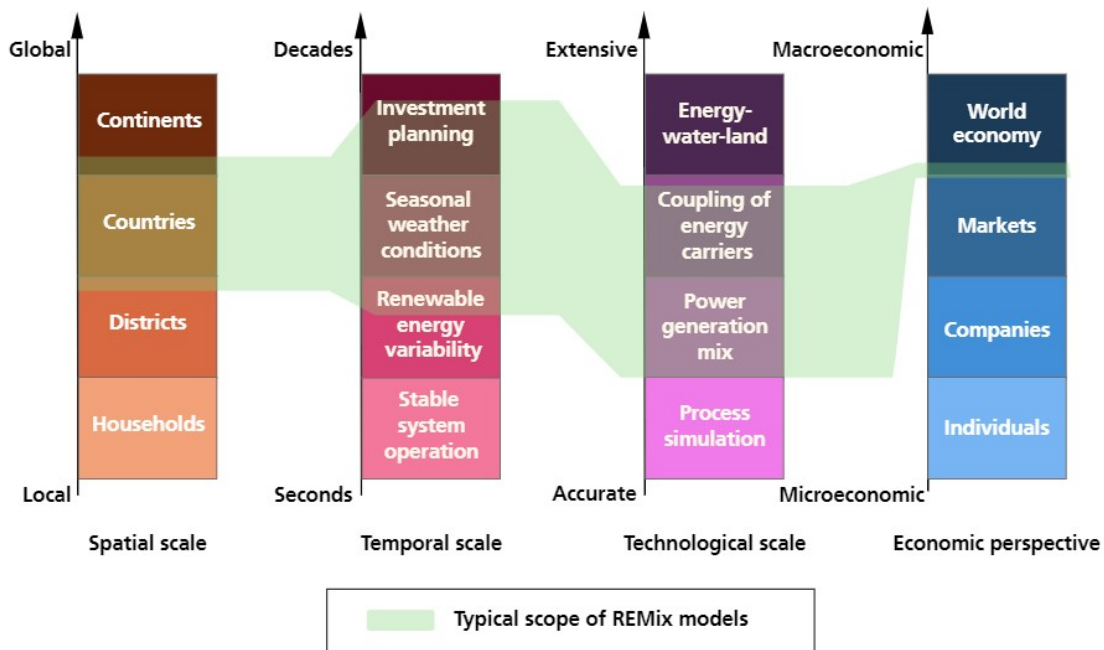
Figure 3.2: REMix Models [56]

3.1.1 Modelling concept in REMix

The data structure in REMix is usually based on technological, geographical and temporal domains. This modelling framework follows a feature-centric approach in the optimization of energy systems [17], consisting of different blocks such as conversion, transport, storage, sources, and sinks. The key parts of this model are the commodity and indicator. The development of REMix has considered using large models with multi-year analysis of energy systems [17]. This means high spatial and technological resolutions are intended in modelling. Figure 3.3 shows a comprehensive structure of REMix modelling.
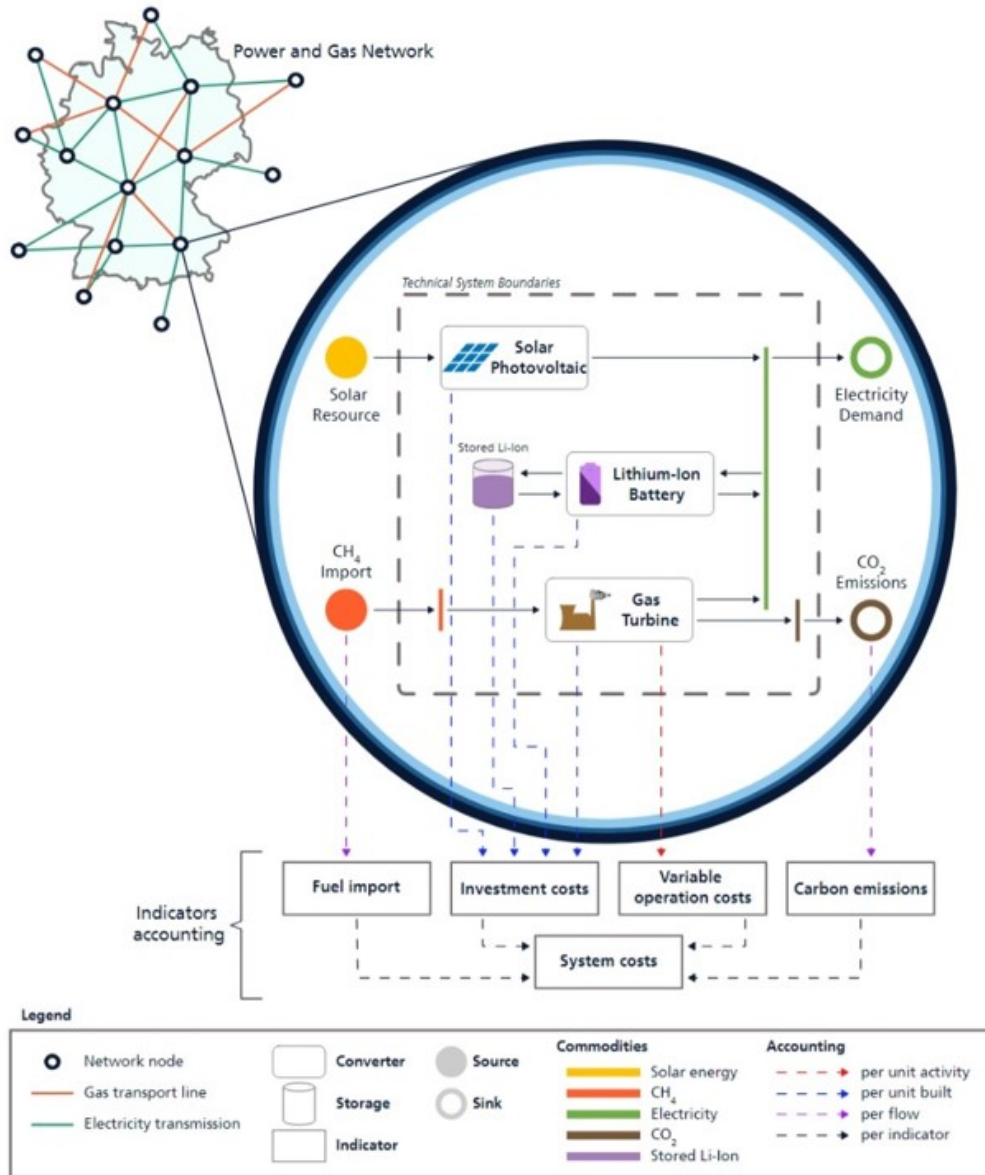
Figure 3.3: Comprehensive structure of a REMix model [57]

3.1.1.1 Commodities

Commodities are energy carriers such as fuels, electricity or heat. Sources and sinks must be specified for every commodity in the model. They are moved between system nodes by transport technologies defined in the model [57].

3.1.1.2 Indicators

Indicators are used for accounting purposes; examples include costs, carbon, capacities, etc. Depending on the model, indicators can be accounted for in a single or multiple-year period [19]. In a similar way, indicators can be evaluated at the level of individual model nodes, at a global level, or based on custom regions [57].

3.1.2 REMix Modules

REMix uses modules divided into three categories: core, framework, and methods. The framework modules provide a basic structure to the model. They do this by calling the model definitions of all the core modules and incorporating the solving methods files [19].

3.1.2.1 Converter

Converters are technologies that convert commodities into other commodities within a node of the model. Their technical characteristics are considered and processed by the core_converter modules, and the core_accounting module takes in the economic parameters as inputs. The conversion activities related to the converters determine the relationships between input and output commodities [57]. Different converters are considered in REMix, including photovoltaic systems, wind turbines, and conventional power generators, among others.

3.1.2.2 Transport

The transport modules are used for commodities exchange between one region of the model to another. They can be facilitated in either a unidirectional or bidirectional manner [57]. During modelling, the capacity for commodity transportation is determined by the constraints on flow and the dimensions of the transport unit, which may either be pre-existing or constructed newly. Moreover, every commodity transported is defined along with its technical specifications, including maximum rated capacity, transmission line, and electrical reactance.

3.1.2.3 Storage technology

This technology allows a commodity to be stored for a given time and released when required. Usually, storage technology is designed to charge during periods with abundant generation and discharge when generation is low.

3.1.2.4 Sources and Sinks

In the modelling of commodity flow from the start region to the end region within a network, sources and sinks are utilized. Sources provide commodities at specific nodes required. Sinks consume the commodities carried by transport technologies. Every commodity defined in the model must have a corresponding sink.

3.1.2.5 Accounting

The parameters in the accounting module describe all the accounting indicators in the model. The objective function is specified by the user and in accordance with the indicators. When

an objective function is to be minimized or maximized, it is done in the core_accounting module. A positive unity means maximization and a negative unity indicates a minimization of an objective function.

3.1.2.6 Balance

This describes the commodity balancing in the model in each time, region, or node of the systems and year specified. This module ensures that all system demands are met at all times and in all regions of the model [19].

3.2 MATLAB

MATPOWER is one of the packages of MATLAB software for solving power flow and optimal power flow problems. It effectively utilizes the robust numerical computing capabilities of the MATLAB language, particularly in matrix operations. This significantly reduces the amount of programming code required and enhances operational efficiency [58]. In modelling with MATPOWER, it utilizes all the conventional steady-state models commonly applied in power flow analysis. For this thesis, MATPOWER is first integrated into the modelling of the project to determine additional network parameters needed for the capacity expansion planning in the REMix model [59]. However, particle swarm optimization is implemented in solving the optimal power flow when additional voltage constraints are to be used. The particle swarm optimization solver allows easy integration of the voltage stability index into the modelling framework to examine the voltage stability of the system during capacity expansion planning.

3.2.1 Modelling with MATPOWER

In the course of this thesis, MATPOWER is used in calculating various network parameters.

3.2.1.1 runpf

In MATPOWER, executing a power flow involves using the `runpf` function and providing a case struct or case file name as the initial argument [60]. Here, the casedata is replaced by IEEE24 bus system data in accordance with the proposed model in REMix. Typically, the `runpf` solves AC power flow using the Newton Raphson's method.

```
results = runpf(casedata, mpopt, fname, solvedcase);
```

After executing the `runpf`, the result information consists of the following, which are part of the algorithm utilized in computing voltage stability line indices;

Table 3.1: runpf Results Information [60]

Name	Description
results.success	Success flag, 1 = succeeded, 0 = failed
results.et	Computation time required for solution
results.iterations	Number of iterations required for solution
results.bus(:, VM)*	Bus voltage magnitudes
results.bus(:, VA)	Bus voltage angles
results.gen(:, PG)	Generator real power injections
results.gen(:, QG)*	Generator reactive power injections
results.branch(:, PF)	Real power injected into "from" end of branch
results.branch(:, PT)	Real power injected into "to" end of branch
results.branch(:, QF)*	Reactive power injected into "from" end of branch
results.branch(:, QT)*	Reactive power injected into "to" end of branch
*AC power flow only.	

results.success is used to determine at what point there exists convergence of the power flow.

3.2.1.2   runopf

runopf executes optimal power flow with a case struct or case filename as the first argument [60]. The result structure here is similar to the runpf.

```
results = runopf(casedata, mpopt, fname, solvedcase);
```

One notable addition to the result information given by the runopf is the results.f, which is the final objective function value of the model. The objective function is expected to be similar to the indicator_accounting_detailed result in REMix for the same modelling task in the two environments.

3.3   Model Topology and OPF for Generic Network

A generic power system network is modelled, and data for the systems are imported into the modelling environment of both REMix and the supporting software. DC-OPF computation are carried out in the REMix environments and both DC-OPF and AC-OPF are executed in the supporting tool.

3.3.1 The Model Topology

The standard network topology selected for this study, the IEEE Reliability Test System (RTS) 24-bus network, is depicted in figure 3.4 through its single-line diagram. This IEEE-24 system features 34 branches, 12 generators, 17 loads, and 24 buses. However, during capacity expansion planning, more generators or branches are added to the network depending on the extent of the expansion in a given time frame.
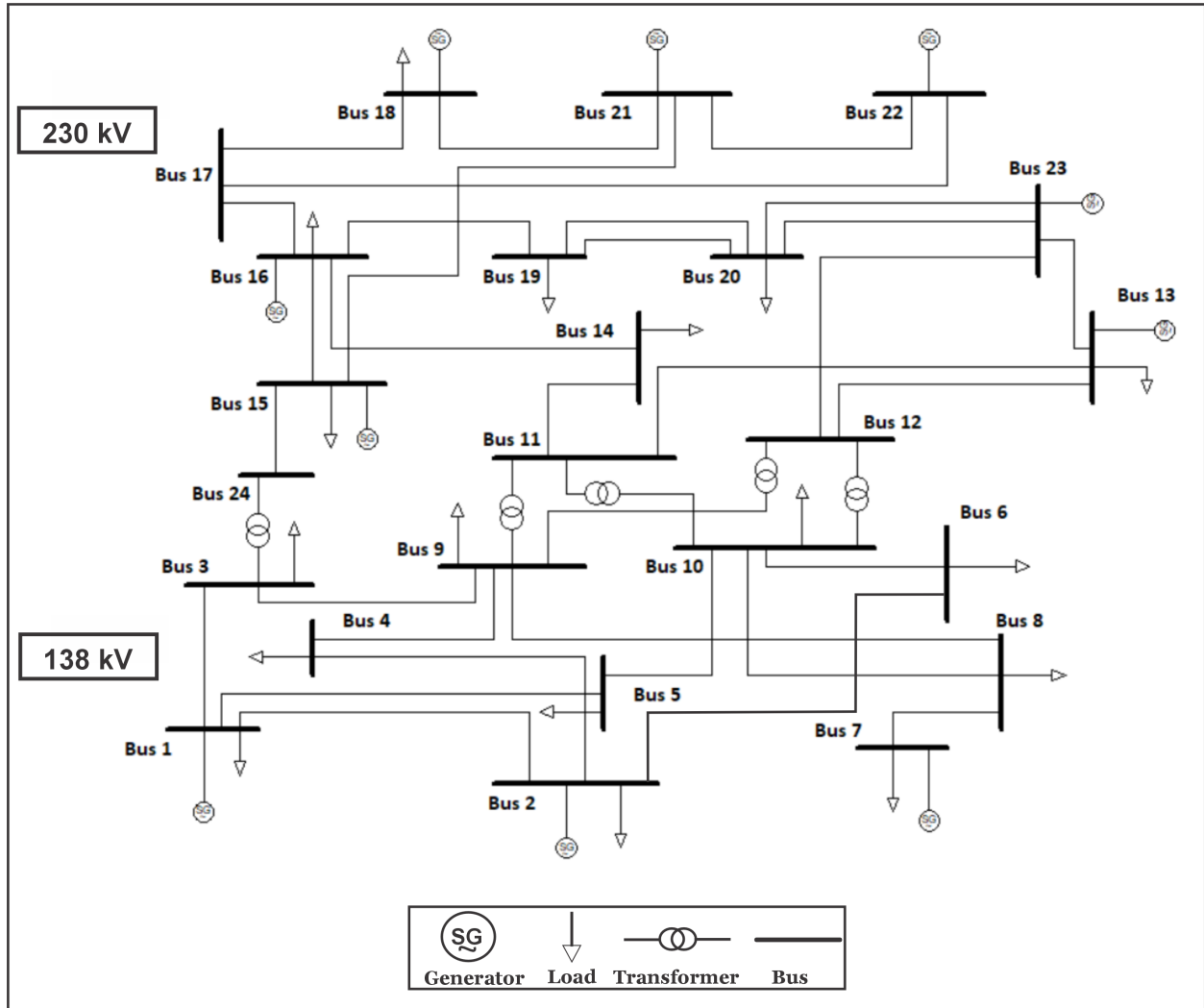
Figure 3.4: Single line diagram of IEEE RTS 24-bus system

In this network, Bus 13 is taken as the slack bus. The generation, transmission, and load data are presented in Appendix A as sourced from [35]. For the base case scenario, the network's total load amounts to 2850 MW. The magnitude and location of each load in the base case are indicated in Table A3. The transmission lines in this network operate at two different voltage levels, 138 kV and 230 kV, with a base power of 100 MVA. The 230 kV lines interconnect with the 138 kV system at tie stations located at buses 11, 12, and 24. Details about the branch parameters are provided in Table A2. Wind turbines are implemented

for the expansion planning involving the integration of a renewable energy source into the model. The wind turbines implemented data are sourced from [61]. A 300 MW wind power plant profile is imported into the model as given in Table A4.

3.3.2 DC-OPF in the REMix Model

To use the REMix framework for running a DC-OPF model, it is important to have data input files in the form of (.*dat*) format. These files are configured in the format in which the REMix framework understands. For this thesis, the IEEE 24 RTS 24-bus system parameters are set up alongside the various technical, economic, and environmental parameters defined for the model in Python. The significant steps involved in preparing the .dat files and running the model are as shown in figure 3.5;
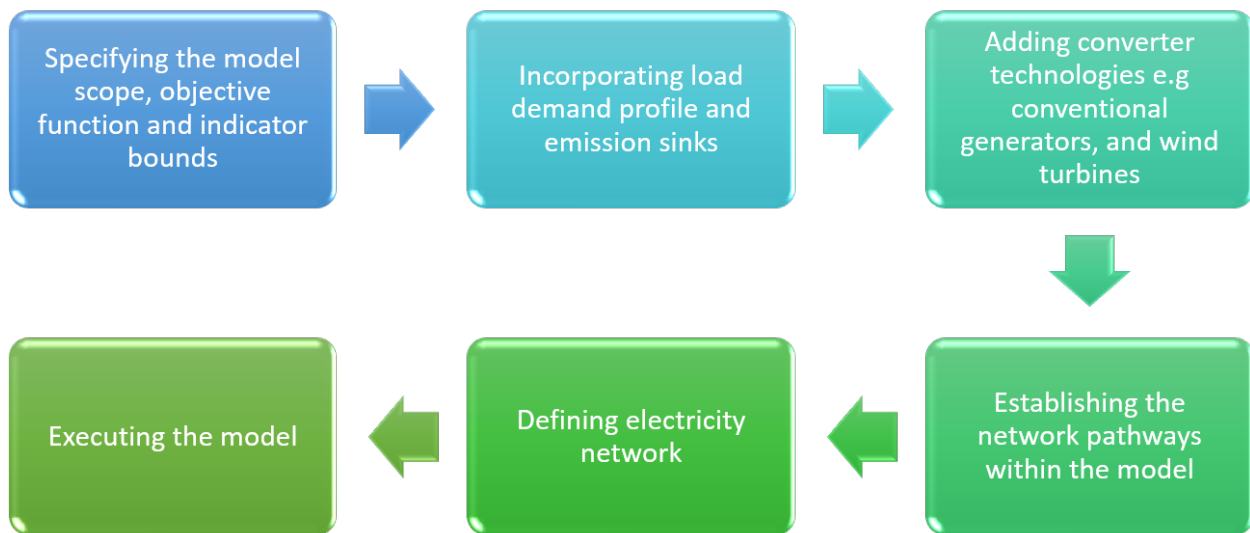
Figure 3.5: DCOPF Model Using REMix Framework

3.3.2.1 Specifying model scope, objective function, and indicator bounds

The model scope defines the fundamental dimensions of the model, which includes the distinct regions and time frame. Throughout the capacity expansion planning, this model uses 24 nodes and optimizes the objective function every hour. The objective function takes the overall system cost as input. The energy system uses indicators for general accounting. To reflect the overall costs of the system, an indicator named 'System cost' is used. This indicator is calculated by summing up the variable operation and maintenance cost (in MEUR/MWh) (OMVar), fix operation and maintenance costs (in MEUR/MW/year) (OMFix), and investment cost for a technology unit (in MEUR/MW) (Invest) with an equal weighting of 1 in the 'accounting_perIndicator' DataFrame. Depending on the scenario being considered, the constituents of the objective function may vary. Indicators can also be used to set soft constraints in the system, such as how much of a specific technology can be

built within a period. This thesis introduces a carbon budget into the model to limit the utilization of conventional technologies and to encourage the implementation of more clean energy sources, in this case, wind power plants.

3.3.2.2 Incorporating load demand profile and emission sinks

The load demands for the system throughout the capacity expansion are indicated in Table A3 in the appendix. For scenarios with conventional generators, Emission sinks are added to take the carbon emission from the generators. The load demand and emission sink are set up as negative values in accordance with the remix framework.

3.3.2.3 Adding converter technologies e.g, conventional generators and wind turbines

To integrate converter technologies into the model, it's essential to define several aspects that the REMix framework expects. Firstly, the produced commodities, which in this scenario are electricity and carbon (for conventional generators). Next, the technical and economic parameters are outlined, as detailed in Table A1. The primary function of this technology is power generation. Additionally, it's important to note that the anticipated lifespan of the generating units is estimated to be 30 and 25 years for conventional generators and wind turbines, respectively. Activity profile, unitsLowerLimit, and unitsUpperLimit for every generator are also defined.

3.3.2.4 Establishing the network pathways within the model

Establishing the network pathway in a power system model involves two major steps, which are setting up a link connection in the data nodes by defining the starting and ending node of each link. secondly, defining the lengths of each of the corridors while also considering the terrain type which can be land or sea. In this model, the terrain type is land for all lines, and the length is calculated based on the reactance. The lengths used for each line are given in Table A4 of Appendix A.

3.3.2.5 Executing the model

In the final step of the optimization process, all the data frames created from previous stages are converted into .dat files for the REMix framework. Before running the model, a few solver settings may be updated based on the scenario. In the case of this model, the opf-method is set to "angle" while other default settings are maintained. After updating the settings, the model is executed.

3.3.3   AC-OPF & DC-OPF in the Supporting Model

The supporting model is set up in a MATLAB environment by replicating the same IEEE RTS 24-bus system model as parametrized in the REMix model. The main purpose of this supporting model is to determine certain power flow parameters that are not available in the DC-OPF model in REMix and, simultaneously, compare the result obtained with the remix model. The AC-OPF model, the power systems variables required to compute the maximum active power that can be transferred in a line are determined. These parameters include bus voltages, the angle of load impedance, and impedance angle. For every proposed system load increase, the AC-OPF is solved iteratively to determine all of these parameters and, by extension, identify the voltage collapse proximity indicator for every line in the network. To test the efficiency of the proposed algorithm, capacity expansion planning is carried out with and without the VCPI constraint added to the optimal power flow using equations (2.4) to (2.13), and (2.29). The DC-OPF experiment in MATLAB is used to validate the results obtained with the REMix model.

3.4   Defining Voltage Stability for the Thesis

3.4.1   Criteria for Stability Index Selection

As mentioned earlier, different types of voltage stability indices are used to assess the stability of power system networks, and these indices vary from the assumptions in their formulations. It is crucial to consider assumptions sensitive to the conditions to forecast voltage collapse accurately. Figure 3.6 compares different voltage stability indices in determining how close a system is to the point of instability. In all three, the loading magnitude is gradually increased until the voltage collapse point is breached. The subplot (a) in Figure 3.6 resulted from increased active power loading on bus 15 only in the base network until one of the VSIs crosses the boundary limit. This subplot (a) now illustrates VSIs on branch 12-13 as the voltage magnitude on bus 15 begins to drop. While VCPI can detect the voltage collapse at the earliest on this branch when active power loading on bus 9 has risen to 1200 MW, NCPI, LQP, and Lmn still ignore this loading as they depict the branch as stable. NCPI and LQP later detected the voltage collapse at a much higher load. The Lmn index can only detect the collapse until the active loading reaches 1585 MW. The reason why Lmn has a low response is that it ignores the effect of active power flow. Thus, the performance of VCPI during increasing active power loading is effective compared to other indices.
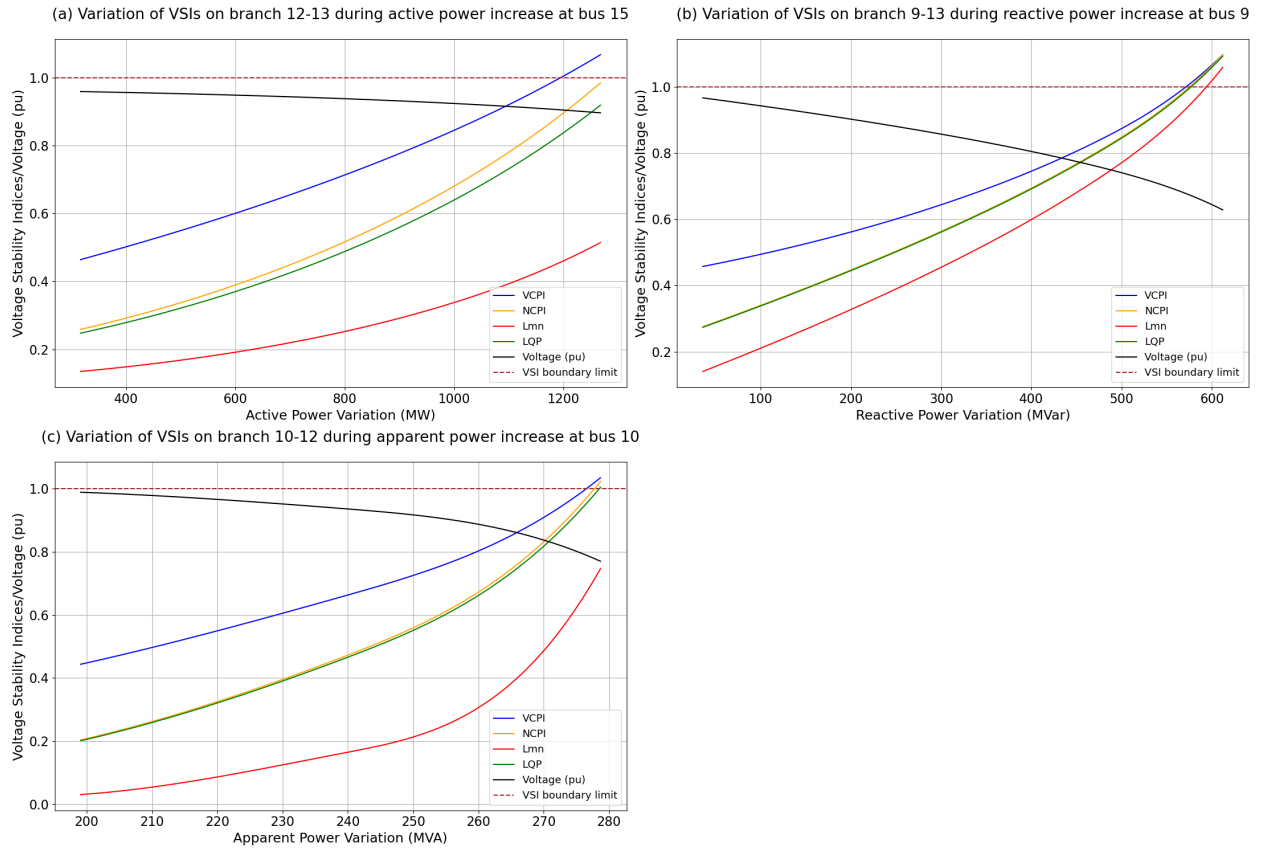
Figure 3.6: Comparison of voltage stability indices during active, reactive and apparent power increase at selected buses using an IEEE 24-bus network

Furthermore, the effectiveness of these indices is examined during the heavy reactive loading condition in the network. the subplot (b) in Figure 3.6 compares the various VSIs when increasing the reactive loading at bus 9 and bus 13 in the IEEE 24-bus base network. The VCPI increases until it approaches the VSI boundary limit of 1.00. This is followed by NCPI, LQP, and Lmn. The NCPI, LQP, and Lmn are quicker when considering the increase in reactive power because they consider the impact of reactive power flow in their formulation. In the last subplot (c) of Figure 3.6, the apparent power loading across the entire network is increased in steps of 10% of their initial values until the solution to the power flow stops converging. This apparent power increase is important because the active and reactive power loading continuously vary in power networks and occurs mostly in power systems. Looking at branch 10-12 and observing the apparent power flow, VCPI first approaches the voltage stability boundary limit at the critical active and reactive power loading of 273 MW and 56 MVar respectively. Whereas the other indices fail to reach the stability limit until a further increase in apparent power occurs. Therefore, the VCPI shows a high performance and effectiveness compared to other indices as a result, It is substantial to incorporate it into capacity expansion planning to ensure voltage stability.

31
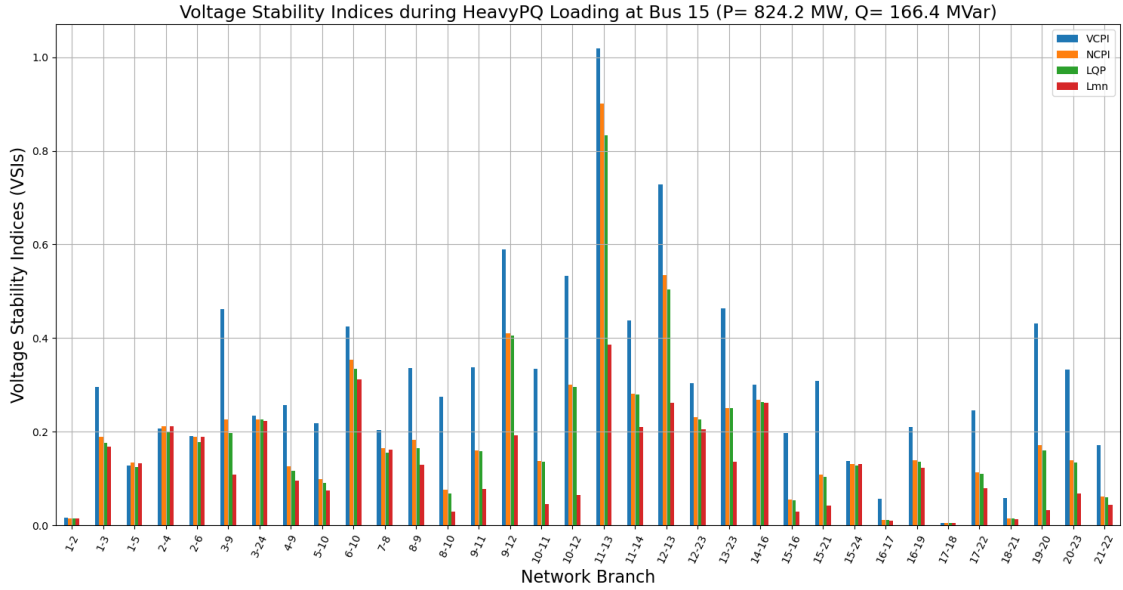
Figure 3.7: Values of Voltage Stability Index for all Transmission Lines in the IEEE 24-Bus System under Heavy Apparent Load Conditions at Bus 15 (P = 824.2 MW, Q = 166.4 MVar)

Figure 3.7 shows the voltage collapse proximity indicator values for all transmission lines in the network when only the active power (P = 824.2 MW) and reactive power (166.4 MVar) loading at Bus 15 are increased. This shows that line 11-13 is the critical line of the network as the VCPI approached the voltage stability limit 1 on that branch. The critical values for the voltage stability indices at this loading condition for VCPI, NCPI, Lmn, and LQP are 1.0189, 0.9008, 0.386, and 0.8330, respectively.

3.4.2   Integration of VCPI into Optimal Power Flow

To ensure an acceptable level of voltage security at the buses and across the lines during capacity expansion planning in the power system network, the voltage collapse proximity indicator is included in the CEP algorithm as an additional constraint to the existing voltage magnitude constraint. The voltage collapse stability limit is set as follows;

$$VCPI_{max} \leq VCPI_{limit} \tag{3.1}$$

Here, the limit of the VCPI represents the threshold value set to maintain a certain level of system security, while $VCPI_{\max}$ denotes the highest possible value of the VCPI index in the network and it is given in equation (3.2).

$$VCPI_{max} = \max(VCPI_i), i = 1...n \tag{3.2}$$

Where n is the total number of lines in the model. The equation (3.1) is added to the constraints of the ac optimal power flow defined from equations (2.5) to (2.13) in the MATLAB environment.

3.4.3 Identifying approach for REMix extension

So far, the REMix framework uses a DC power flow algorithm for optimization; as a result, direct computation of voltage collapse stability limit across any power system network modelled in this environment is currently impossible. The model is first replicated in the Matlab environment to incorporate the concept of voltage modelling along with capacity expansion planning in REMix. The supporting model determines the $VCPI_{\text{limit}}$ of each line. This $VCPI_{\text{limit}}$ determines the maximum load to stabilize the network voltage and the final load is imported into the CEP model. As a result, the REMix model would then account for the investment, operation, and maintenance costs and determine the optimal sizes and locations of both the new generation capacities and transmission lines to be added at the final load stage of the capacity expansion.

3.5 Integration of Voltage Stability Constrained Optimal Power Flow into GEP Model

The GEP OF model adopted for this thesis work optimizes Investment cost (or capital cost) and operation and maintenance cost. This model is set up as 'accounting_perindicator' within the REMix tool. The GEP model is given in equation (3.3);

$$GEP = \min \sum_{t \in P} (C_{I,t} + C_{OM,t}) \tag{3.3}$$

Where P is the planning period, for the thesis, only a planning horizon is used, $C_{I,t}$ and $C_{O,t}$ are the capital cost, and operation and maintenance cost in a given period. To achieve an optimal solution, sets of technical and economic constraints are considered in the model, including capacity upper and lower limits, power balances, and environmental constraints. REMix can solve this model, and an optimal solution can be obtained. However, when the concept of voltage stability is to be introduced, the GEP model is implemented in the supporting tool. The voltage stability index is then added to the supporting tool. This index is an additional constraint to the voltage magnitude limit in the power flow equation. Due to the intermittent generation of renewable energy generation components, the existing voltage magnitude limit cannot guarantee an acceptable level of voltage stability in the network model. As such, the voltage stability index is considered and integrated into the optimal power flow algorithm. The VSI constraint added to the generation expansion planning is given in equation (3.1).

3.5.1 Model Framework

The voltage constraint optimal power flow algorithm implemented for this thesis is given in figure 3.8 to ensure voltage stability in the network while executing capacity expansion

planning.
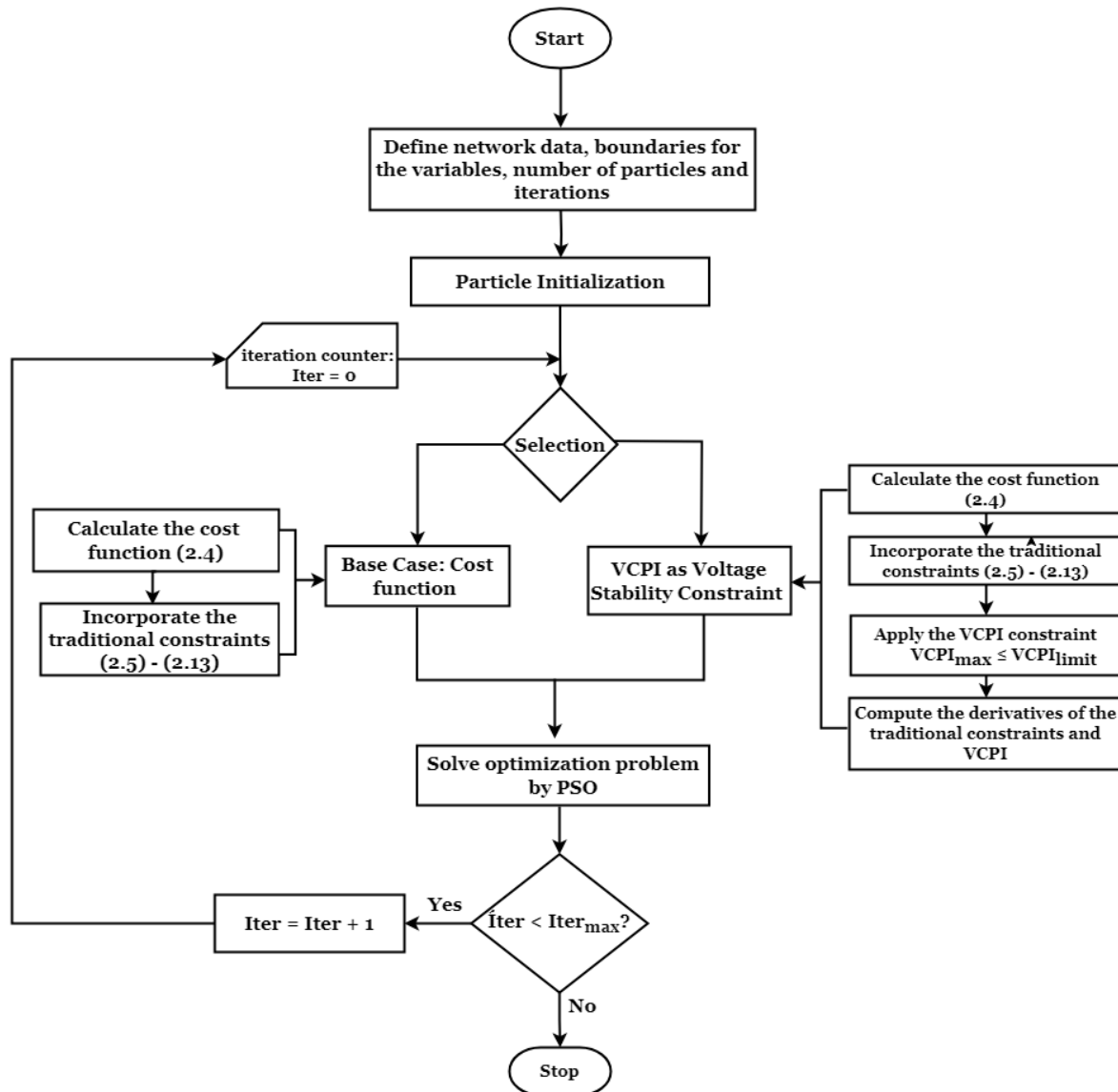
Figure 3.8: Flowchart for the Voltage Security Constrained Optimal Power Flow Algorithm

The methodology employed for the supporting software in this thesis operates within a MATLAB-based power system framework. The PSO solver algorithm was originally developed by [62, 63, 64, 65] and has been modified and adapted for this particular thesis through the integration of a Voltage Collapse Proximity Index (VCPI) into its structure. Moreover, For this thesis, an IEEE 24-bus network is implemented. The algorithm takes the network data of the IEEE 24 bus system and sets up the boundaries for all the variables initiated for its optimization, including the load demand defined for the model. In terms of the purpose of the optimization, the algorithm selects whether to use the voltage stability index or not. When solving with VCPI, the VCPI is used as an additional constraint to the optimal power flow. When the VCPI is used as a constraint, the optimization research aims to confine the VCPI index from 0 to a specific $VCPI_{\text{limit}}$ in order to secure a targeted level of voltage

stability and, at the same time, assess how the voltage security influences investment in new generators, operation and maintenance cost of installed and planned generators. It aims to improve the model voltage stability and minimize the power losses for the latter.

In most parts of the research, VCPI is adopted as a constraint in the generation expansion planning. Each selection has well-defined other constraints as shown in the flow chart figure 3.8. The optimization tool within Matlab is then implemented to solve the problem. In each iteration, the voltage stability condition of the model is assessed. When the model accomplishes the maximum optimization iterations, the algorithm's execution stops; otherwise, it starts again.

3.5.2 Model Framework for Integrating VSC - OPF Algorithm Concept into REMix

The flow diagram in figure 3.9 illustrates the functioning process employed in executing the generation expansion planning defined for the thesis. The first step involves initializing the model structure of the REMix framework and preparing the data frame for all the input required by the framework. These data are converted into the *.dat* format expected by the REMix structure. Two routes are possible for the GEP. The first is executing the GEP without considering the concept of voltage stability of the network. In this instance, the optimal solution should determine the size, type, and number of new generators that should be installed.

The second pathway considers the introduction of the concept of voltage stability index as the capacity expansion progresses. In this method, the algorithm developed in the supporting modelling environment is used to determine the expected voltage stability limit of the line for each step in the expansion stage. The corresponding load demand to keep the system stable is imported into the REMix environment, and the GEP is solved for each scenario defined for the thesis. If the program sees an optimal solution., this will generate the GEP solution. Otherwise, the model is modified until satisfactory steady-state operation is accomplished.
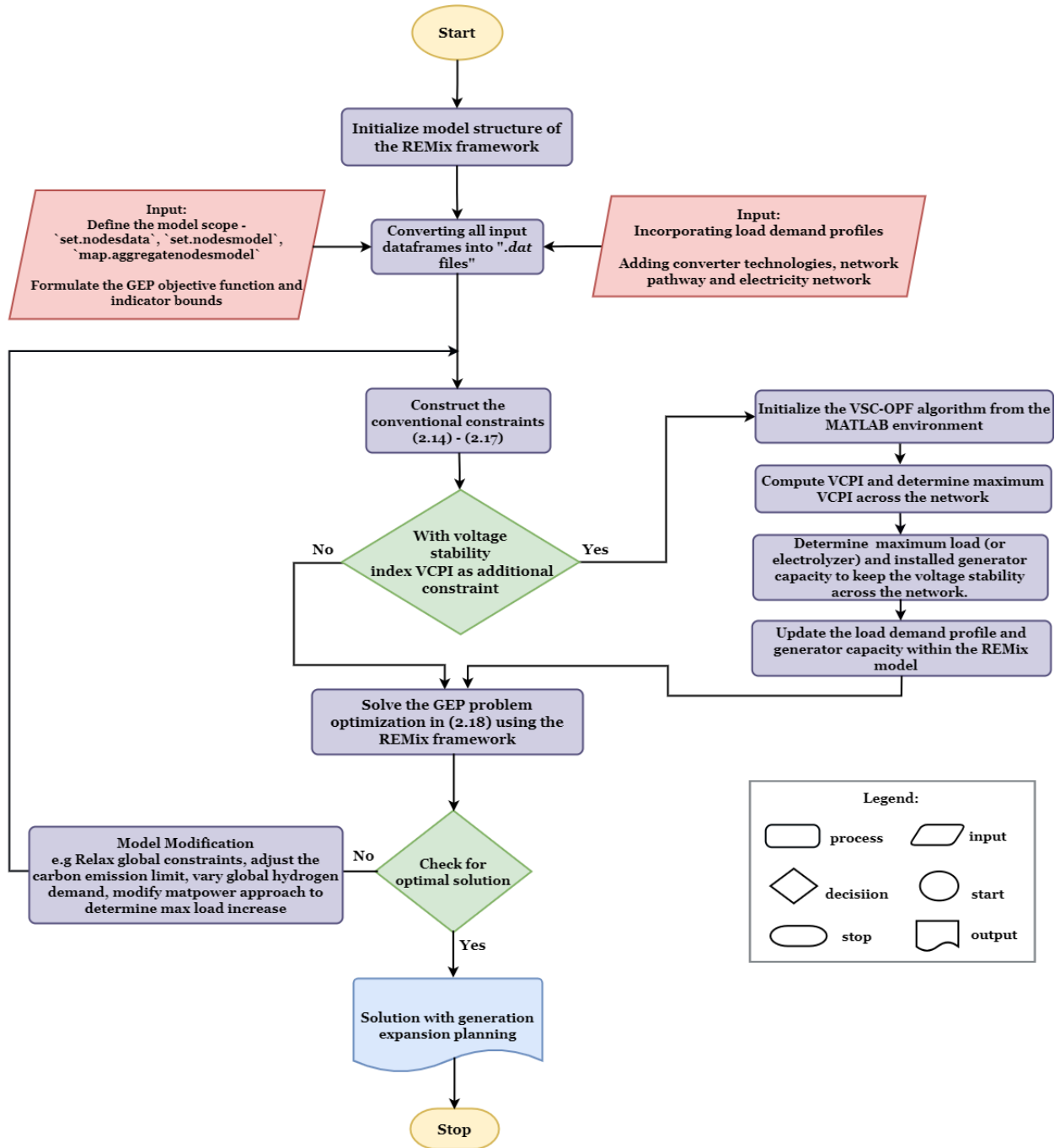
Figure 3.9: Integrated Generation Expansion and VSC-OPF Algorithm Process Flowchart

3.5.3 Capacity expansion model development process

All the network data consisting of generators, transmission lines, bus, transformers, and load for the IEEE RTS 24-bus system are written into a .csv (command-separated values) format and imported into the Python environment. These data are transformed into data frames and then converted into '.dat' (data file) format using Python. This thesis uses Visual Studio's Python environments window to implement the '.dat' file and execute all the REMix

codes. Behind this REMix framework is the general algebraic modelling system (GAMS), a high-level modelling system for mathematical optimization. The GAMS tool executes optimizing the modelling problem to find the best solution. After the result from the REMix environment has been generated, the voltage stability of the output is assessed using MATLAB. At this stage, the GEP solutions without considering VCPI are obtained. However, when the CEP now involves the incorporation of the voltage stability index, the MATLAB model is modified to include VCPI. the result from the MATLAB model is exported into a .xlsx (Microsoft Excel Spreadsheet) and then imported back into the Python environment, where the load and generator data are updated. The REMix tool is then used to execute the model where an optimized and reliable generation expansion solution is obtained. The optimization model's result is obtained through the GAMS interface. Lastly, MATLAB is also used to verify the voltage stability of the resulting GEP solution. Figure 3.10 presents a diagram that illustrates the process of implementing the CEP model considering voltage stability.
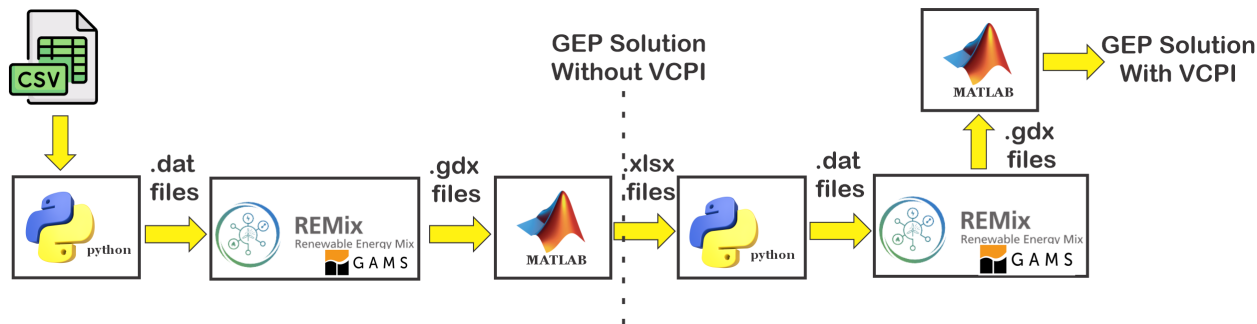
Figure 3.10: Capacity expansion planning model development process

3.6   GEP Case Studies

Two case studies consisting of four scenarios are considered for the generation expansion planning defined in this thesis work. The base model of the standard IEEE 24-bus RTS is assumed to have conventional generations, and the system is in stable condition. The base network has been modified to turn the system into a GEP problem. It is assumed that not all generator units of the base network are completely installed. Also, uniform characteristics exist across all system transmission lines within the same corridor. During the capacity expansion, the system starts to experience disturbances across the transmission lines and various nodes. The voltage stability is of concern in this work. This fluctuation in voltage might be due to large or small disturbances, which can either extend for the short term or the long term. For this thesis, the network disturbance is modelled as the load variations during the capacity expansion planning. Figure C.1 illustrates the system load profile over the planning horizon for the case studies examined in this thesis.

3.6.1 Case 1: Fully Conventional Generators

The GEP model is formulated with only conventional generators in this case study. First, the model is solved in the REMix framework without considering any additional voltage stability limit. In the second instance, GEP will be optimized while incorporating the concept of voltage stability index. The potential for installing new generations is applied within the model across all network nodes. The optimal solution will determine the size and location where new conventional generators should be installed across the period of the capacity expansion. The voltage stability of the final model is also assessed to measure the strength of the solution. The schematic model for the resulting optimal GEP solution is drawn, and plots for analyzing results are made. Two scenarios are defined for this case study 1.

3.6.1.1 Scenario 1

This is the first scenario considered in case study 1, where only conventional generators are in the network. Here, the Generation Expansion Planning is carried out without the use of additional voltage stability constraints in the modelling framework. The maximum base load and maximum final load in this scenario are 2650.5 MW and 3106.5 MW, respectively.

3.6.1.2 Scenario 2

This scenario involves considering additional voltage stability constraints during the generation expansion planning. This additional voltage constraint is first set in the Matlab environment to determine the installed generation and load demand at each stage of the expansion while maintaining the voltage stability of the system. The load demand and installed generator capacity at the final expansion stage are imported into the REMix environment. Scenario 2 models the load as an electrolyzer in the REMix framework. In this scenario, the maximum base load is 2650.5 MW, and 10.944 GW of hydrogen demand over the planning horizon is placed on the network. This hydrogen demand corresponds to the expected final load for case study 1.

3.6.2 Case 2: Conventional and Wind Turbine Generators

In this scenario, a potential for installing a wind power plant is applied across the network. This is in addition to the existing base case scenario consisting of only conventional generators. A carbon limit is set within this model to restrict implementation of the conventional generators and encourage more installation of wind power plants. The proposed model and algorithm decide the size, location, and type of the generator to be installed while solving the GEP problem. The voltage stability of the network is also assessed before and after the GEP. As in the previous case, the schematic model for the resulting optimal GEP solution

is drawn, and plots for analyzing the economic and operational results are made, including the voltage stability of the network. Two scenarios are also defined under this case study.

3.6.2.1 Scenario 3

This is the first scenario in case study 2. No additional voltage constraint is added to the generation expansion planning model in this scenario. The results from the REMix tool obtained through the GAMS interface are exported as Excel files into the MATLAB environment to determine the stability of the GEP solution. At this point, the actual voltage stability of the network is studied.

3.6.2.2 Scenario 4

Scenario 4 considers additional voltage stability constraints in the generation expansion planning model's modelling framework. The system also optimizes the incorporation of wind power plants into the model. The GEP models are set up in REMix, and the supporting MATLAB software is used to determine the voltage stability of the optimized GEP solutions. In this scenario, the maximum base load is 5073 MW at t018, and 58.14 GW of hydrogen demand over the planning horizon is placed on the network. This hydrogen demand corresponds to the expected final load for case study 2. The Figure C.1 further depicts the system load profile over the planning horizon.

Chapter 4

Results and Discussion

This chapter describes the outcomes of implementing the generation expansion planning model alongside the algorithm for the voltage stability constraint optimal power flow using the simulation scenarios defined in section 3.6. Various graphical representations, including the modified IEEE RTS 24 bus network single-line diagrams, are implemented to expatiate the results and showcase a clear understanding of the proposed concept for the thesis. The system stability margin of the base case network is also assessed before the implementation of the capacity expansion. Detailed explanations are also given for the four scenarios defined for the thesis.

4.1   Base Case Network

4.1.1   Network Voltage Magnitude and Voltage Stability Index

Before the base case network is introduced into the generation expansion planning model, it is essential to know the stability of the system. As such, this subsection presents the findings from both power flow and optimal power simulations to determine the base case network's node voltages and transmission network voltage stability indices. As shown in the network single line diagram of Figure 3.4, the transmission line of the IEEE RTS 24-bus operates under two different voltage levels of 138 kV and 230 kV. These are the voltages at the two sides of the network. Both the power flow and optimal power flow solutions are carried out on the system. The power flow computation gives the steady-state operating conditions of the base network.

On the other hand, the optimal power flow reveals the optimal operating conditions for the system, considering various constraints and objectives. Here, the main objective to be optimized is the operation cost. The simulation result in Figure 4.1 shows the voltage magnitude at the buses. The constraint for the voltage magnitude is defined for 0.95 to 1.05 pu in the optimization problem. The voltage magnitudes of the base case network fluctuate

between the magnitude of 0.99 pu to 1.05 pu for the optimal power flow optimization of the operation cost. Observing the power flow computation, the maximum voltage magnitude does not exceed 1 pu, and the least voltage magnitude is 0.96 pu. Thus, the voltage magnitudes fall within the defined range to ensure the system stability.
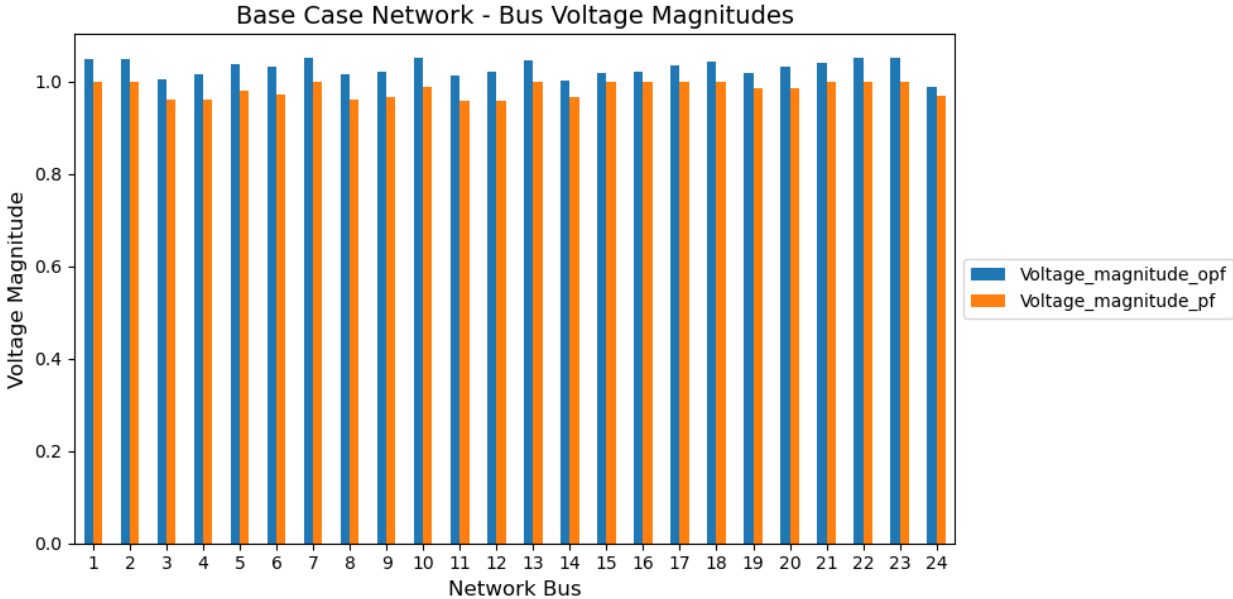
Figure 4.1: Base Case Network - Bus Voltage Magnitudes

Furthermore, Figure 4.2 illustrates the voltage stability indices from the base case network for the two simulations involving optimal power flow and power flow.
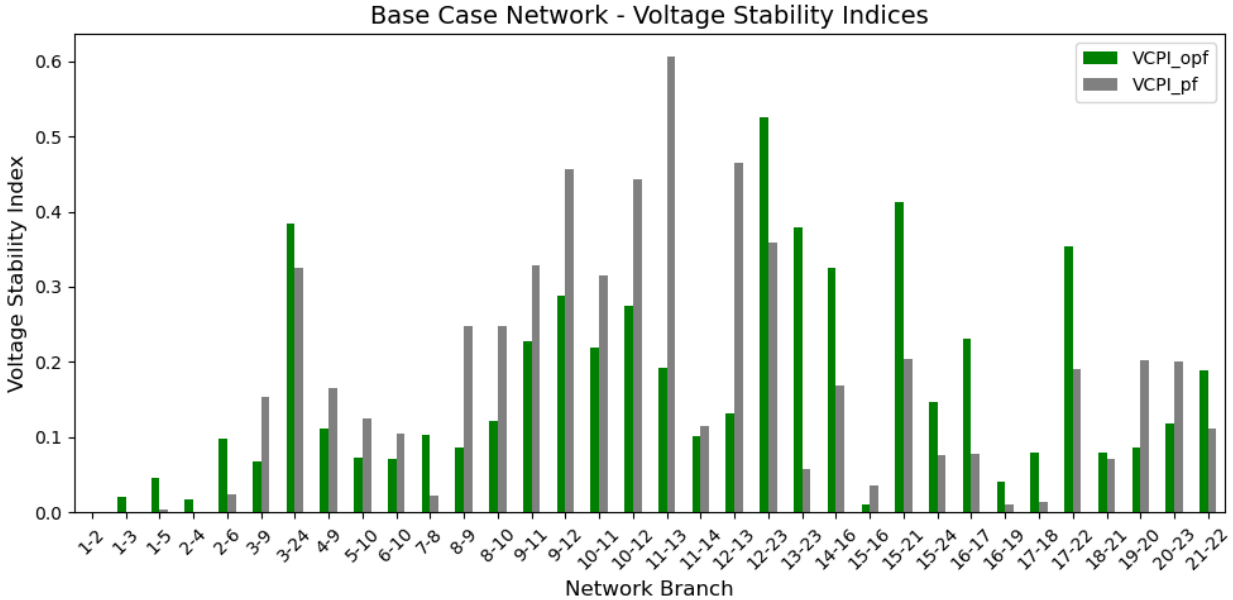
Figure 4.2: Base Case Network - Voltage Stability Indices

The maximum voltage stability index for the optimal power flow computation is 0.53, which

occurred on the branch between bus 12 and bus 23, whereas that during the power flow computation is 0.61 at the branch connecting bus 11 to bus 13. The voltage stability index introduced here is the voltage collapse proximity indicator, which measures the ratio of the real power transferred to the receiving end to the maximum real power that could be transferred to that end. For stability, the VSI should not exceed 1, the maximum permissible loading condition. Thus, as shown in Figure 4.1, VSIs during the computation of the optimal power flow and power for the base case network do not exceed the allowable limit. As a result, the network is in a stable condition.

4.1.2 DCOPF in REMix and Supporting Models

DCOPF algorithms available in the two modelling frameworks allow comparison of certain parameters. Here, the key parameters are the generator's operation and maintenance cost, generation output at the nodes, and active power flow across the transmission lines using the base case network. Executing the DC-OPF on the REMix model of the base case network, the operating cost is equal to what is obtained from the Supporting model (or MATLAB model) which is equivalent to 30 Mio USD.
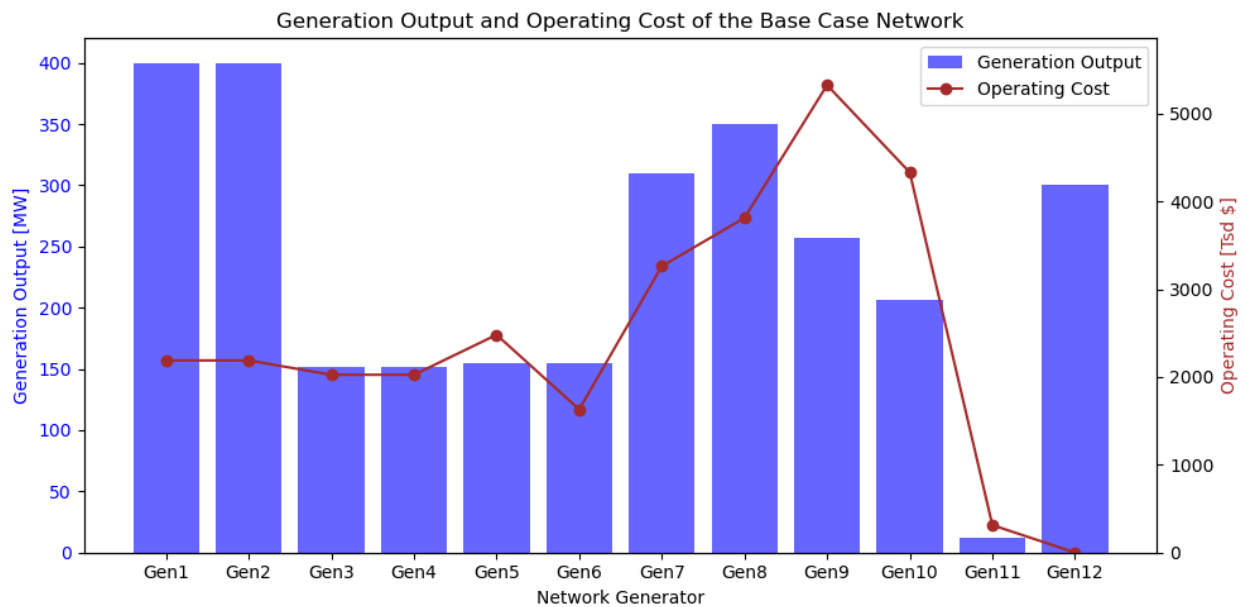
Figure 4.3: Base Case Network - Generation Output and Operating Cost

Figure 4.3 gives the generator output and the operation cost of each generating unit in the system. All the network-generating units are presented in Table A1 of the appendix section. Since Gen 12 has no cost for its operation, the optimization algorithm uses all of the generator capacity. Gen 9 has the maximum operating cost among all the generating units of the network. This means the optimization algorithm reduces usage to minimize the overall system cost. The generator's output at designated nodes is the same as the MATLAB

result.

The active power flow across various network branches is illustrated in Table 4.1. The loading of the branches is indicated in percentage within the column of Line loading as shown in Table 4.1. This measures the maximum load for each line. The top three loaded branches are

Table 4.1: Active Line Power Flow Across the Base Case Network

From Bus	To Bus	P_{ij} [MW]	Line Loading [%]	From Bus	To Bus	P_{ij} [MW]	Line Loading [%]
1	2	12.26	7%	11	13	92.73	18.6%
1	3	17.50	10%	11	14	169.04	33.8%
1	5	49.23	28.1%	12	13	65.82	13.2%
2	4	26.49	15.1%	12	23	226.48	45.3%
2	6	40.78	23.3%	13	23	216.70	43.3%
3	9	19.29	11.0%	14	16	363.04	72.6%
3	24	216.78	54.2%	15	16	80.02	16.0%
4	9	47.51	27.2%	15	21	446.80	44.7%
5	10	21.77	12.4%	15	24	216.78	43.4%
6	10	95.23	54.4%	16	17	320.20	64.0%
7	8	132.15	75.5%	16	19	92.18	18.4%
8	9	30.44	17.4%	17	18	179.36	35.9%
8	10	8.41	4.8%	17	22	140.83	28.2%
9	11	109.20	27.3%	18	21	112.36	11.2%
9	12	124.47	31.1%	19	20	88.82	8.9%
10	11	152.57	38.1%	20	23	216.82	21.7%
10	12	167.83	42.0%	21	22	159.17	31.8%

7-8, 14-16, and 16-17, with loading capacities of 75.5%, 72.6%, and 64%, respectively. The power flows and line loading capacities are the same in the REMix and Supporting models. With the increase in load demand on the network, the line power flow increases, resulting in a gradual voltage drop across the line and at the receiving bus. The line losses also increase whenever there is an increase in the line power flow.

4.2   GEP with Conventional Generators Only

This section examines the scenarios when the base case network with system load profile as presented in Table A.5 are introduced into the generation expansion model, and the voltage stability is observed for the system. The MATLAB model is first used to determine the maximum loadability of the network in this scenario, in which an optimal solution can be obtained. The load in Table A.5 is then scaled for the generation expansion to solve. In this case study, when the GEP is done in the REMix environment without additional

voltage stability constraints to the framework, this is referred to as Scenario 1. The second instance considering the voltage security-constrained algorithm during the generation expansion planning is termed Scenario 2. This additional voltage constraint is first set in the Matlab environment to determine the installed generation and load demand at each stage of the expansion while maintaining the voltage stability of the system. The load demand and installed generator capacity at the final expansion stage are imported into the REMix environment. Scenario 2 models the load as an electrolyzer in the REMix framework. At the final stage of this case study, the results of the two scenarios are compared to know to what extent an expansion can be carried out using the REMix framework while maintaining the voltage stability of the network.

4.2.1 GEP Solution from Scenario 1 in the REMix Framework

In this sub-section, the voltage stability during capacity expansion planning in REMix is observed. The maximum system load is increased from 2650.5 MW to 3106.5 MW, indicating a 17.2% maximum load increase for the expansion planning. The final system load limit over the planning horizon is further verified in the REMix environment to ensure that an optimal solution is available. There are specific emissions used for the operation of the conventional power plants of 21 kt.
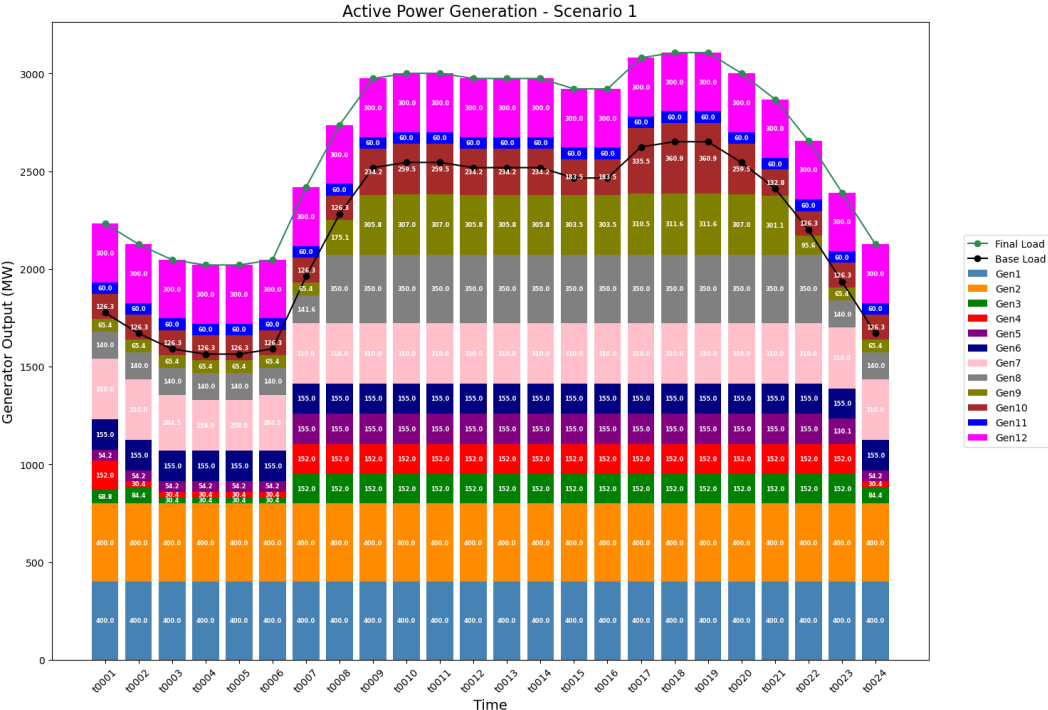
Figure 4.4: Active Power Generation from Scenario 1 Model

Figure 4.4 illustrates the power plants combination and capacity dispatch across the expansion planning horizon according to the REMix modelling output. All the system's generators

44

cover the base load except Gen11 and Gen12. As the system load grew, more generators were committed to the network at optimal cost. The GEP is carried out by considering the potential of all the generating units in the network. Table 4.2 gives the installed generator capacity, and the systems cost at the end of the generation expansion planning horizon.

Table 4.2: GEP Solution for Scenario 1

Node	Installed Generator	Capacity	Investment Cost	Operation Cost
		[MW]	[Tsd USD]	[Tsd USD]
1	Gen3	152	10269.7	39204.3
2	Gen4	152	4417.05	38873.1
7	Gen9	312	18880.9	101416
13	Gen10	361	22285	121721
15	Gen5, Gen11	215	9665.94	62986.6
16	Gen6	155	7364.42	39134.4
18	Gen1	400	20632.3	52512
21	Gen2	400	27025.4	52512
22	Gen12	300	18525.5	-
23	Gen7,Gen8	660	30597.5	214124
Total			169663.71	722483.4
System Cost			892147.11	

The full limit of the generator capacity potential at the nodes is built for Gen1 (400MW), Gen2 (400MW), Gen3 (152MW), Gen4 (152MW), Gen5 (155MW), Gen6 (155MW), Gen7 (310MW), Gen8 (350MW), Gen11 (60MW) and Gen12 (300MW). However, for Gen9, 312 MW is built out of a potential of 350 MW; in the case of Gen10, 361 MW is built from a potential of 591 MW. The optimized system cost for installing and operating all the generators at the final load is about 892 Mio USD. However, the knowledge of the network's voltage stability could not be ascertained from the result obtained from REMix.

Using the supporting modelling tool, the voltage magnitude at the buses and voltage stability indices across lines are computed at each stage of the capacity expansion to evaluate the stability of the network depicted from the REMix environment. Across the expansion stage, the branch between bus 12 and bus 23 is the most unstable line while trying to optimize the system cost. The maximum value of the VCPI during the expansion period is 0.598, occurring in branch 12-13 during time model t0001. The actual voltage at bus 12 and bus 23, making up this branch, are 230 kV and 241.5 kV, respectively. During the maximum hour loading of t0018, the highest VCPI across the branches of the network is 0.511, occurring at branch 12-13, which indicates that any continuous increase in the load will cause the branch to be cut off from the network, thus introducing instability in the network. Figure 4.5 shows the voltage magnitude variation at t0018 when the system is under maximum loading.
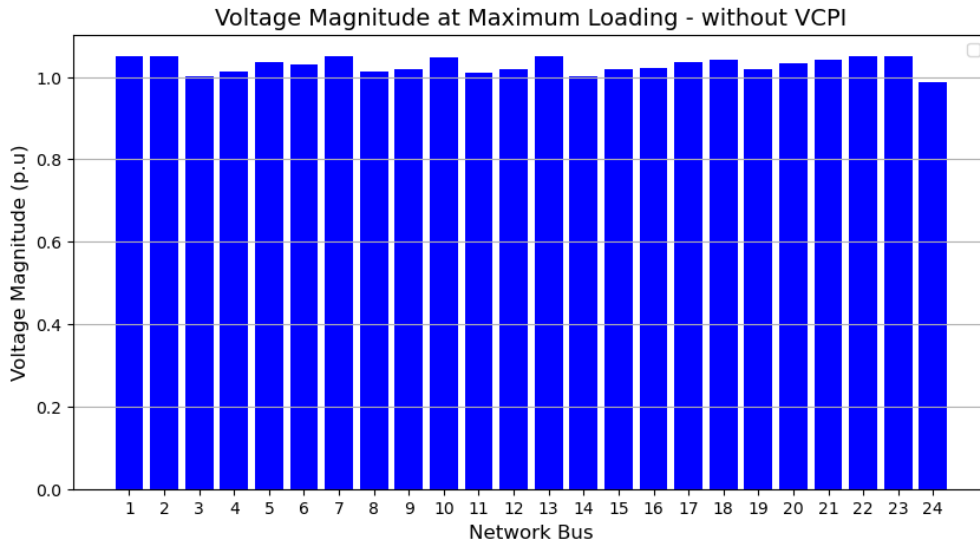
Figure 4.5: Voltage magnitude during maximum loading at t0018 - Scenario 1

At t0018, the voltage across the network quickly jumped from 0.989 pu at Bus 24 to 1.05 pu at Buses 1, 7, 13, 22, and 23, causing instability in the network.

4.2.2 GEP Solution from Scenario 2 in the REMix Framework

In this scenario, the voltage stability during the capacity expansion is observed with the introduction of VCPI as an additional constraint into the supporting modelling framework. The load increase in this scenario is modelled as an electrolyzer, as shown in Figure 4.6, to serve as a flexible load across the network. Here, the hydrogen demand set for the REMix model is 10.944 GWh according to the maximum system loadability derived from MATLAB for the network and across the planning horizon. The REMix model determined that 456 MW of electrolyzer should be installed across the network during the expansion planning horizon for each timestamp. These electrolyzers are distributed as given in appendix Table C.1 with the maximum electrolyzer capacity of 53.28 MW installed at node 18 and a minimum electrolyzer capacity of 11.36 MW at node 5 of the IEEE-24 bus network. Figure 4.6 further illustrates that depending on the set hydrogen demand in the REMix model, the distribution of the electrolyzer will be optimized to follow the demand.
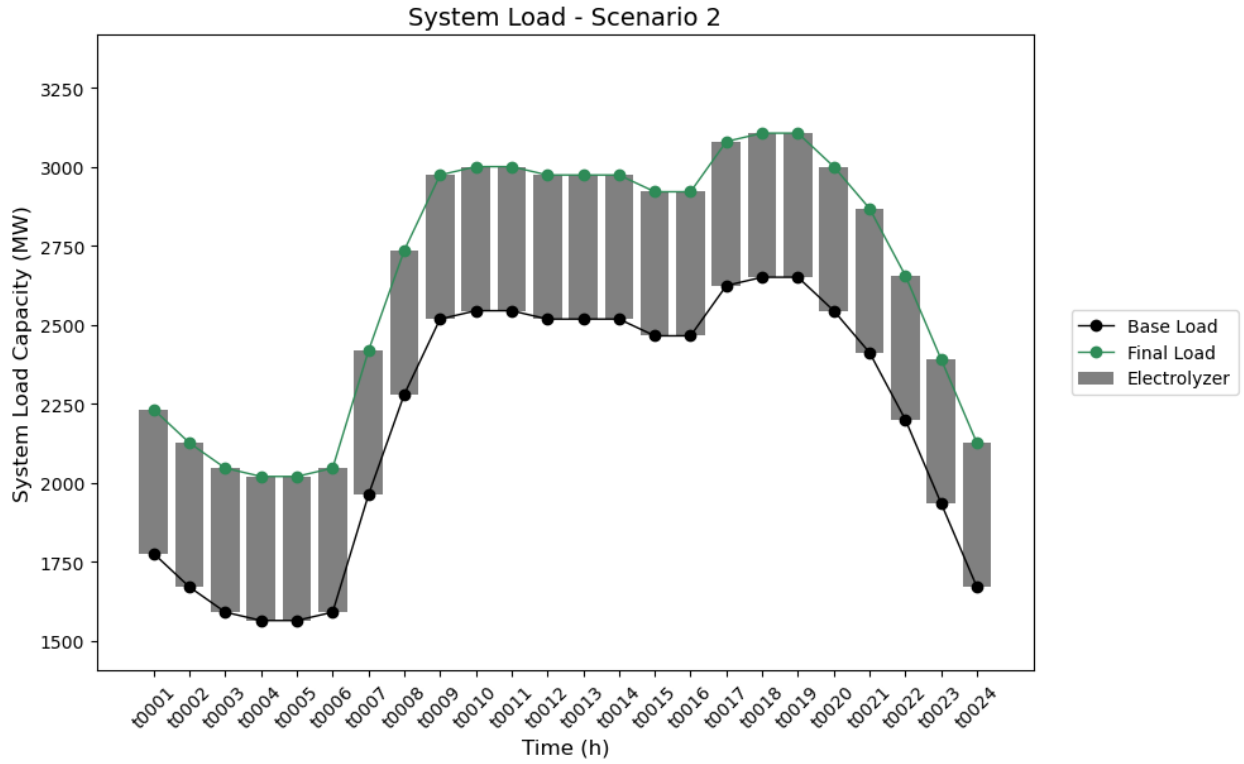
Figure 4.6: Installed electrolyzer capacity for Scenario 2

The installed generator combination and capacity dispatch during the network expansion are given in Figure 4.7. As the load increases from the base loading to the final loading, the generators are committed to the network at optimal cost according to the modelling framework in REMix. The hydrogen demand is used for the load expansion from the base loading of the IEEE-24 Bus network. In this scenario 2, the hydrogen demand set for the model is 10.944 GWh for the expansion. Since there are only conventional generators in this scenario, a 20.389 kt emission capacity accompanied the generation expansion planning model. While other generators are available across the expansion period, Gen 7 is not available from time t0001 to t0006, and after that, not dispatched again from t0023 to t0024; Gen 5 is only committed to the capacity expansion within the period of t0009 to t0021.
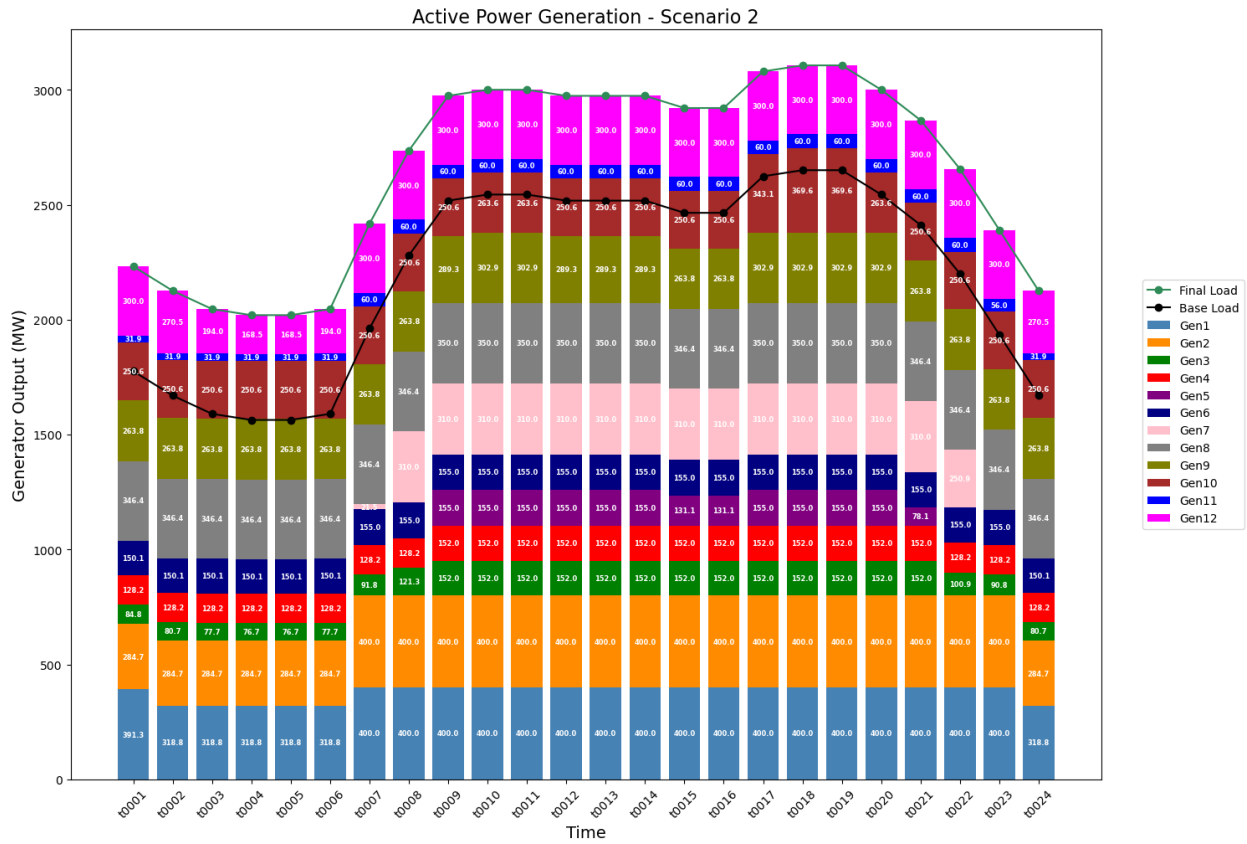
Figure 4.7: Active Power Generation from Scenario 2 Model

At the final loading of the network, Table 4.3 gives the installed generator capacity and the systems cost at the end of the generation expansion planning horizon considering VCPI. As the model optimizes the solution while considering voltage stability across the network, more generator capacities are available and dispatched, increasing the overall system cost to about 963 Mio USD.

At the end of the expansion planning horizon and as presented in Table 4.3, the generators Gen1 (400MW), Gen2 (400MW), Gen3 (152MW), Gen4 (152MW), Gen5 (155MW), Gen6 (155MW), Gen7 (310MW), Gen8 (350MW), Gen11 (60MW) and Gen12 (300MW) were installed, utilizing their full potential. Gen9 was able to build up to 303 MW out of a potential 350 MW, whereas Gen10 could build up to 370 MW out of a possible 591 MW. Across the expansion planning and the inclusion of an additional voltage security constraint into the modelling environment in Matlab, the voltage magnitude at the buses and voltage stability indices across lines are examined from the base loading to the final loading stage to evaluate the stability of the network depicted from the REMix environment. Here, the model solution tries to keep the voltage across the buses close to their nominal values. The maximum VCPI value across the network during the capacity expansion is 0.539, occurring in branch connecting bus 1 to bus 3 during the periods t0015 and t0016. The actual voltages at bus 1 and 3 are 137 kV and 138 kV, respectively. Figure 4.8 illustrates the voltage magnitude

Table 4.3: GEP Solution for Scenario 2

Node	Installed Generator	Capacity	Investment Cost	Operation Cost
		[MW]	[Tsd USD]	[Tsd USD]
1	Gen3	152	10269.7	39106
2	Gen4	152	4417.05	45108.5
7	Gen9	312	18352.9	139563
13	Gen10	361	22823.2	166697
15	Gen5, Gen11	215	9665.94	43284.3
16	Gen6	155	7364.42	38772.3
18	Gen1	400	20632.3	49799.8
21	Gen2	400	27025.4	48095.6
22	Gen12	300	18525.5	-
23	Gen7,Gen8	660	30597.5	223072
Total			169673.91	793498.5
System Cost			963172.41	

stabilization during maximum loading time at t0018. Moreso, Figure 4.8 further shows that the VSC-OPF generation expansion planning model can maintain the voltage across all the buses with the maximum voltage of 1.02 pu at node 7 and the minimum voltage of 0.99 pu at node 18 of the network. This indicates a small deviation from the nominal voltage at the buses.
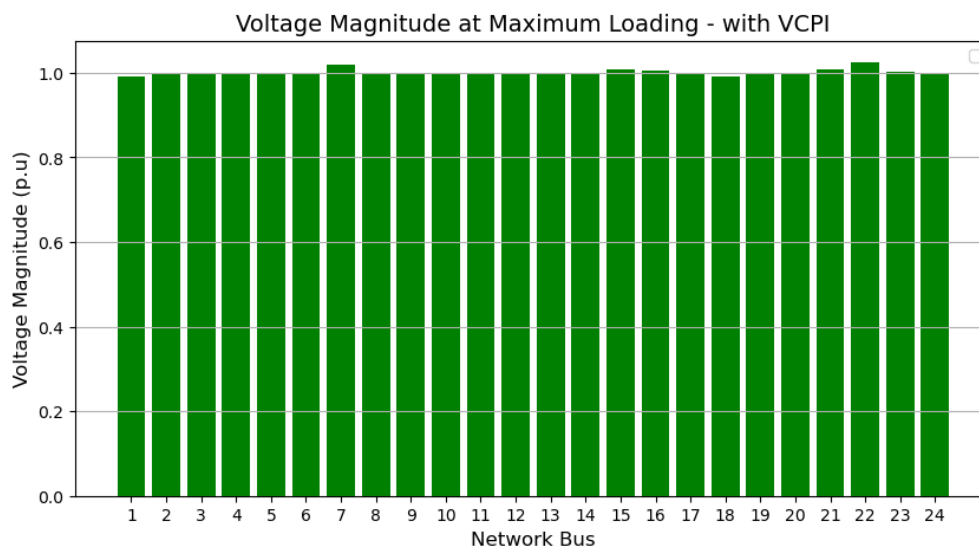
Figure 4.8: Voltage magnitude during maximum loading at t0018 with voltage improvement-Scenario 2

4.2.3 Comparison of GEP Solution from Scenario 1 and Scenario 2

This sub-section presents a comparative analysis of the capacity expansion solutions obtained using Scenario 1 (without VCPI) and Scenario 2 (with VCPI) in case study 1 involving only conventional generators in the expansion problem. It further emphasizes the impact of incorporating additional voltage stability constraints into the planning process on the voltage stability improvement and minimization of power losses across the network. Figure 4.9 presents a comparison of the results obtained from the two scenarios in capacity expansion planning in terms of the system cost comprising of operational cost and investment cost, maximum VCPI across the network branches, and the maximum active power loss across the network branches, all at final loading of the network.
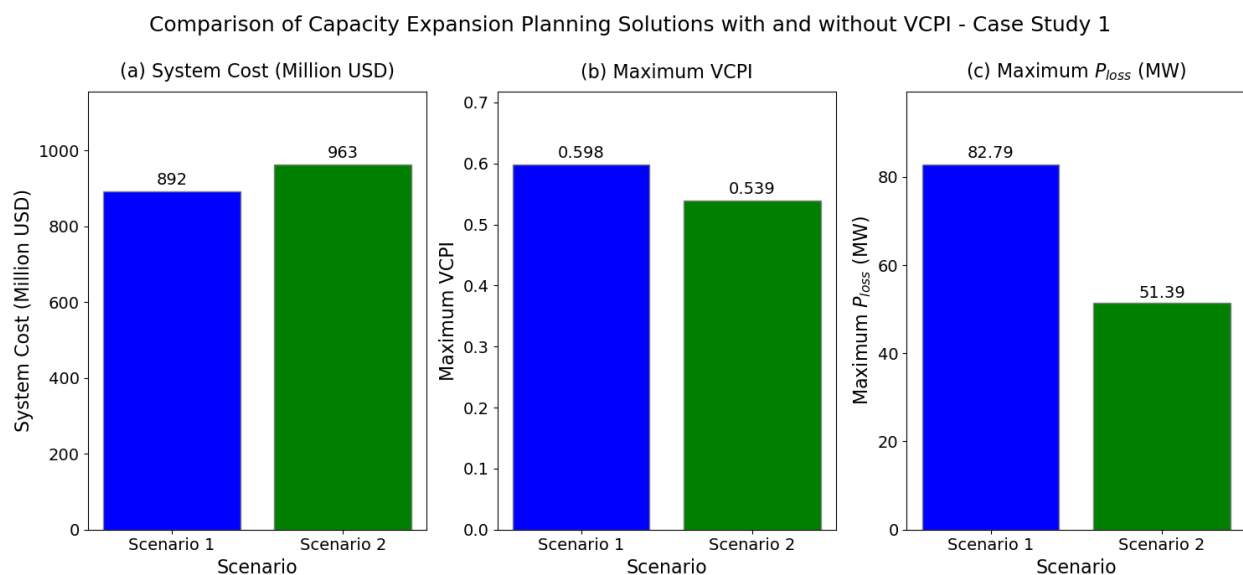
Figure 4.9: Comparison of the capacity expansion planning solutions with and without voltage stability index - Case 1

From Figure 4.9, significant differences are observed between Scenario 1 and Scenario 2 across the three metrics shown above. It can be seen from Figure 4.9(a) that Scenario 2 shows an increase in the system cost, reaching about 963 Mio USD compared to about 892 Mio USD in Scenario 1. This increment suggests that integrating VCPI into the CEP process would require additional generation capacity, leading to more operational cost and investment due to installing voltage stability measures to ensure overall system stability at the end of the expansion period.

From Figure 4.9(b), There is an appreciable reduction in the maximum VCPI from 0.598 in Scenario 1 to 0.539 in Scenario, indicating a 9.86% improvement in voltage stability of the network. This reduction is substantial as VCPI predicts voltage stability as implemented in the modelling framework for capacity expansion planning. The power losses are significantly

reduced in Scenario 2 (51.39 MW) compared to Scenario 1 (82.79 MW), demonstrating a substantial efficiency gain of 37.92% in the system branches as depicted in Figure 4.9(c). This reduction in losses signifies a more efficient operation with less energy wasted which provides a cost savings in the long term.

Furthermore, Figure 4.10 illustrates the voltage magnitude across eight network buses at final loading, with and without VCPI, during the capacity expansion planning.
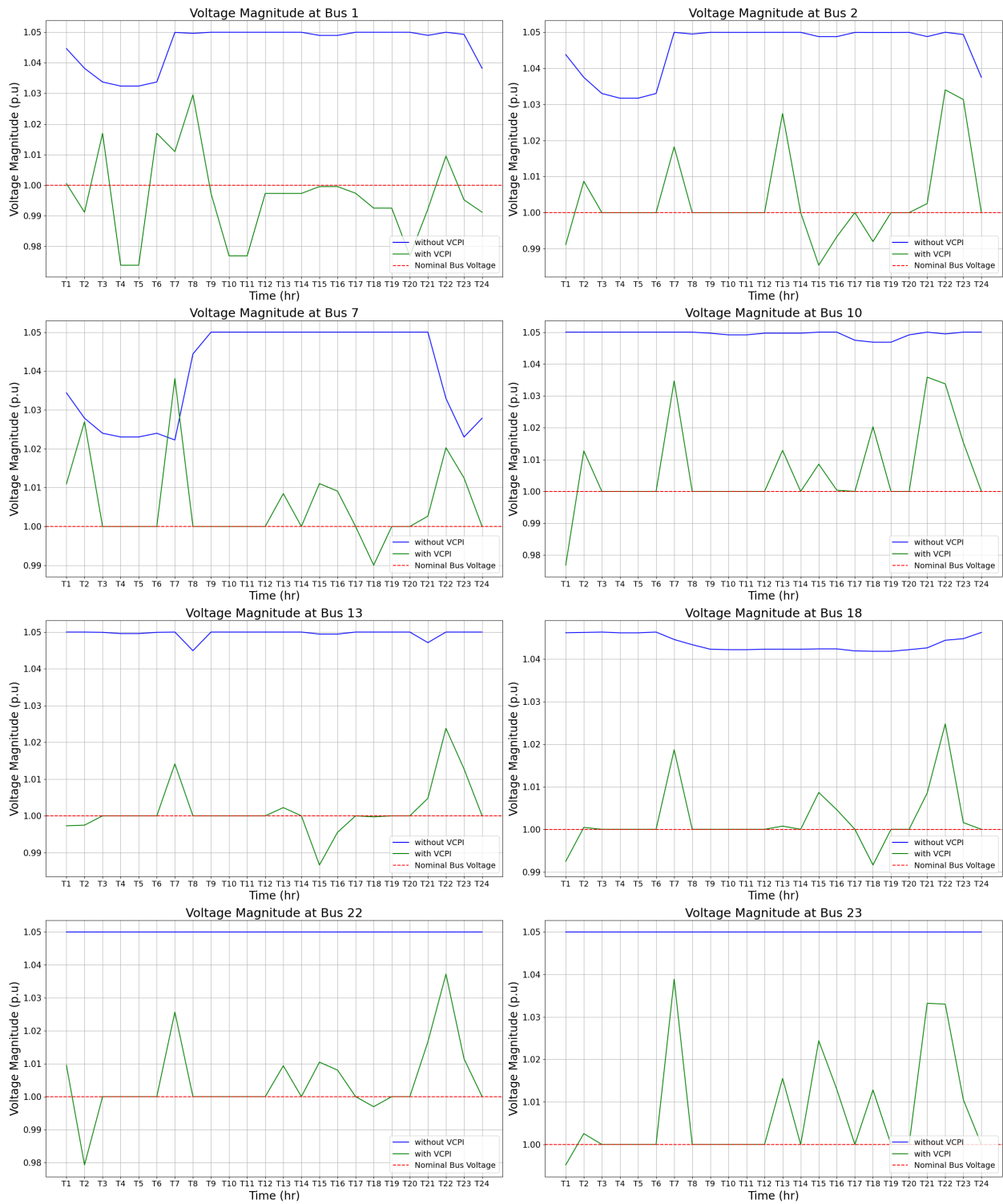
Figure 4.10: Comparison of Voltage Magnitude Across Selected Network Buses in Scenario 1 and Scenario 2

The selected buses are Bus 1, Bus 2, Bus 7, Bus 10, Bus 13, Bus 18, Bus 22, and Bus 23. Each plot contains two lines, the first representing the voltage magnitude with VCPI and the other without VCPI incorporated into the model. The red dashed line across each graph indicates the nominal voltage level of 1 per unit, which serves as a reference for the desired

stable voltage level at the network buses. From the plots, it is evident that VCPI stabilizes the voltage magnitude across the buses. Looking at the instances without VCPI across the eight examined buses, the voltage magnitude peaked at 1.05 pu for all buses except bus 18, which had a maximum voltage magnitude of 1.046 pu. Due to the loading on the system, the voltage levels have deviated well from their reference voltage magnitude of 1.0 pu. The increase implies that voltage at buses 1, 2, 7, and 10 has increased from the expected 138 kV to 144.9 kV, which implies a 5% increase, high enough to cause line outage across the network. However, for buses 13, 22, and 23, the voltage level increased from 230 kV to 241.5 kV, and in bus 18, the increase is from 230 kV to 240.48 kV, introducing unstable conditions in the entire network.

In contrast, looking at the lines with VCPI, the highest voltage magnitude across the observed buses is 1.038 pu, occurring at Bus 7. It can seen across Figure 4.10 that the voltage, when considering the VCPI, undulates around the reference bus voltage magnitude, trying to keep the voltage magnitude as close as possible while ensuring the stability of the overall network. In several instances, the voltage magnitude without VCPI shows considerable deviations from the desired nominal level, indicating an unstable system. These deviations can be spikes or dips, reflecting under or over-voltages at the buses, which are undesirable in the network. On the other hand, the voltage magnitude with VCPI appears to be more controlled and closer to the nominal voltage level, suggesting that VCPI contributes positively to stabilizing the system voltage. Figure 4.11 gives the final outlook of the solution obtained from the generation expansion planning with voltage improvement in case study 1. The resultant system operates under two voltage situations of 138 kV and 230 kV. 12 conventional generators are installed, with 34 active transmission lines and 5 transformers. The maximum load experienced by the system is 3106.504 MW.
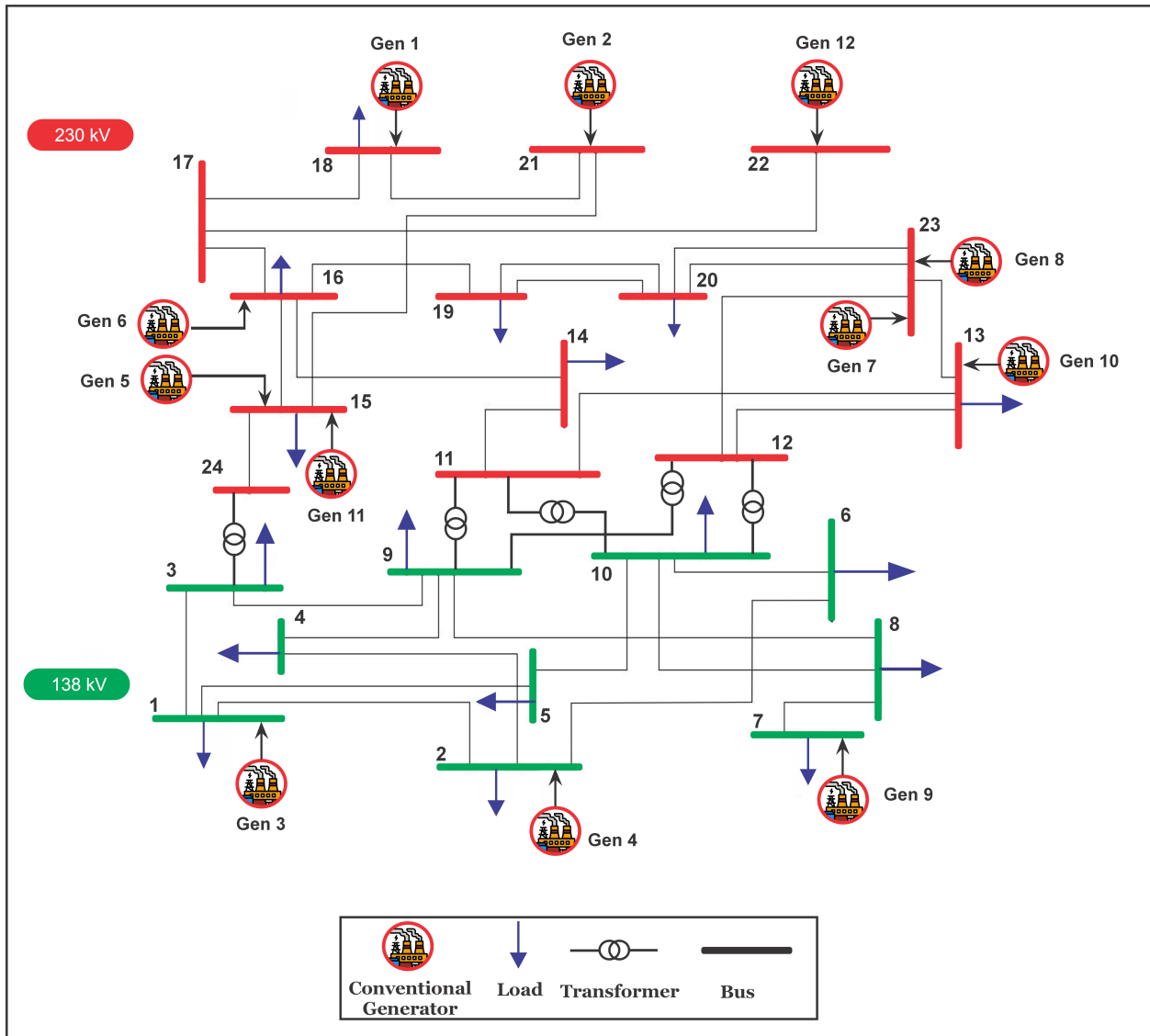
Figure 4.11: IEEE RTS 24-bus network solution with Voltage Profile Improvement - Case 1

4.3 GEP with Wind Turbines and Conventional Generators - Case 2

This section presents the results of the impact of integrating renewable energy plants on the voltage stability of power networks during capacity expansion planning. In a similar way as in case 1 involving only conventional generators, the maximum loadability of the network is determined using the supporting modelling tool. The system load is then scaled according to the maximum loadability derived for the generation expansion planning to solve. At the end, the results of the two scenarios are also compared to better expansion planning using the REMix framework and maintaining the voltage stability of the network.

4.3.1 GEP Solution from Scenario 3 in the REMix Framework

This subsection details the findings derived from modelling GEP without considering additional voltage constraints. The potential for installing a wind power plant is set for all the nodes where conventional generators are installed. The maximum hourly network load is increased from 2650.5 MW to 5073 MW, indicating a 91.4% maximum load increase for the network expansion. An emission limit is set for the conventional generators to ensure that more wind turbines are implemented in the GEP solution. Figure 4.12 depicts the power plant combination and capacity dispatch across the expansion planning horizon determined from the REMix environment.
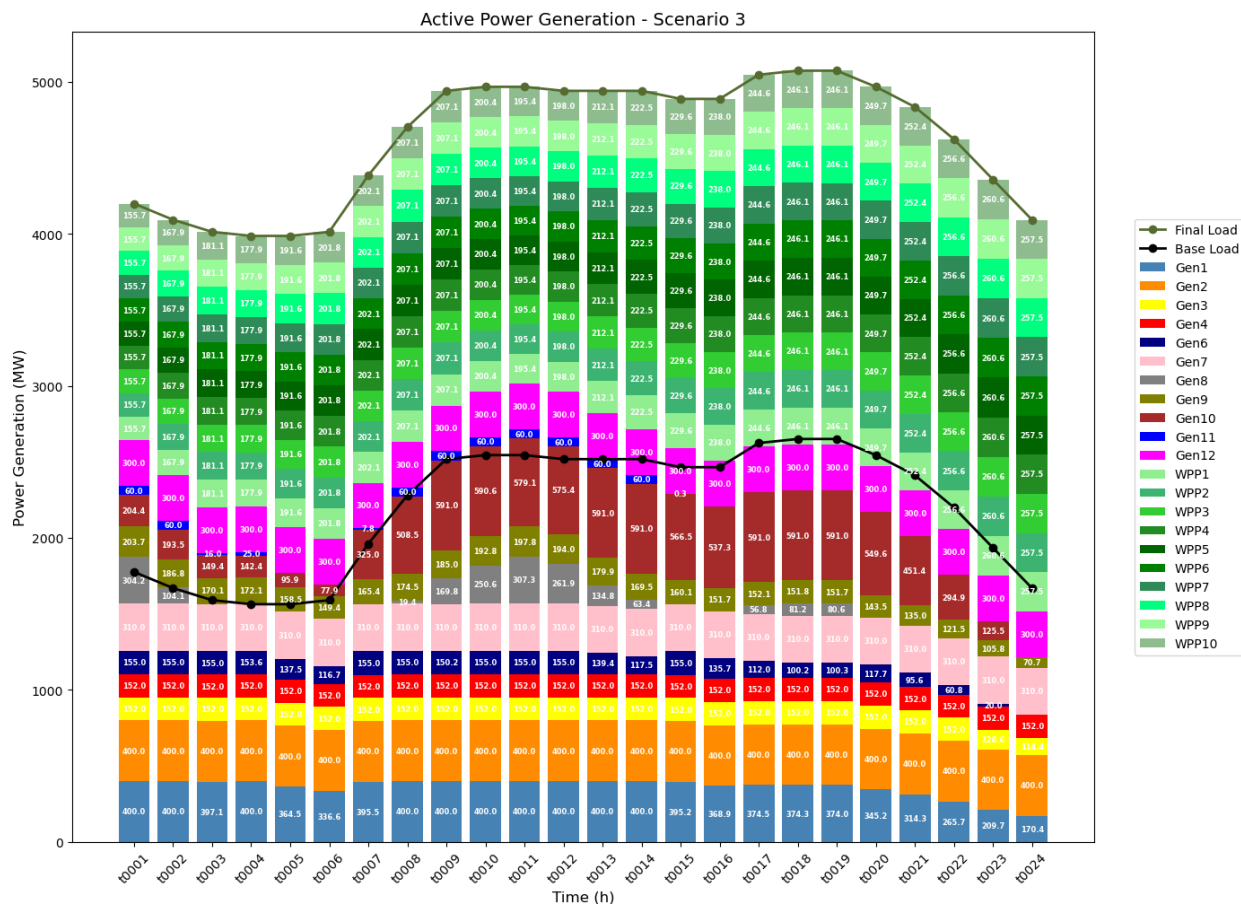
Figure 4.12: Active Power Generation from Scenario 3 Model

From Figure 4.12, it can be inferred that the conventional generator capacities are sufficient to cover all of the base load. As the loading on the system increases, more generator capacities are installed and dispatched during the expansion planning. Here, most of the additional generators are wind turbines. Gen 5 is entirely replaced by a 300 MW wind farm at Bus 15. The several units of wind turbines installed constitute the wind power plants shown in Figure 4.12. These wind power plants are installed based on the optimal solution found by the modelling framework. Table 4.4 below outlines the installed generators, both conventional

55

and wind turbines, and system cost consisting of investment and operational costs at the end of the planning horizon. A 16.551 kt emission accompanied all the conventional generators in the optimal solution. Upon optimizing the capacity expansion set up in the modelling framework, the resulting total system cost is about 1007 Mio USD at the end of the planning horizon.

Table 4.4: GEP Solution for Scenario 3

Node	Generator	Capacity [MW]	Wind Power Plant (WPP)	Capacity [MW]	Investment Cost [Tsd USD]	Operation Cost [Tsd USD]
1	Gen 3	152	WPP 3	300	37797.6	37640.7
2	Gen 4	152	WPP 4	300	31945	44591.7
7	Gen 9	198	WPP 8	300	36743.4	52640.9
13	Gen 10	591	WPP 9	300	64023.2	247860
15	Gen 11	60	WPP 5	300	27645.2	135.798
16	Gen 6	155	WPP 6	300	32935.6	19676.8
18	Gen 1	400	WPP 1	300	46837.9	39226.7
21	Gen 2	400	WPP 2	300	54553.4	52512
22	Gen 12	300	WPP 10	300	46053.5	-
23	Gen 7, Gen 8	606	WPP 7	300	41825.8	92657
Total					420360.6	586941.598
System Cost					1,007302.198	

The full potential of the wind turbines placed in the network is installed as part of the optimal capacity expansion planning. These wind turbines are clustered to establish the full capacity of a 300 MW wind power plant at each node, as shown in Table 4.4. Ten wind power plants are installed at the end of the expansion period. For the conventional generators, the Gen1 (400 MW), Gen2 (400 MW), Gen3 (152 MW), Gen4 (152 MW), Gen6 (155 MW), Gen7 (310 MW), Gen8 (350 MW), Gen11 (60 MW) and Gen12 (300 MW) were installed, utilizing their full potential. 296 MW capacity of Gen 8 is built out of a potential of 350 MW. For Gen9, 198 MW capacity is built from a potential of 350 MW. The full 591 MW potential capacity of Gen10 is built to ensure a stable network. The supporting model in the MATLAB environment is used to investigate the voltage stability of the capacity expansion solution from REMix.
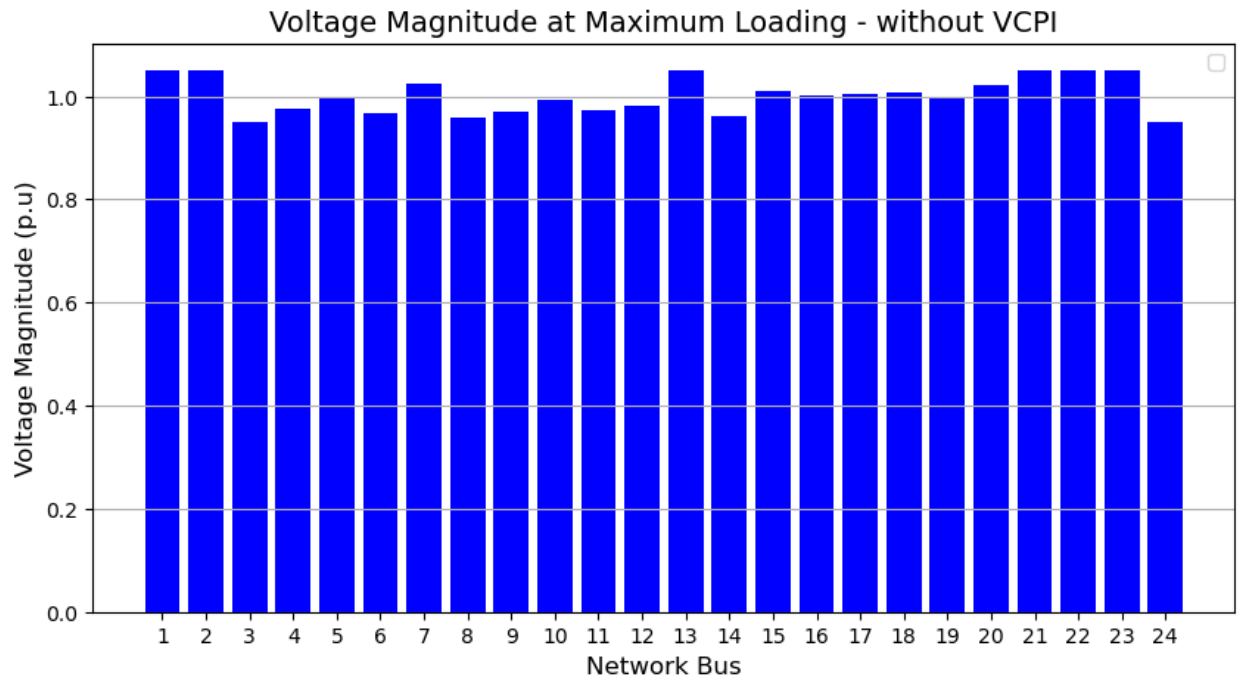
Figure 4.13: Voltage magnitude during maximum loading at t0018 - Scenario 3

Figure 4.13 shows the magnitude of the voltage variation across the examined network while it is under the highest loading. At t0018, when the system is under maximum loading, this results in unstable conditions in the network. At this period, the voltage across the network peaked at 1.05 pu at bus 1, bus 2, bus 13, bus 21, bus 22, and bus 23, as shown in Figure 4.13. During this period, the maximum VCPI level in the network is 0.838, occurring on the branch between bus 12 and bus 23. Also, this index value happens to be the maximum VCPI across the expansion planning horizon. The index value of 0.838 indicates that a further increase in the power flow across the line or more load in the network load would lead to intense voltage instability, as seven different buses are already at their peaked voltage levels.

4.3.2 GEP Solution from Scenario 4 in the REMix Framework

Scenario 4 system is used to analyze the result of the voltage security-constrained model. As in scenario 2, the increase in load is modelled by an electrolyzer and depicted in Figure 4.14. For this scenario, a hydrogen demand of 58.14 GWh is implemented in the expansion planning to activate the electrolyzers in the network. However, the optimization model determines the installation of the electrolyzers totaling 2422.5 MW at each hour to meet the demand for hydrogen. At the end of the planning horizon, the allocation of these electrolyzers is given in Appendix Table C.2 ranging from the largest capacity of 283.05 MW at node 18 and the smallest capacity of 60.35 MW at node 5 at the final stage of the expansion period.
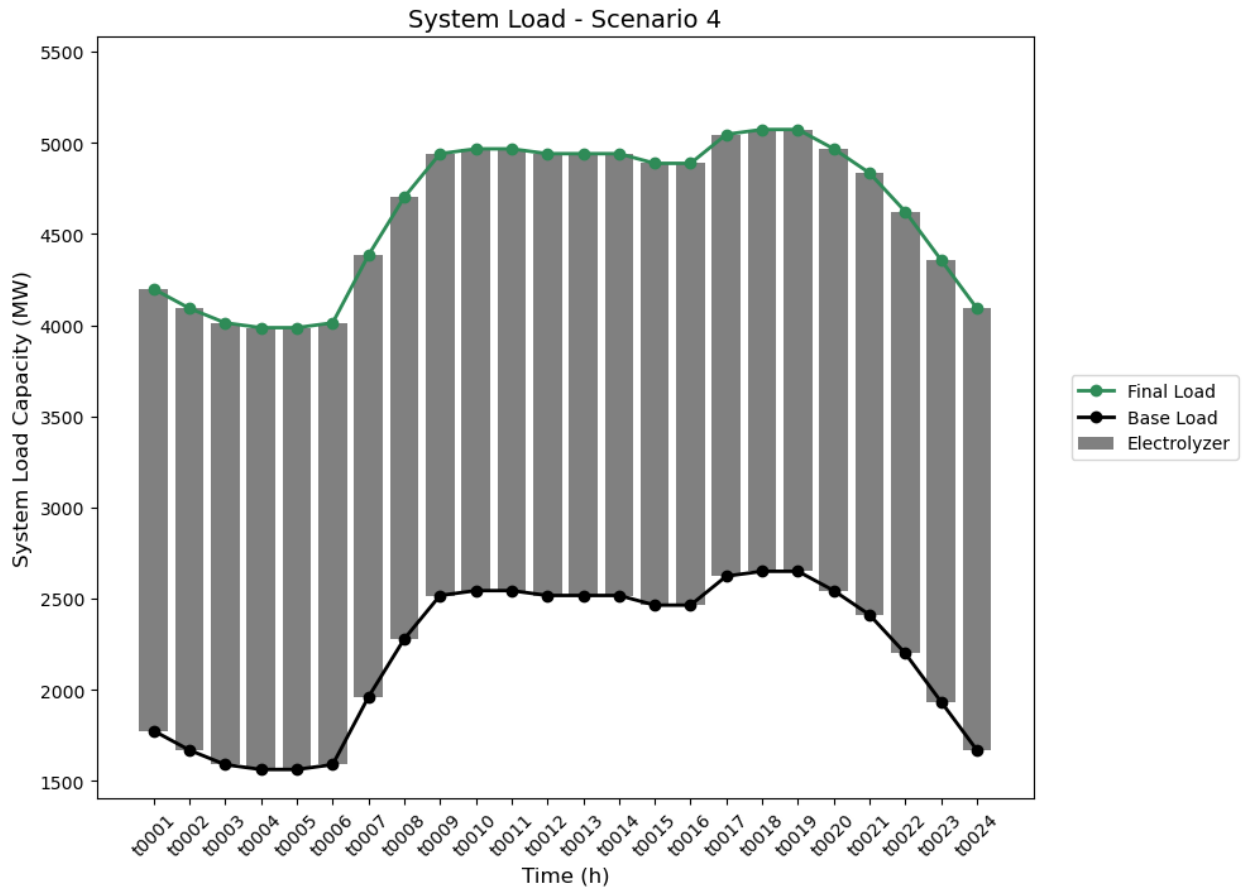
Figure 4.14: Electrolyzer Capacity from Scenario 4 Model

To ensure that the demand from the electrolyzers is satisfied by the wind turbines' supply, the wind power plants' output is scaled to optimize their potential better. Figure 4.15 illustrates the combination of the installed generators and the dispatch capacity across the expansion period. The demand for hydrogen is used for the load expansion from the base loading of the IEEE-24 Bus network. Conventional generators satisfy most of the base load, and the wind turbines' electricity satisfies the electrolyzer's demand. Since more wind turbines are used to satisfy the more significant load, the emission level is now 16.551 kt. While other conventional generators are available across the expansion period, Gen 5 and Gen 11 are entirely replaced by the network's wind power plants at node 15.
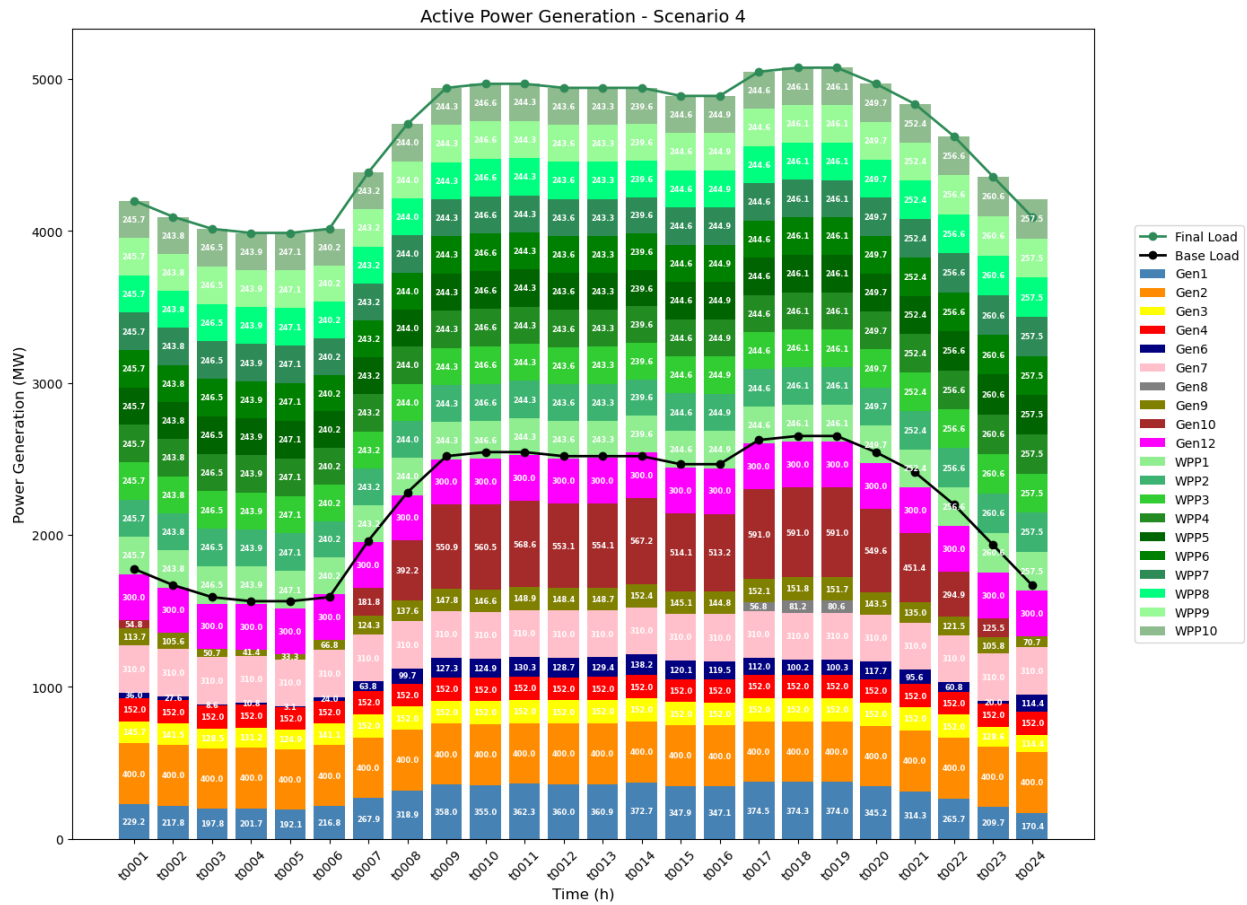
Figure 4.15: Active Power Generation from Scenario 4 Model

Table 4.5 gives the installed generator capacity and the systems cost at the end of the generation expansion planning horizon while incorporating VCPI into the model. As the model optimizes the solution while considering voltage stability across the network, more generator capacities are dispatched; however, the system cost is 990 Mio USD. The full potential of 300 MW for the wind power plants is built at the end of the planning horizon, reducing the operation cost.

Less conventional generators are installed across the planning horizon, and with the introduction of wind turbines into the modelling framework, more wind power plants are built. With this integration, the impact of the alternating generation output, especially on the voltage stability of the new, is observed and controlled. Ten wind power plants are built at the end of the capacity expansion. Looking at the conventional generators as shown in Table 4.5, Aside from Gen2 (400 MW), Gen3 (152 MW), Gen4 (152 MW), Gen7 (310 MW), Gen10 (591 MW), and Gen12 (300 MW) that built their full potential, the model only built a fraction of the other conventional generators. 375 MW capacity of Gen 1 is built out of a potential of 350 MW. For Gen9, 153 MW capacity is built from a potential of 350 MW. 82 MW capacity of Gen 8 is built out of a potential of 350 MW. For Gen 6, 139 MW is built from a potential of 155 MW. The optimized solution of the model entirely replaces Gen 11

Table 4.5: GEP Solution for Scenario 4

Node	Generator	Capacity [MW]	Wind Power Plant (WPP)	Capacity [MW]	Investment Cost [Tsd USD]	Operation Cost [Tsd USD]
1	Gen 3	152	WPP 3	300	37797.6	46458.8
2	Gen 4	152	WPP 4	300	31945	48591.4
7	Gen 9	153	WPP 8	300	36764.5	60451.4
13	Gen 10	591	WPP 9	300	64023.2	214229
15	-	-	WPP 5	300	27528	-
16	Gen 6	139	WPP 6	300	34092.6	19972.3
18	Gen 1	375	WPP 1	300	46843.7	39024.4
21	Gen 2	400	WPP 2	300	54553.4	52512
22	Gen 12	300	WPP 10	300	46053.5	-
23	Gen 7, Gen 8	392	WPP 7	300	41836.4	85546.7
Total					421437.9	566786.0012
System Cost					988223.9012	

and Gen 5. Figure 4.16 gives the variation of voltage magnitude across during maximum loading on the network with the incorporation of voltage stability index in the modelling framework consisting of wind turbines and conventional generators. The voltage peaked at 1.022 pu at Bus 15 during this period is examined. During this period, the maximum VCPI level in the network was 0.7266, occurring on the branch line between bus 7 and bus 8. This implies that even at the highest loading time, the network can keep the voltage at the bus as close as possible to 1 pu, ensuring the voltage stability of the system.
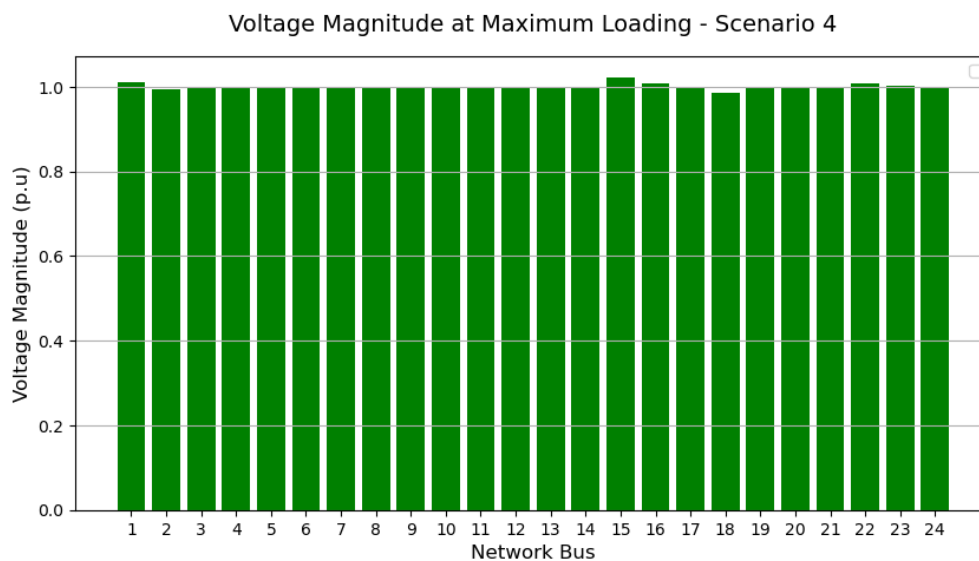
Figure 4.16: Voltage magnitude during maximum loading at t0018 with voltage improvement- Scenario 4

4.3.3 Comparison of GEP Solution from Scenario 3 and Scenario 4

This section elucidates comparing Scenario 3 (without VCPI) and Scenario 4 (with VCPI) by integrating wind power plants in the modelling framework. Moreover, it deliberates the impact of having additional voltage stability in capacity expansion planning. Figure 4.17 illustrates this comparison regarding system cost and maximum VCPI over the expansion period and maximum active power loss across the network in a single period.
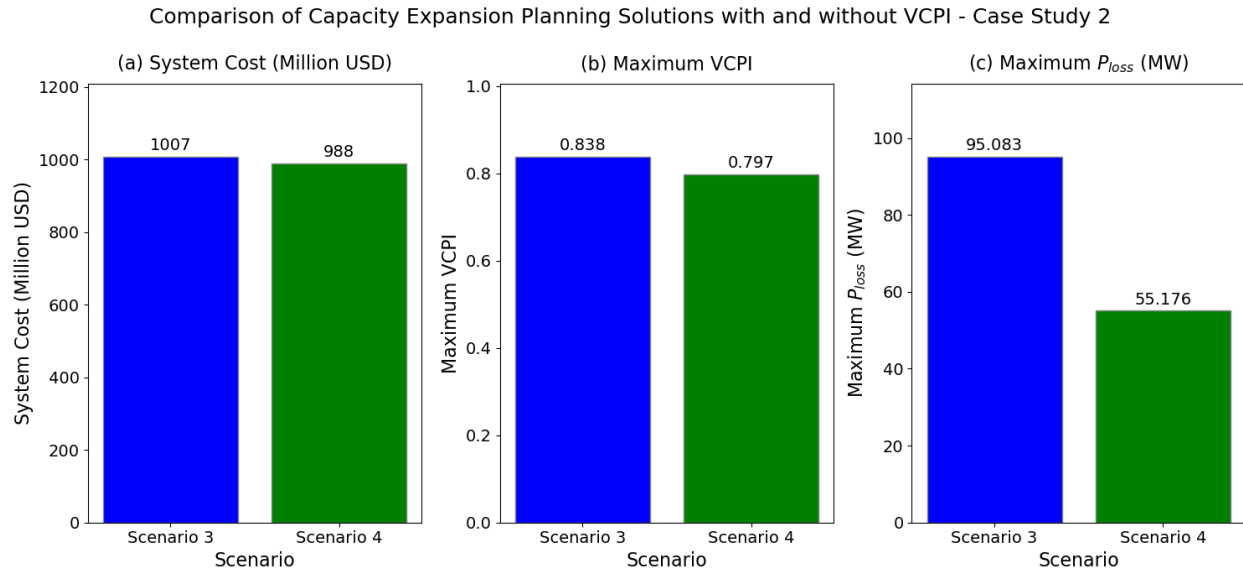
Figure 4.17: Comparison of the capacity expansion planning solutions with and without voltage stability index - Case 2

Figure 4.17 highlights the notable difference between Scenario 3 and Scenario 4 across the three observed vital indicators. From the subplot 4.17(a), It is evident that Scenario 4 resulted in a lower system cost of about 990 Mio USD, slightly lower than in Scenario 3 with about 1007 Mio USD. This is a result of the different operational costs of the two scenarios. Scenario 3 has more conventional generators built, giving it more operation cost than Scenario 4, with more wind turbines having no operation cost. However, scenario 4 has a higher investment cost of about 422 Mio USD as more capacity can ensure sufficient dispatch to maintain the system stability.

Furthermore, in Figure 4.17(b), an improvement is observed with a significant decrease in the maximum VCPI from 0.838 in Scenario 3 to 0.797 in Scenario 4, reflecting a 4.89% enhancement in the network's voltage stability. This improvement is vital because VCPI is integral to modelling voltage stability within the capacity expansion framework despite the fluctuation in the voltage magnitude at the buses due to the presence of wind turbines in the expansion model and high load demand. The subplot 4.17(c) depicts a notable decrease in the active power losses in Scenario 4, resulting in 55.176 MW compared to 95.83 MW in

Scenario 2. This reduction in power loss indicates an improvement of 41.97% in the network flow. In addition, Figure 4.18 compares the impact of incorporating VCPI in the capacity expansion planning by elaborating on the voltage magnitude profile of eight network buses at the last stage of the expansion planning.
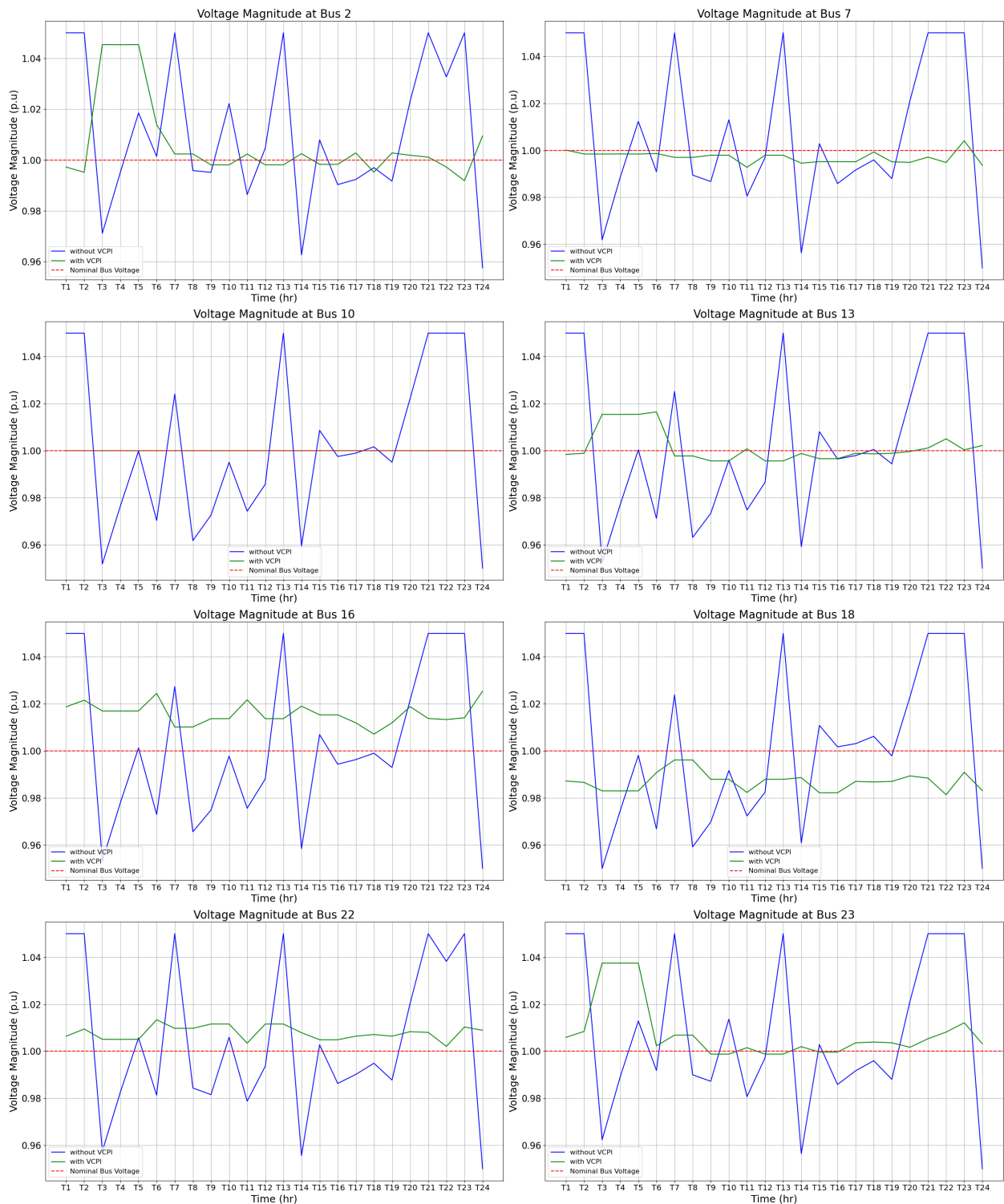
Figure 4.18: Comparison of Voltage Magnitude Across Selected Network Buses in Scenario 3 and Scenario 4

To examine the variation of the VCPI's impact on the system voltage stability when renewable energy sources are in the network, Figure 4.18 illustrates these impacts on selected buses. The buses in focus for the analysis include Bus 2, Bus 7, Bus 10, Bus 13, Bus 16, Bus 18, Bus 22 and Bus 23. Similarly, as in the case 1 analysis, the graphs of the buses consist of two curves, each representing the voltage magnitude when the VCPI is factored into the model, and the other shows the voltage level without VCPI consideration. The effect of having a voltage stability index as part of the modelling framework during capacity expansion planning can be seen as it helps to maintain the voltage at the buses close to the desired levels. In Scenario 3, where VCPI is not included, the voltage magnitude across all the buses fluctuates rapidly from values as low as 0.95 pu to a maximum value of 1.055 pu, resulting in instability in the system. This frequent fluctuation in the voltage level can be majorly attributed to the continuous variation in the wind power plant outputs built during the capacity expansion planning.

On the other hand, with the incorporation of VCPI in the model and as seen in the results of Scenario 4, the voltage magnitude fluctuates less rapidly across the reference voltage level, and their values are close to the reference voltage magnitude of 1 pu. At Bus 2, the voltage peaks at 1.045 pu (144.21 kV) and the lowest with a magnitude of 0.992 pu (136.90 kV). At this bus, the voltage level varies close to the reference bus voltage. At Buses 7, 13, 16, 18, 22, and 23, the voltage is maintained close to the reference voltage level. For Bus 10, the voltage level is maintained at 1 pu (138 kV), ensuring the system stability. Lastly, without VCPI, the voltage magnitudes exhibit significant swings away from the optimal value, signifying an unstable system with potential over or under-voltage situations. Conversely, the voltage readings with VCPI remain better regulated and closer to the ideal voltage level desired in the power network during and after expansion, underscoring VCPI's crucial role in the system voltage's stability. Figure 4.19 gives the final outlook of the solution obtained from the generation expansion planning with voltage improvement in case study 2. The resultant system operates under two voltage situations of 138 kV and 230 kV. 10 conventional generators and 10 wind power plants are installed, with 34 active transmission lines and 5 transformers. The maximum load experienced by the system is 5073 MW.
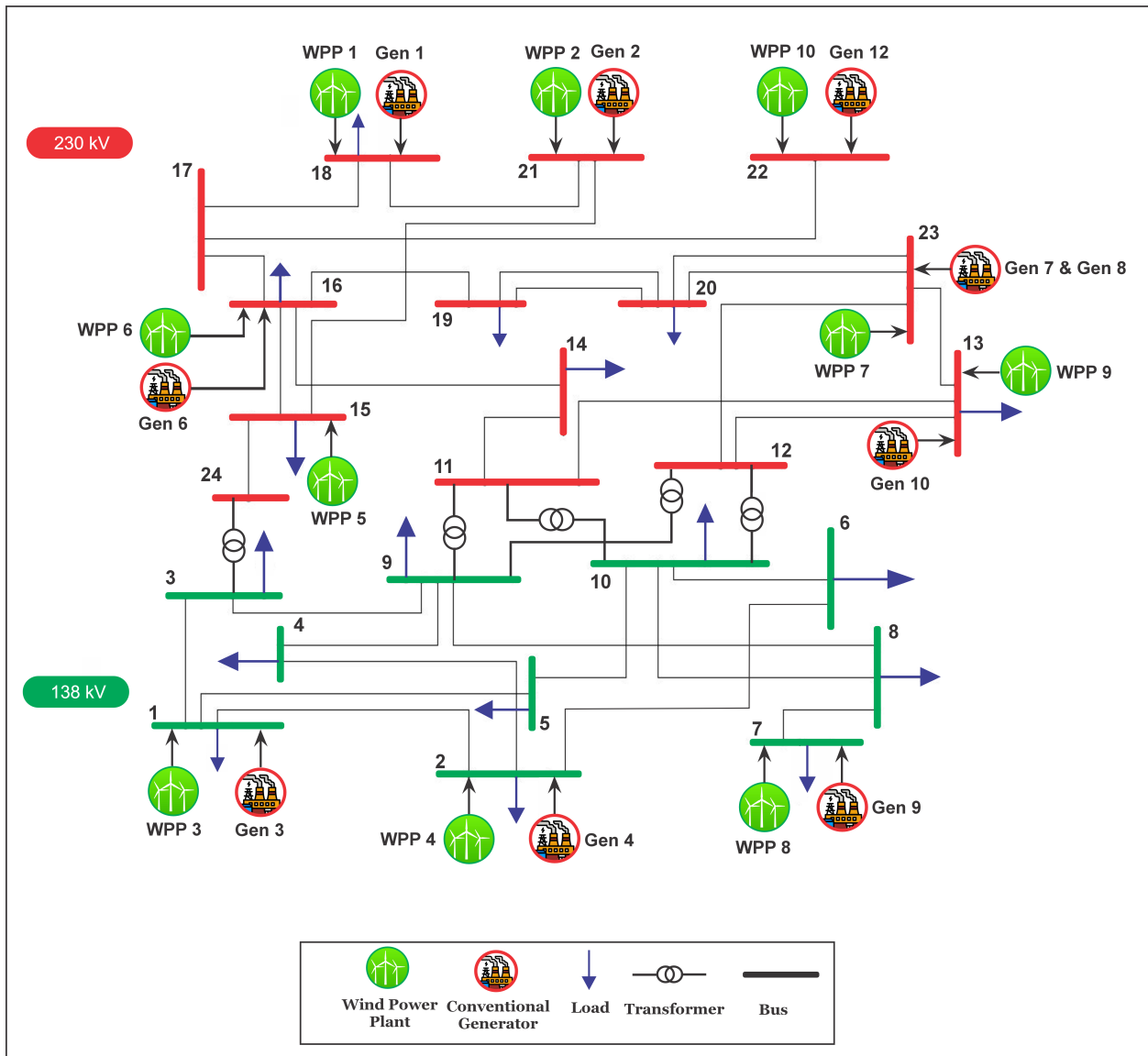
Figure 4.19: IEEE RTS 24-bus Network Solution with Voltage Profile Improvement - Case 2

Chapter 5

Conclusions and Future Research Outlook

This thesis has successfully introduced and applied a method of incorporating the concept of voltage stability during Capacity Expansion Planning in REMix, especially for networks with high renewable energy integration. Through a systematic methodology involving algorithm development for Voltage Security Constrained Optimal Power Flow (VSC-OPF) and adaptation of the Generation Expansion Planning (GEP) model to enhance voltage stability while optimizing system cost. Using only the conventional voltage magnitude constraint cannot ensure the desired level of voltage stability in a power system, majorly due to the dynamic nature and nonlinearity of the power system, especially under stressed conditions [66]. Simple voltage magnitude measures may not capture the nonlinear and dynamic interactions between loads, generation, and transmission network components, which can lead to voltage instability. As such, VCPI is applied in the capacity expansion planning model.

By defining voltage stability indices, investigating different scenarios for generation expansion planning, and validating the proposed models to ensure voltage stability during CEP modelling in REMix, this master thesis provides a solid foundation for enhancing the reliability and sustainability of electricity networks. The study's contribution is bridging the gap where energy system optimization models, such as REMix, need to be kept simple, thereby developing an advanced model that combines optimization capabilities with stability measures to ensure a secure power supply for future systems. The research objectives have been gaining an in-depth understanding of voltage stability analysis methods, integrating voltage stability constraints into optimal power flow algorithms, and developing models and scenarios tailored for networks with renewable energy sources.

In the first instance, the algorithm is applied to the IEEE RTS 24-bus system with 34 lines and 12 base generators within the supporting modelling framework model—the weakest buses and lines in the existing network before the network expansion are identified. The most critical line is the branch between Bus 12 and Bus 23 while trying to optimize the fuel cost.

A DC-OPF model is then set up in REMix to compare the result obtained in the validation model within MATLAB. When the DC-OPF is executed in the REMix model of the base case network, the operating cost is optimized to be the same as that obtained in the Supporting model.

Two case studies are implemented to analyze the impact of the voltage stability index on the power system network during capacity expansion. In each case, there are two scenarios where capacity expansion planning is executed with or without the integration of VCPI in the modelling framework. In case 1, which involves generation expansion planning with only conventional generators, there are Scenarios 1 and 2. In this case study, the maximum load for which the GEP is solved is 3106.5 MW. In case 2, the maximum load within the planning horizon is 5073 MW, and the wind power plants are now incorporated into the modelling framework. This second case study consists of Scenario 3 (without VCPI) and Scenario 4 (with VCPI).

In Scenario 1 of the capacity expansion planning model, only conventional generators were considered without incorporating additional voltage stability constraints. The solution comprises 12 generators to satisfy the defined system loading within the planning horizon formulated in the REMix environment. The built system is then implemented in the supporting software to analyze the system's voltage stability. The results showed a system cost of about 892 Mio USD, a maximum VCPI of 0.598, and a maximum active power loss of 82.79 MW. In Scenario 2, the capacity expansion planning model incorporated additional voltage stability constraints through VCPI. The result indicated an increase 7.96% in the system cost but showed significant improvements in voltage stability, with the maximum VCPI reduced to 0.539. These additional costs are acceptable to improve the system security as the network grows more prominent. Additionally, there was a substantial decrease in power losses to 51.39 MW, demonstrating a more efficient network operation with a 37.92% reduction in losses compared to Scenario 1. Integrating VCPI into the planning process resulted in additional generation capacity, leading to increased operational and investment costs, ultimately enhancing system stability and efficiency while providing long-term cost savings.

Furthermore, In case study 2 with a high share of renewable energy sources, in this instance, the study of a wind power plant, the voltage level across the network of buses continuously fluctuates more rapidly due to constant variation in the output of the wind turbines, making the wind farms. In Scenario 3 of the capacity expansion planning model, 11 conventional generators with a minimum capacity of 60 MW (Generator 11), a maximum capacity of 591 MW (Generator 10), and 10 Wind Power Plants, each with 300 MW capacity, were built. The voltage levels varied widely, ranging from as low as 0.95 pu to a maximum of 1.055 pu, resulting in system instability. These fluctuations were attributed to continuous variations in wind farm output during the expansion planning. Without VCPI, the voltage

magnitudes exhibited significant swings away from the optimal values, indicating an unstable system with potential over or under-voltage situations.

In Scenario 4, VCPI was integrated, resulting in more stable voltage magnitudes across the network buses. The system load is modelled as an electrolyzer for easy demand flexibility. The voltage fluctuations in this scenario were rapidly reduced, with values closer to the reference voltage magnitude of 1 pu. The results showed improved voltage stability, with the maximum VCPI reduced from 0.838 in Scenario 3 to 0.797 in Scenario 4, reflecting a 4.89% enhancement. Active power losses notably decreased by 41.97%, depicting improved network flow efficiency. Including VCPI in Scenario 4 helped maintain voltage levels close to the desired values, ensuring system stability and efficient network operation during the expansion planning phase.

The implementation and testing of the developed model on the IEEE 24 bus system demonstrate the effectiveness of incorporating voltage security constraints in generating expansion planning. This highlights the importance of considering voltage stability in capacity expansion planning to address renewable energy integration challenges.

This thesis improves the modelling framework REMix by supporting it with results obtained from the MATLAB tool, which integrates a voltage security-constrained GEP method. As a result, this thesis contributes valuable insights into electrical engineering and offers practical solutions for maintaining voltage stability in the face of evolving power system dynamics.

The capacity expansion studied by authors in [67], which aimed at implementing wind generation capacity expansion using a voltage stability constrained problem, showed a similar result to this thesis research, as more wind capacity are dispatched to the grid as determined by the optimization algorithm when considering the impact of the voltage stability constraint. Moreover, the work of [5] that studied the impact of voltage stability-constrained low-carbon generation, and transmission expansion planning revealed that introducing this additional constraint increases the GEP system cost and decreased the values of the voltage stability index across the network. These outcomes are also in line with the observations in this thesis project.

The approach used in integrating VCPI into CEP for voltage stability in power systems with high renewable integration offers several benefits but also comes with limitations. A critical appraisal recognizes the enhanced ability to identify and mitigate voltage stability issues preemptively, thus improving grid reliability. However, limitations include the complexity of accurately modelling renewable energy variability and the potential computational challenges of integrating advanced voltage stability indices into large-scale CEP models. These aspects underline the need for continued innovation in modelling techniques and computational strategies to fully realize the benefits while mitigating the drawbacks.

In future research, the voltage security-constrained optimal power flow could be inte-

grated into a linearized optimal power flow model implemented in the REMix environment. This would provide an avenue to further employ REMix in studies involving more large-scale power system projects while considering voltage stability. Also, aside from the use of particle swarm optimization solvers for optimal power flow, other solvers such as salp swarm optimization or other powerful solvers that could be easily compatible with the REMix framework could be introduced. The recommendations for future research underscore the ongoing transition towards more sustainable and reliable electricity networks, emphasizing the significance of integrating voltage stability considerations into CEP methodologies for a secure and efficient power supply in the era of renewable energy integration.

Appendix A

Parameter for IEEE RTS 24-Bus Network

Table A.1: Generating Units Data for the Base Case Network [35]

Gen	Bus	$P_{\max}$ [MW]	$P_{\min}$ [MW]	c_g [Tsd USD/MW]
g1	18	400	100	5.47
g2	21	400	100	5.47
g3	1	152	30.4	13.32
g4	2	152	30.4	13.32
g5	15	155	54.25	16
g6	16	155	54.25	10.52
g7	23	310	108.5	10.52
g8	23	350	140	10.89
g9	7	350	75	20.7
g10	13	591	206.85	20.93
g11	15	60	12	26.11
g12	22	300	0	0

Table A.2: Reactance and Capacity of Transmission Lines for the Base Case Network [35]

From Bus	To Bus	Reactance [p.u.]	Capacity [MVA]	From Bus	To Bus	Reactance [p.u.]	Capacity [MVA]
1	2	0.0139	175	11	13	0.0476	500
1	3	0.2112	175	11	14	0.0418	500
1	5	0.0845	175	12	13	0.0476	500
2	4	0.1267	175	12	23	0.0966	500
2	6	0.192	175	13	23	0.0865	500
3	9	0.119	175	14	16	0.0389	500
3	24	0.0839	400	15	16	0.0173	500
4	9	0.1037	175	15	21	0.0245	1000
5	10	0.0883	175	15	24	0.0519	500
6	10	0.0605	175	16	17	0.0259	500
7	8	0.0614	175	16	19	0.0231	500
8	9	0.1651	175	17	18	0.0144	500
8	10	0.1651	175	17	22	0.1053	500
9	11	0.0839	400	18	21	0.013	1000
9	12	0.0839	400	19	20	0.0198	1000
10	11	0.0839	400	20	23	0.0108	1000
10	12	0.0839	400	21	22	0.0678	500

Table A.3: Load Data for the Base Case Network [35]

Bus	Load [MW]	Bus	Load [MW]
1	108	10	195
2	97	13	265
3	180	14	194
4	74	15	317
5	71	16	100
6	136	18	333
7	125	19	181
8	171	20	128
9	175		

Table A.4: Reactance and Length Implemented for REMix

From Bus	To Bus	Reactance [p.u.]	Reactance [Ω]	Length [km]
1	2	0.01	2.65	0.26
1	3	0.21	40.22	4.02
1	5	0.08	16.09	1.61
2	4	0.13	24.13	2.41
2	6	0.19	36.56	3.66
3	9	0.12	22.66	2.27
3	24	0.08	15.98	1.60
4	9	0.10	19.75	1.97
5	10	0.09	16.82	1.68
6	10	0.06	11.52	1.15
7	8	0.06	11.69	1.17
8	9	0.17	31.44	3.14
8	10	0.17	31.44	3.14
9	11	0.08	15.98	1.60
9	12	0.08	15.98	1.60
10	11	0.08	15.98	1.60
10	12	0.08	15.98	1.60
11	13	0.05	9.06	0.91
11	14	0.04	7.96	0.80
12	13	0.05	9.06	0.91
12	23	0.10	18.40	1.84
13	23	0.09	16.47	1.65
14	16	0.04	7.41	0.74
15	16	0.02	3.29	0.33
15	21	0.02	4.67	0.47
15	24	0.05	9.88	0.99
16	17	0.03	4.93	0.49
16	19	0.02	4.40	0.44
17	18	0.01	2.74	0.27
17	22	0.11	20.05	2.01
18	21	0.01	2.47	0.25
19	20	0.02	3.77	0.38
20	23	0.01	2.06	0.21
21	22	0.07	12.91	1.29

Table A.5: Load Profile for the Base Network over 24 hour period [68]

Hour	System Load [MW]	Hour	System Load [MW]
1	1775.835	13	2517.975
2	1669.815	14	2517.975
3	1590.3	15	2464.965
4	1563.795	16	2464.965
5	1563.795	17	2623.995
6	1590.3	18	2650.5
7	1961.37	19	2650.5
8	2279.43	20	2544.48
9	2517.975	21	2411.955
10	2544.48	22	2199.915
11	2544.48	23	1934.865
12	2517.975	24	1669.815

Table A.6: Investment Data for Generation Units [5]

Invest	perUnitBuild	useAnnuity	amorTime	Interest
gen1	710.0	1.0	30.0	0.06
gen10	850.0	1.0	30.0	0.06
gen11	900.0	1.0	30.0	0.06
gen12	850.0	1.0	30.0	0.06
gen2	930.0	1.0	30.0	0.06
gen3	930.0	1.0	30.0	0.06
gen4	400.0	1.0	30.0	0.06
gen5	510.0	1.0	30.0	0.06
gen6	654.0	1.0	30.0	0.06
gen7	417.0	1.0	30.0	0.06
gen8	834.0	1.0	30.0	0.06
gen9	834.0	1.0	30.0	0.06
wpp	1173.0	1.0	25.0	0.06

Appendix B

Wind Power Plant Generation Profile

Table B.1: Generation Profile of 300 MW Enercon Wind Power Plant [61]

Timestamp	Windpower (MW)
t0001	155.700838
t0002	167.880559
t0003	181.119721
t0004	177.913328
t0005	191.603252
t0006	201.808547
t0007	202.109903
t0008	207.05633
t0009	207.051154
t0010	200.388788
t0011	195.380545
t0012	198.020346
t0013	212.129439
t0014	222.49669
t0015	229.634505
t0016	237.978391
t0017	244.608817
t0018	246.057117
t0019	246.139536
t0020	249.702098
t0021	252.42247
t0022	256.550328
t0023	260.574171
t0024	257.47948

Appendix C

Other Results and Plots [REMix and MATLAB]

Table C.1: Electrolyzer Capacity - Scenario 2

Node	Electrolyzer Capacity (MW)	Node	Electrolyzer Capacity (MW)
1	17.28	10	31.2
2	15.52	13	42.4
3	28.8	14	31.04
4	11.84	15	50.72
5	11.36	16	16
6	21.76	18	53.28
7	20	19	28.96
8	27.36	20	20.48
9	28		

Table C.2: Electrolyzer Capacity - Scenario 4

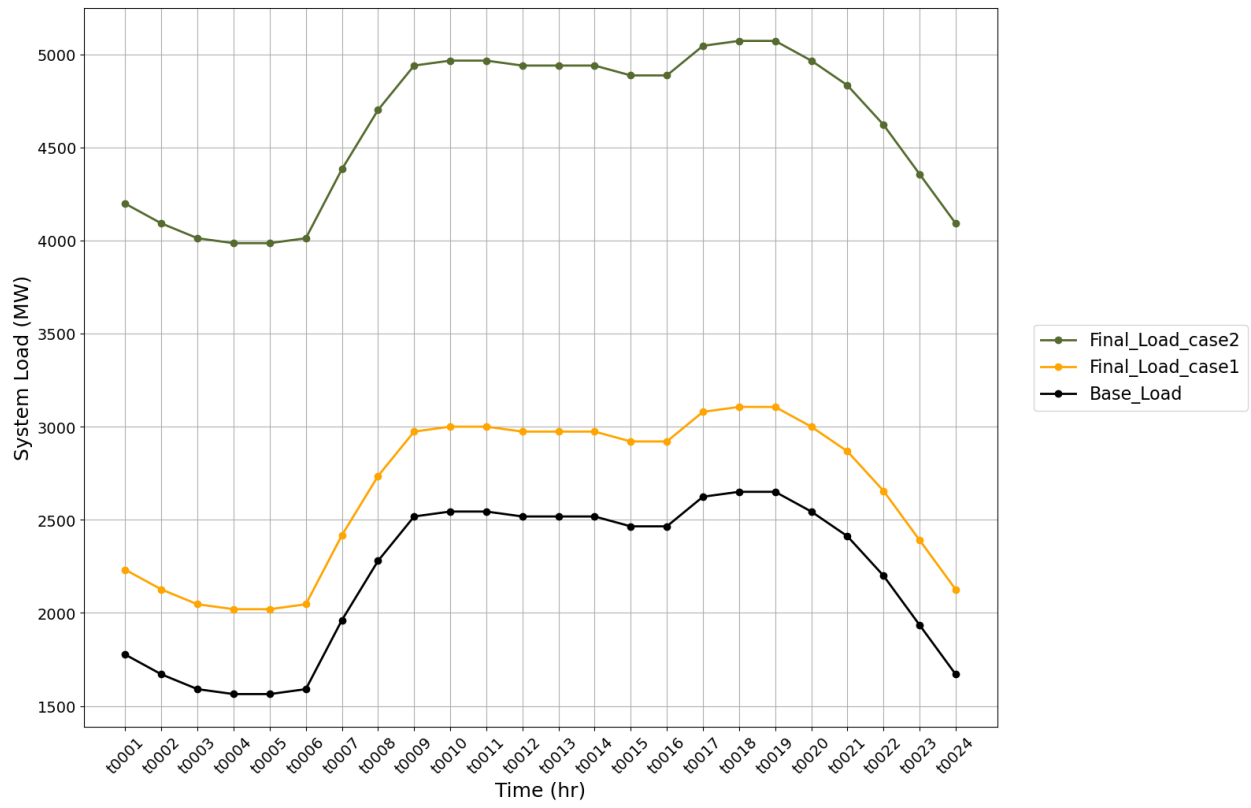| Node	Electrolyzer Capacity (MW)	Node	Electrolyzer Capacity (MW)
1	91.8	10	165.75
2	82.45	13	225.25
3	153	14	164.9
4	62.9	15	269.45
5	60.35	16	85
6	115.6	18	283.05
7	106.25	19	153.85
8	145.35	20	108.8
9	148.75		

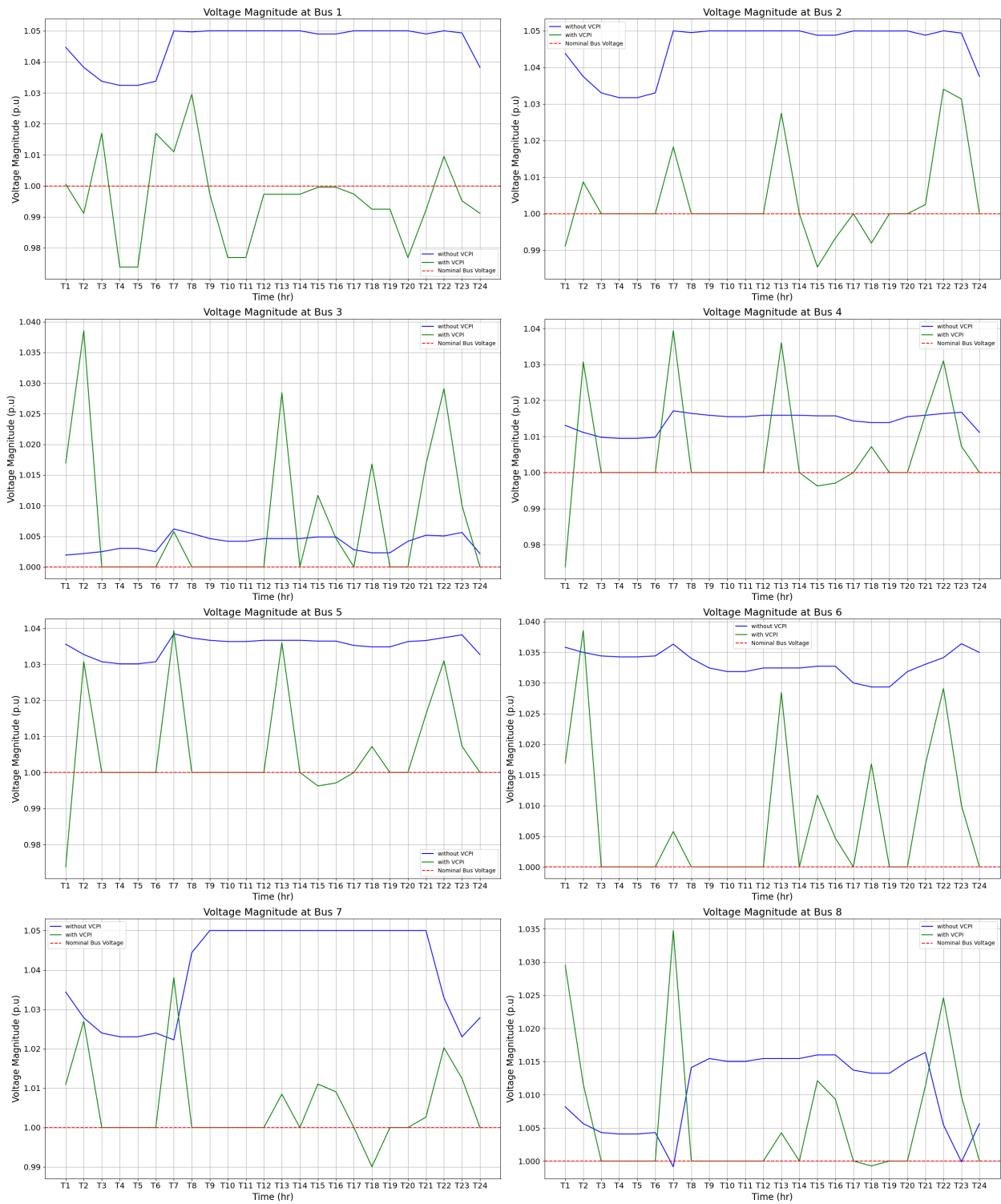Figure C.1: System Load Profile Over the Planning Horizon

Figure C.2: Comparison of Voltage Magnitude Across Network Buses in Scenario 1 and Scenario 2 - Bus 1 to Bus 8
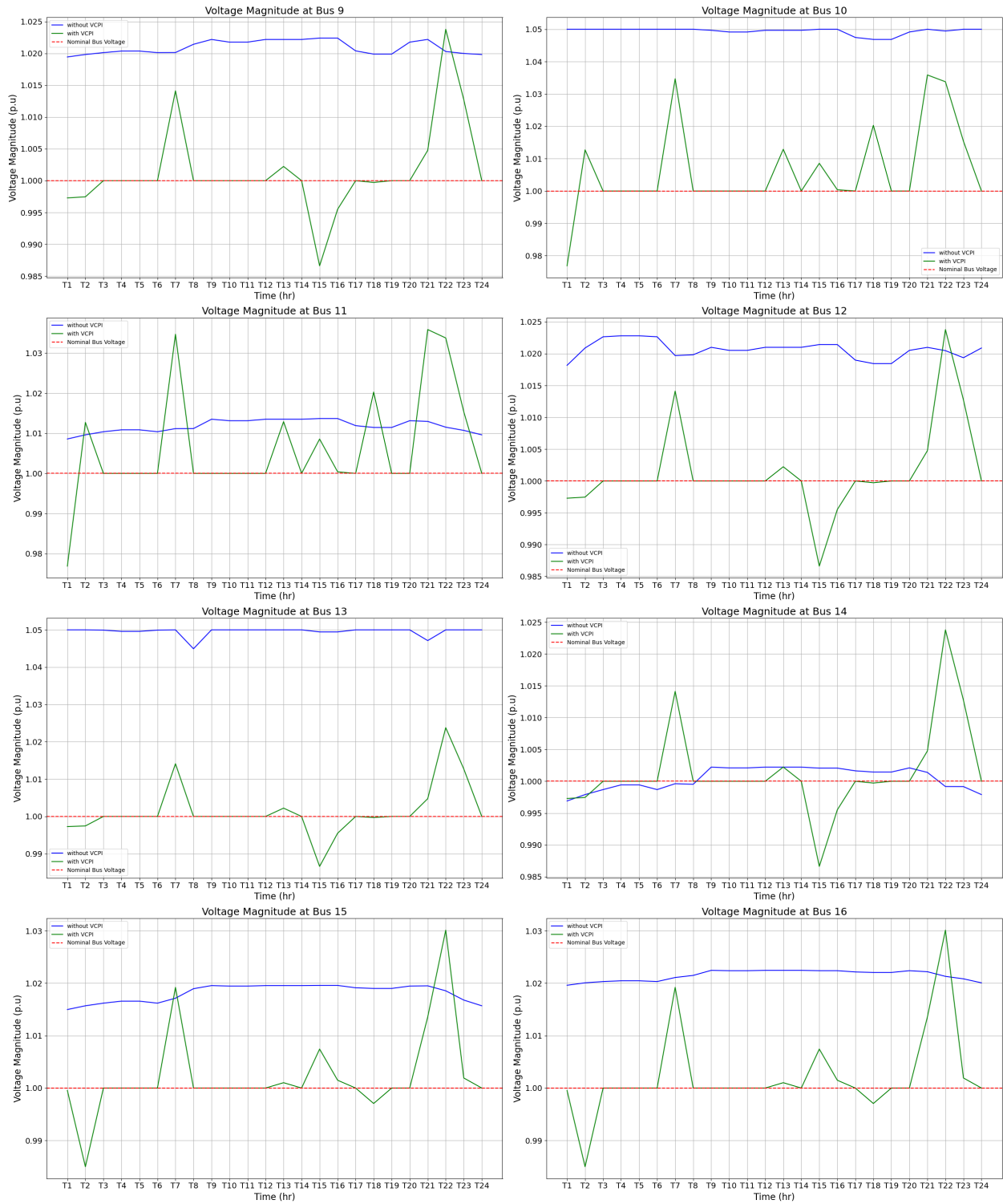
Figure C.3: Comparison of Voltage Magnitude Across Network Buses in Scenario 1 and Scenario 2 - Bus 9 to Bus 16
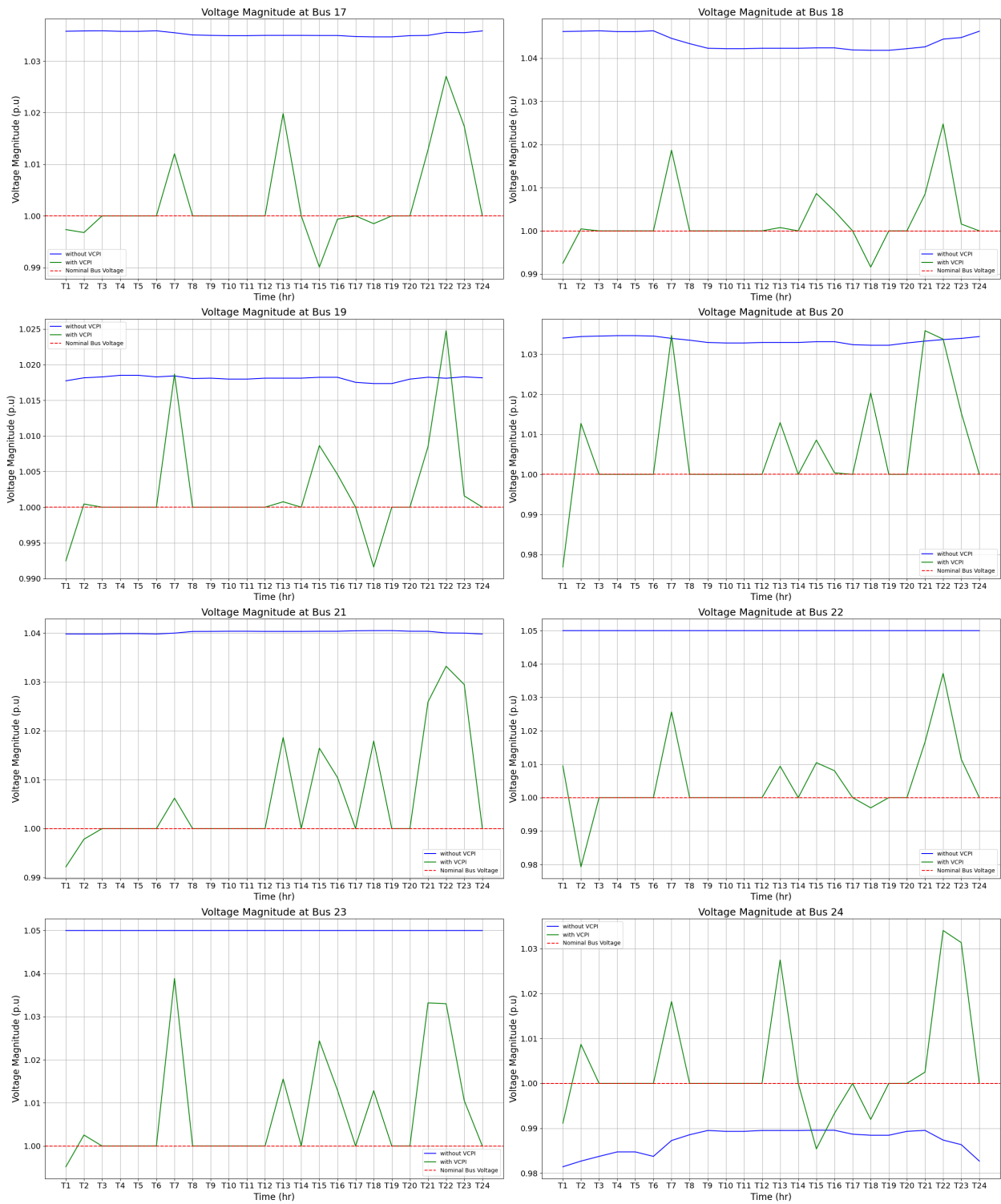
Figure C.4: Comparison of Voltage Magnitude Across Network Buses in Scenario 1 and Scenario 2 - Bus 17 to Bus 24
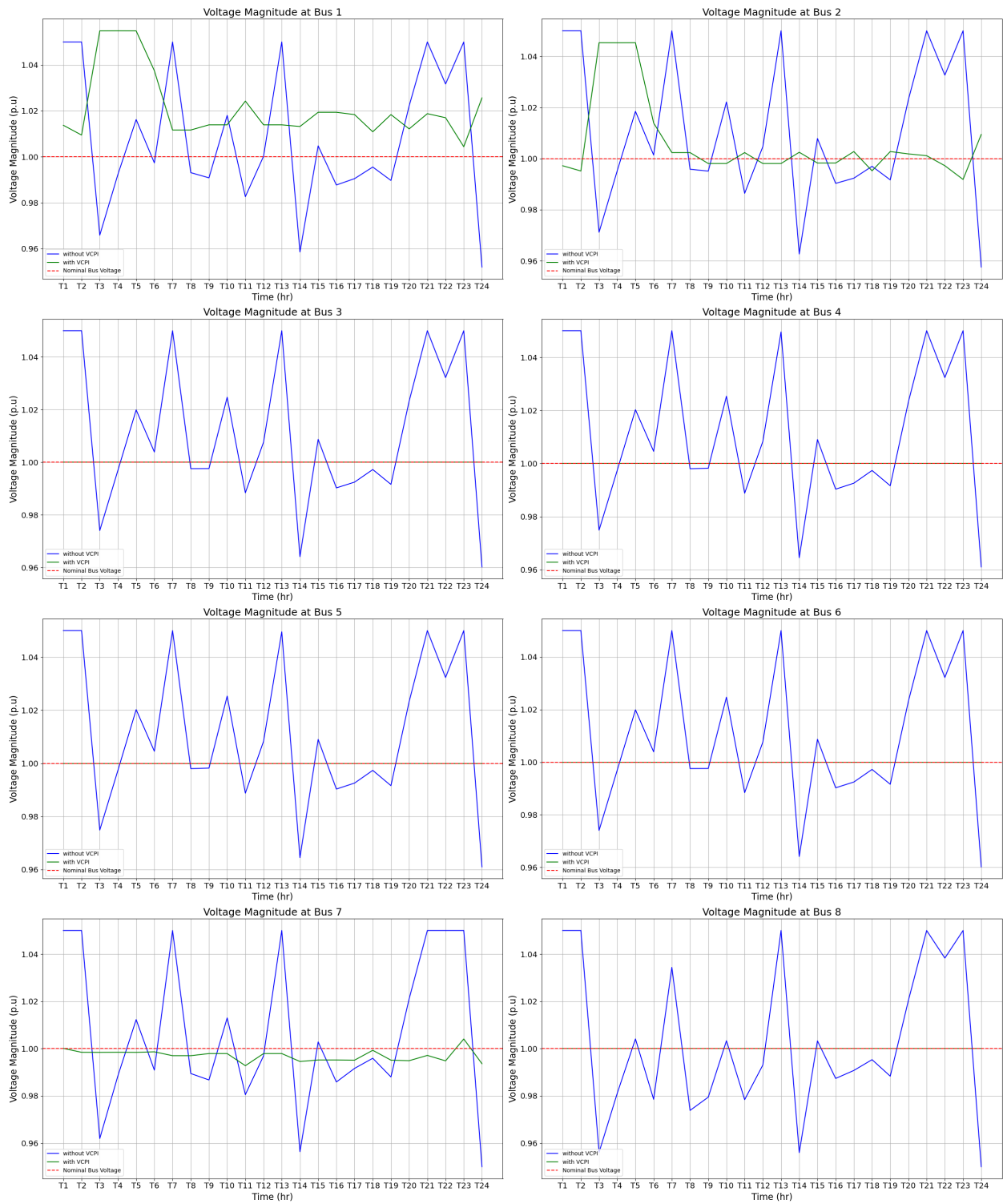
Figure C.5: Comparison of Voltage Magnitude Across Network Buses in Scenario 3 and Scenario 4 - Bus 1 to Bus 8
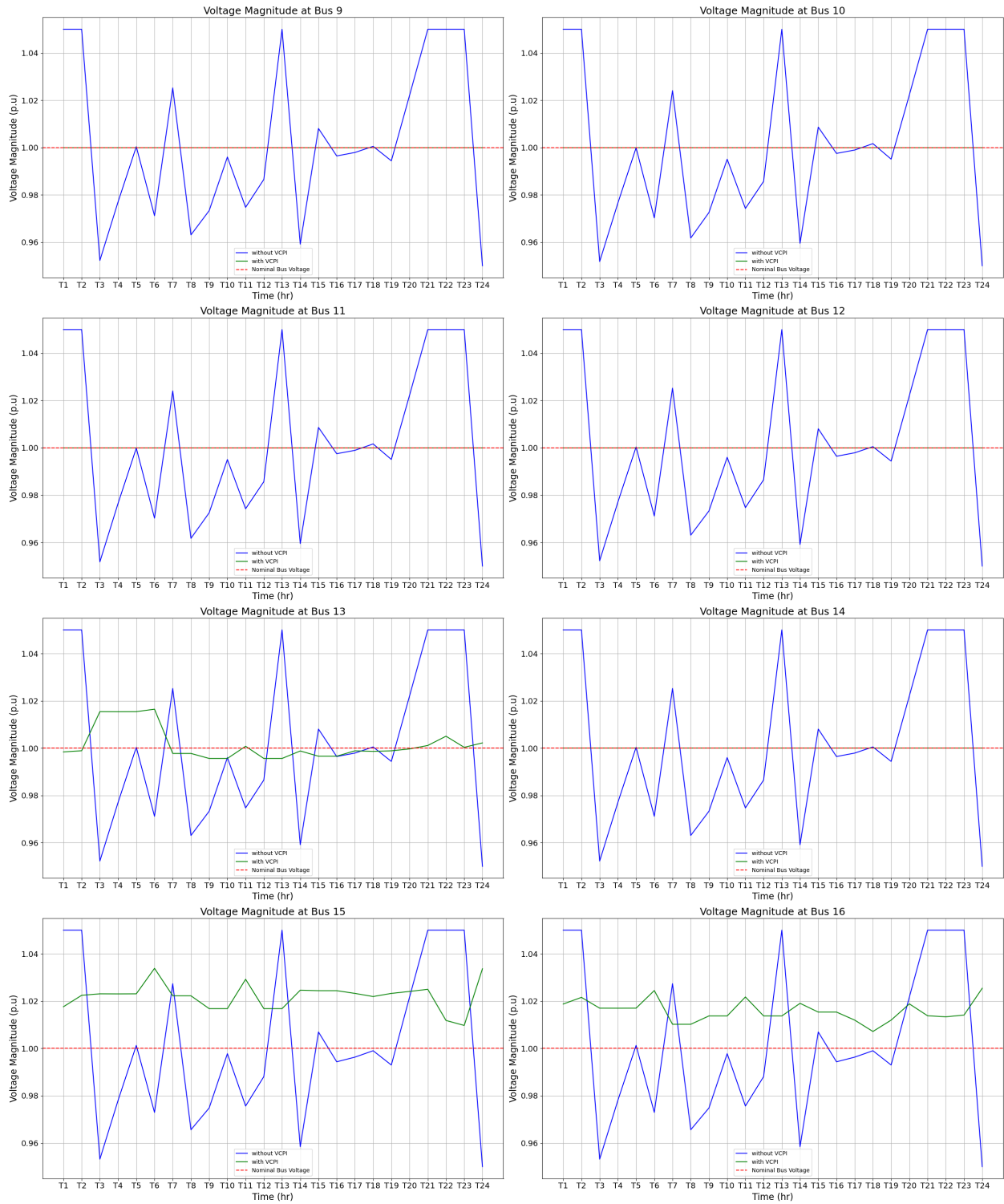
Figure C.6: Comparison of Voltage Magnitude Across Network Buses in Scenario 3 and Scenario 4 - Bus 9 to Bus 16
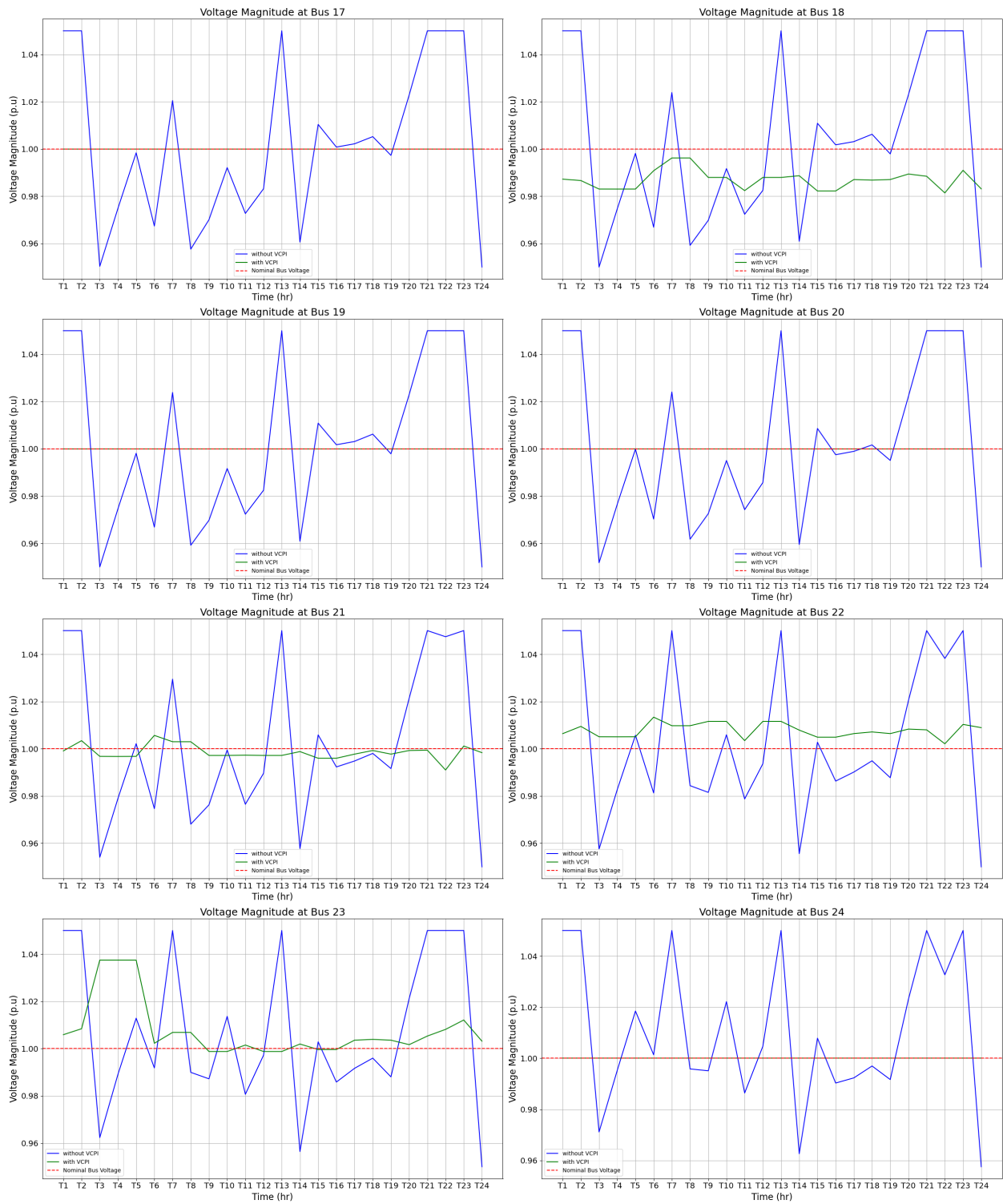
Figure C.7: Comparison of Voltage Magnitude Across Network Buses in Scenario 3 and Scenario 4 - Bus 17 to Bus 24

References

[1] T. Zabaiou, L.-A. Dessaint, and I. Kamwa, "Preventive control approach for voltage stability improvement using voltage stability constrained optimal power flow based on static line voltage stability indices," *IET Generation, Transmission & Distribution*, vol. 8, no. 5, pp. 924–934, 2014.

[2] K. Yamashita, S.-K. Joo, J. Li, P. Zhang, and C.-C. Liu, "Analysis, control, and economic impact assessment of major blackout events," *European Transactions on Electrical Power*, vol. 18, no. 8, pp. 854–871, 2008.

[3] C. A. Canizares *et al.*, "Voltage stability assessment: Concepts, practices and tools," *IEEE/PES power system stability subcommittee special publication*, no. SP101PSS, 2002.

[4] P. Kundur, J. Paserba, and S. Vitet, "Overview on definition and classification of power system stability," in *CIGRE/IEEE PES International Symposium Quality and Security of Electric Power Delivery Systems, 2003. CIGRE/PES 2003.*, IEEE, 2003, pp. 1–4.

[5] V. Asgharian and M. Abdelaziz, "Voltage stability constrained low-carbon generation & transmission expansion planning," in *2020 IEEE Canadian Conference on Electrical and Computer Engineering (CCECE)*, IEEE, 2020, pp. 1–5.

[6] M. Moradzadeh and M. Abdelaziz, "Reducing the loss of life of distribution transformers affected by plug-in electric vehicles using electric water heaters," in *2019 IEEE Canadian Conference of Electrical and Computer Engineering (CCECE)*, IEEE, 2019, pp. 1–5.

[7] P. Kessel and H. Glavitsch, "Estimating the voltage stability of a power system," *IEEE Transactions on power delivery*, vol. 1, no. 3, pp. 346–354, 1986.

[8] V. Balamourougan, T. Sidhu, and M. Sachdev, "Technique for online prediction of voltage collapse," *IEE Proceedings-Generation, Transmission and Distribution*, vol. 151, no. 4, pp. 453–460, 2004.

[9] M. Haque, "Use of local information to determine the distance to voltage collapse," *International Journal of Emerging Electric Power Systems*, vol. 9, no. 2, 2008.

[10] C.-F. Yang, G. G. Lai, C.-H. Lee, C.-T. Su, and G. W. Chang, "Optimal setting of reactive compensation devices with an improved voltage stability index for voltage stability enhancement," *International Journal of Electrical Power & Energy Systems*, vol. 37, no. 1, pp. 50–57, 2012.

[11] I. Musirin and T. A. Rahman, "On-line voltage stability based contingency ranking using fast voltage stability index (fvsi)," in *IEEE/PES Transmission and Distribution Conference and Exhibition*, IEEE, vol. 2, 2002, pp. 1118–1123.

[12] M. Moghavvemi, G. Jasmon, *et al.*, "New method for indicating voltage stability condition in power system," in *Proc. 3rd International Power Engineering Conference*, vol. 1, 1997, pp. 223–227.

[13] M. Moghavvemi and O. Faruque, "Real-time contingency evaluation and ranking technique," *IEE Proceedings-Generation, Transmission and Distribution*, vol. 145, no. 5, pp. 517–524, 1998.

[14] A. Mohamed, G. Jasmon, and S. Yusoff, "A static voltage collapse indicator using line stability factors," *Journal of industrial technology*, vol. 7, no. 1, pp. 73–85, 1989.

[15] S. Mokred, Y. Wang, and T. Chen, "A novel collapse prediction index for voltage stability analysis and contingency ranking in power systems," *Protection and Control of Modern Power Systems*, vol. 8, no. 1, p. 7, 2023.

[16] M. Cupelli, C. D. Cardet, and A. Monti, "Comparison of line voltage stability indices using dynamic real time simulation," in *2012 3rd IEEE PES Innovative Smart Grid Technologies Europe (ISGT Europe)*, IEEE, 2012, pp. 1–8.

[17] Y. Scholz, "Renewable energy based electricity supply at low costs: Development of the remix model and application for europe," 2012.

[18] DLR Institute of Engineering Thermodynamics, *Dlr energy system model remix short description*, Online, 2016. [Online]. Available: `https://www.dlr.de/tt/Portaldata/41/Resources/dokumente/institut/system/Modellbeschreibungen/DLR_Energy_System_Model_REMix_short_description_2016.pdf`.

[19] A. M. Gamba Cardenas *et al.*, "Modeling line outages and transmission line expansion in remix-miso," Ph.D. dissertation, Carl von Ossietzky Universität Oldenburg, 2021.

[20] T. M. Inc., *Matlab version: 9.13.0 (r2021a)*, Natick, Massachusetts, United States, 2021. [Online]. Available: `https://www.mathworks.com`.

[21] H. Saadat, *Power System Analysis*. PSA Pub., 2010, ISBN: 9780984543809. [Online]. Available: `https://books.google.de/books?id=s_IbSQAACAAJ`.

[22] M. Kezunovic, A. Abur, G. Huang, A. Bose, and K. Tomsovic, "The role of digital modeling and simulation in power engineering education," *IEEE transactions on power systems*, vol. 19, no. 1, pp. 64–72, 2004.

[23] N. Hatziargyriou *et al.*, "Stability definitions and characterization of dynamic behavior in systems with high penetration of power electronic interfaced technologies," *IEEE PES Technical Report PES-TR77*, 2020.

[24] T. Van Cutsem and C. Vournas, *Voltage stability of electric power systems*. Springer Science & Business Media, 2007.

[25] T. Yong, M. Shiying, and Z. Wuzhi, "Mechanism research of short-term large-disturbance voltage stability," in *2006 International Conference on Power System Technology*, IEEE, 2006, pp. 1–5.

[26] H. Pourbabak, J. Luo, T. Chen, and W. Su, "A novel consensus-based distributed algorithm for economic dispatch based on local estimation of power mismatch," *IEEE Transactions on Smart Grid*, vol. 9, no. 6, pp. 5930–5942, 2017.

[27] H. Pourbabak, Q. Alsafasfeh, and W. Su, "Fully distributed ac optimal power flow," *IEEE Access*, vol. 7, pp. 97 594–97 603, 2019.

[28] A. J. Wood, B. F. Wollenberg, and G. B. Sheblé, *Power generation, operation, and control*. John Wiley & Sons, 2013.

[29] J. Hörsch, H. Ronellenfitsch, D. Witthaut, and T. Brown, "Linear optimal power flow using cycle flows," *Electric Power Systems Research*, vol. 158, pp. 126–135, 2018.

[30] A. Castillo *et al.*, "Essays on the acopf problem: Formulations, approximations, and applications in the electricity markets," Ph.D. dissertation, Johns Hopkins University, 2016.

[31] A. Verma, *Power grid security analysis: An optimization approach*. Columbia University, 2010.

[32] K. Lehmann, A. Grastien, and P. Van Hentenryck, "Ac-feasibility on tree networks is np-hard," *IEEE Transactions on Power Systems*, vol. 31, no. 1, pp. 798–801, 2015.

[33] F. C. Schweppe, M. C. Caramanis, R. D. Tabors, and R. E. Bohn, *Spot pricing of electricity*. Springer Science & Business Media, 2013.

[34] T. Akbari and M. Tavakoli Bina, "Linear approximated formulation of ac optimal power flow using binary discretisation," *IET Generation, Transmission & Distribution*, vol. 10, no. 5, pp. 1117–1123, 2016.

[35] A. Soroudi, *Power system optimization modeling in GAMS*. Springer, 2017, vol. 78.

[36] V. Phillipe, A. Street, J. M. Colmenar, *et al.*, "A milp-based heuristic algorithm for transmission expansion planning problems," 2022.

[37] W. Gandulfo, E. Gil, and I. Aravena, "Generation capacity expansion planning under demand uncertainty using stochastic mixed-integer programming," in *2014 IEEE PES General Meeting— Conference & Exposition*, IEEE, 2014, pp. 1–5.

[38] H. Akbarzade and T. Amraee, "A multi-stage generation expansion planning for low carbon power systems," in *2020 28th Iranian Conference on Electrical Engineering (ICEE)*, IEEE, 2020, pp. 1–5.

[39] H. Akbarzade and T. Amraee, "A model for generation expansion planning in power systems considering emission costs," in *2018 Smart Grid Conference (SGC)*, IEEE, 2018, pp. 1–5.

[40] J. Wu *et al.*, "Study on medium and long-term generation expansion planning method considering the requirements of green low-carbon development," in *2018 IEEE PES Asia-Pacific Power and Energy Engineering Conference (APPEEC)*, IEEE, 2018, pp. 689–694.

[41] P. Vilaca, A. Street, and J. M. Colmenar, "A milp-based heuristic algorithm for transmission expansion planning problems," *Electric Power Systems Research*, vol. 208, p. 107882, 2022.

[42] S. S. Torbaghan and M. Gibescu, "Optimum transmission system expansion offshore considering renewable energy sources," in *Optimization in Renewable Energy Systems*, Elsevier, 2017, pp. 177–231.

[43] P. Thongbouasy and R. Chatthaworn, "Transmission expansion planning considering solar photovoltaic using novel binary particle swarm optimization," *Energy Reports*, vol. 9, pp. 1145–1153, 2023.

[44] M. S. S. Danish, T. Senjyu, S. M. S. Danish, N. R. Sabory, N. K, and P. Mandal, "A recap of voltage stability indices in the past three decades," *Energies*, vol. 12, no. 8, p. 1544, 2019.

[45] M. Moghavvemi and F. Omar, "Technique for contingency monitoring and voltage collapse prediction," *IEE Proceedings-Generation, Transmission and Distribution*, vol. 145, no. 6, pp. 634–640, 1998.

[46] S. Punitha and K. Sundararaju, "Voltage stability improvement in power system using optimal power flow with constraints," in *2017 IEEE International Conference on Electrical, Instrumentation and Communication Engineering (ICEICE)*, IEEE, 2017, pp. 1–6.

[47] J. Modarresi, E. Gholipour, and A. Khodabakhshian, "A comprehensive review of the voltage stability indices," *Renewable and Sustainable Energy Reviews*, vol. 63, pp. 1–12, 2016.

[48] A. Nageswa Rao, P. Vijaya, and M. Kowsalya, "Voltage stability indices for stability assessment: A review," *International Journal of Ambient Energy*, vol. 42, no. 7, pp. 829–845, 2021.

[49] A. Chebbo, M. Irving, and M. Sterling, "Voltage collapse proximity indicator: Behaviour and implications," in *IEE Proceedings C (generation, transmission and distribution)*, IET, vol. 139, 1992, pp. 241–252.

[50] S. A. Adegoke and Y. Sun, "Power system optimization approach to mitigate voltage instability issues: A review," *Cogent Engineering*, vol. 10, no. 1, p. 2 153 416, 2023.

[51] J. Zhu, *Optimization of power system operation*. John Wiley & Sons, 2015.

[52] G. D. KS, "Hybrid genetic algorithm and particle swarm optimization algorithm for optimal power flow in power system," *J. Comput. Mech. Power Syst. Control*, vol. 2, pp. 31–37, 2019.

[53] T. Fukuda, T. Ueyama, Y. Kawauchi, and F. Arai, "Concept of cellular robotic system (cebot) and basic strategies for its realization," *Computers & electrical engineering*, vol. 18, no. 1, pp. 11–39, 1992.

[54] M. Imran, R. Hashim, and N. E. Abd Khalid, "An overview of particle swarm optimization variants," *Procedia Engineering*, vol. 53, pp. 491–496, 2013.

[55] A. Slowik and H. Kwasnicka, "Nature inspired methods and their industry applications—swarm intelligence algorithms," *IEEE Transactions on Industrial Informatics*, vol. 14, no. 3, pp. 1004–1015, 2017.

[56] K.-K. Cao *et al.*, "Bridging granularity gaps to decarbonize large-scale energy systems—the case of power system planning," *Energy Science & Engineering*, vol. 9, no. 8, pp. 1052–1060, 2021.

[57] REMix, *Modeling concept – dlr developer documentation*, `https://remix.pages.gitlab.dlr.de/framework/dev/documentation/modeling-concept/index.html`, Accessed on: December 27, 2023.

[58] S. Shengyan, S. Xiaoliu, and G. Yawei, "Research on calculation of low voltage distribution network theoretical line loss based on matpower," in *2011 International Conference on Advanced Power System Automation and Protection*, IEEE, vol. 1, 2011, pp. 22–25.

[59] R. D. Zimmerman, C. E. Murillo-Sánchez, and R. J. Thomas, "Matpower: Steady-state operations, planning, and analysis tools for power systems research and education," *IEEE Transactions on power systems*, vol. 26, no. 1, pp. 12–19, 2010.

[60] R. D. Zimmerman and C. E. Murillo-Sánchez, "Matpower user's manual. 2019," *URL https://matpower. org/docs/MATPOWER-manual. pdf. Accessed*, vol. 27, 2020.

[61] I. Staffell and S. Pfenninger, "Using bias-corrected reanalysis to simulate current and future wind power output," *Energy*, vol. 114, pp. 1224–1239, 2016.

[62] H. Bouchekara, M. Abido, and M. Boucherma, "Optimal power flow using teaching-learning-based optimization technique," *Electric Power Systems Research*, vol. 114, pp. 49–59, 2014.

[63] F. Berrouk, H. Bouchekara, A. Chaib, M. Abido, K. Bounaya, and M. Javaid, "A new multi-objective jaya algorithm for solving the optimal power flow problem," *Journal of Electrical Systems*, vol. 14, no. 3, pp. 165–181, 2018.

[64] H. Bouchekara, "Solution of the optimal power flow problem considering security constraints using an improved chaotic electromagnetic field optimization algorithm," *Neural Computing and Applications*, vol. 32, no. 7, pp. 2683–2703, 2020.

[65] H. R. E.-H. Bouchekara and M. A. Abido, "Optimal power flow using differential search algorithm," *Electric Power Components and Systems*, vol. 42, no. 15, pp. 1683–1699, 2014.

[66] N. Hatziargyriou *et al.*, "Definition and classification of power system stability–revisited & extended," *IEEE Transactions on Power Systems*, vol. 36, no. 4, pp. 3271–3281, 2020.

[67] S. Nikkhah and A. Rabiee, "Voltage stability constrained multi-objective optimisation model for long-term expansion planning of large-scale wind farms," *IET Generation, Transmission & Distribution*, vol. 12, no. 3, pp. 548–555, 2018.

[68] A. J. Conejo, M. Carrión, J. M. Morales, *et al.*, *Decision making under uncertainty in electricity markets*. Springer, 2010, vol. 1.

Declaration of Authorship

I hereby confirm that this thesis is entirely my own work. I confirm that no part of the document has been copied from either a book or any other source – including the internet - except where such sections are clearly shown as quotations and the sources have been correctly identified within the text or in the list of references. Moreover, I confirm that I have taken notice of the 'Leitlinien guter wissenschaftlicher Praxis' of the University of Oldenburg.

_____

Place, Date

_____

Author's signature